SECOND LIFE AND RECYCLING: ENERGY AND ENVIRONMENTAL SUSTAINABILITY PERSPECTIVES FOR HIGH-PERFORMANCE LITHIUM-ION BATTERIES

A Thesis

Presented to the Faculty of the Graduate School

of Cornell University

in Partial Fulfillment of the Requirements for the Degree of

Master of Science

by

Yanqiu Tao

May 2021

ABSTRACT

Sustainability of retired automotive lithium-ion batteries (LIBs) has drawn growing attention as large volumes of LIBs will start to retire in the coming decade, while LIB demand continues to grow. Second life and recycling are considered sustainable solutions to waste management of LIBs. However, the environmental and economic benefits of second life and recycling depend on specific battery chemistries. Here we show that high-performance LIBs could provide more environmental benefits through full material and energy recovery. Moreover, LIB's second life in stationary energy storage systems could lessen the heterogeneity between different types of LIBs and different recycling methods in terms of both environmental and economic performances. When connected to the power grid in Texas, we found that introducing second life into the life cycle of multiple promising high-performance LIBs reduces carbon footprint and cumulative energy demand (CED) by 6%–11% and CED by 4%–8%, respectively. The corresponding carbon footprint and CED can be further reduced by 16% and 27% in major LIB manufacturing and consuming countries (The United States and China) due to projected renewable energy transition by 2050. Lastly, direct cathode recycling is found to have the most reduction in environmental impacts, although its economic performance is less ideal, compared to pyrometallurgical recycling.

BIOGRAPHICAL SKETCH

Yanqiu Tao was born and raised in Nanjing, China. She graduated with a Bachelor's degree in Life Science and Medical Bioscience from Waseda University, Japan in August 2016. In August 2017, she was enrolled in the Master of Science Program in Biostatistics at University of Pennsylvania. In June 2018, she was enrolled in the Master of Science Program in Chemical Engineering at Cornell University. During her graduate study at Cornell University, she first focused on assessing the environmental and economic feasibility of thermochemical conversions for agricultural wastes in the food-energy-water-waste nexus. She also participated in several researches on spatial analysis of agricultural waste with one publication in ACS Sustainable Chemistry & Engineering. Inspired by the increasing incorporation of remoting sensing data with the agricultural research, she classified cover crop existence during the off-season via applying machine learning methods on the satellite images and presented the results on the 3rd Annual CIDA Digital Agriculture Workshop. Then she devoted to assessing the environmental and economic benefits of second life and recycling for various lithium-ion batteries. She planned to pursue her PhD degree in Systems Engineering at Cornell University later in Spring 2021.

ACKNOWLEDGMENTS

Foremost, I would like to express my deepest appreciation to my parents, for their generous financial support and precious spiritual support to me during my graduate study. Without their encouragement and unconditional love, it is impossible for me to fulfill my dream of being engaged in courses and researches at one of the top universities in the world.

I would also like to extend my deepest gratitude to my advisor, Professor Fengqi You, for his patience, constructive instructions, and relentless support. I have been always deeply inspired by his enthusiasm to research, his dedication to work, and his expertise across various fields of study. It is a great honor to be supervised by him.

I also had great pleasure of working with my committee member, Professor Jefferson Tester. He has been generous with his time and insightful suggestions for the revision of this thesis paper.. I was profoundly impressed by his hard working, and his unremitting high productivity.

Special thanks to my boyfriend, Ning Zhao, who has always been my person and always been there for me. During my graduate study, we have been supporting with each other on both academics and emotions. Thanks should also go to my dependable and adorable friend, Buttercup, for his two-year company.

Last but not least, I gratefully acknowledge the assistance of all my current and past colleagues. The academic success of Dr. Liang Zhao, Dr. Zuwei Liao, Dr. Li Sun, Dr. Inkyu Lee, Dr. Chao Shang, and Chao Ning motivates me on my academic career. Xueyu Tian and Raaj Bora were always patient to me and provided me many useful advices. My thanks also go to other colleagues including, Jiwei Yao, Wei-Han Chen, Xiang Zhao, Akshay Ajagekar, Abdulelah Alshehri, Musuizi Lei, Vanessa Ferreira de Almeida, and Shipu Zhao, thank you guys for all the good memories.

TABLE OF CONTENTS

LIST OF FIGURES

LIST OF TABLES

LIST OF ABBREVIATIONS

Abbreviation	Full name
ACN	Acetonitrile
BMS	Battery management system
CED	Cumulative energy demand
CHP	Combined heat and power generation
DMC	Dimethyl carbonate
DOD	Depth of discharge
EC	Ethylene carbonate
EIA	Energy Information Administration of the U.S. Department of Energy (DOE)
EOL	End-of-life
ESS	Energy storage system
EV	Electric vehicle
LCA	Life cycle assessment
LCI	Life cycle inventory
LFP	Lithium iron phosphate
LIB	Lithium-ion battery
LMO	Lithium manganese oxide
NCA	Lithium nickel cobalt aluminum oxide
NMC	Lithium nickel manganese cobalt oxide
NMP	N-Methyl-2-Pyrrolidone
OCV	Open circuit voltage
PC	Propylene carbonate
PE	Polyethylene
PET	Polyethylene terephthalate
PP	Polypropylene
PVDF	Polyvinylidene fluoride
SOC	State of charge
U.S.	United States

USEPA	United States Environmental Protection Agency

CHAPTER 1

INTRODUCTION

Owing to the rapid growth of the electric vehicle (EV) market since 2010 and the increasing need of massive electrochemical energy storage (reached 30 gigawatt-hours of storage capacity in 2017, around 60% increase in storage capacity from 2016),[1] the demand of lithium-ion batteries (LIBs) is expected to double by 2025 and quadruple by 2030.[2,3] As a consequence, global demands of critical materials used in LIBs, such as lithium and cobalt, are expected to grow at similar rates, leading to increasing supply risk.[2,4] To be specific, the shares of demand for lithium and cobalt used in batteries are expected to increase from 14% and 25% in 2010 to 76% and 53% in 2025, respectively.[5] Concerns about lithium depletion have been extensively addressed in previous studies by showing that lithium does not face major supply risk in the mid-term future.[6,7] However, cobalt supply could be of great risk due to its by-product dependence and geopolitical concentration of both its mining in Congo and refining in China.[8,9] Additionally, the scale of retired LIBs is expected to grow rapidly in the coming decade.[10,11] All of these aspects contribute to the growing concerns on the resource depletion and environmental impacts of the coming boom in retired LIBs.[4]

Avoidance of using critical materials, such as cobalt in LIBs, is the most important approach in LIB waste management.[4,6] Along this line, both research and market interests shift towards low-cobalt LIBs and no-cobalt alternatives due to the susceptibility of cobalt supply to potential supply chain disruption, and the resulting price volatility and uncertainty.[2,5,8,12] Re-use applications of LIBs, such as energy storage systems (ESS) after automotive use, are another ideal way to manage waste. Such a “second-life” approach for automotive LIBs may improve both emission reduction benefits and economic performance.[13] Existing literature on cascaded use (first use and second use)

of LIBs focused on their technical and economic feasibility, as well as economic impacts on the global EV market. [11,14-16] Previous life cycle assessment (LCA) studies on second-life applications of LIBs focused mainly on only one type of battery chemistry (lithium manganese oxide (LMO) or lithium iron phosphate (LFP)).[17-22] Three studies considered different battery chemistries,[13,23,24] however, none of them explicitly investigated the differences in environmental and economic benefits of different battery chemistries. Nevertheless, due to incomplete data on the LIB recycling, the scopes of these pioneering studies were all confined to the assessment of carbon footprint and cumulative energy demand (CED) over only part of second-life LIBs' life cycle. To the best of our knowledge, none of the existing work has systematically investigated the implications on environmental sustainability and economics of reused automotive LIBs across various battery chemistries and recycling alternatives. Furthermore, a comprehensive and systematic assessment of life cycle environmental impacts and the identification of environmental hotspots, such as processes or materials associated with high levels of environmental impacts, for different automotive LIBs with second life remains a knowledge gap.

Another less desirable strategy for retired LIB management integrates recycling, energy recovery, and disposal. However, LIB recycling remains rather unsupervised and unpracticed due to various technical, economic, and environmental challenges.[25,26] Currently, the only commercialized LIB recycling technology is the pyrometallurgical process.[27] Due to lack of available data, existing LCA studies excluded or simplified the end-of-life (EOL) phase from the scope of their study.[28-32] In particular, low-value materials recovery was incorporated into battery disposal in some of these studies. Existing LCA studies do not include sufficient details of LIB recycling technologies. Specifically, LIB recycling in existing LCA analyses was obscured by omitting part of critical steps and essential materials, so the resulting environmental benefits could

be overestimated. Furthermore, to the best of our knowledge, existing LCA studies on LIB recycling did not consider complete recovery of all cathode active materials, metals, and energy, or enhancement of the recovery rates based on promising experimental data. In this regard, the environmental benefits of LIB recycling might be underestimated.

To fill the aforementioned knowledge gaps, this study aims to investigate the environmental and economic benefits of automotive LIBs with different battery chemistries from second life and recycling, and to identify the environmental hotspots throughout their life cycles, emphasizing maximum material and energy recovery. Specifically, life-cycle carbon footprint, CED, a comprehensive list of environmental indicators (given in Section 2.1 LCA assumptions),[33] and life cycle costs are examined for seven promising automotive LIBs, namely LFP, lithium nickel manganese cobalt oxide (NMC333, NMC532, NMC622, and NMC811), LMO+NMC532 blend, and lithium nickel cobalt aluminum oxide (NCA). The assumed specific energy density are 177, 229, 234, 243, 255, 265, and 262 Wh/kg for LFP, LMO+NMC532, NMC333, NMC532, NMC622, NMC811, and NCA LIB packs, respectively. Moreover, to investigate the environmental benefits of second life adoption, two LIB use scenarios are proposed as depicted in Figure 1. The first one only subjects the LIBs to automotive use, and the other one considers the stationary ESS application of energy arbitrage using LIBs after automotive use. Owing to the integration of the less-demanding stationary ESS use, conventional functional units based on weight, driving distance, or energy storage capacity are inappropriate to evaluate the prolonged life-cycle environmental and economic performance of the LIBs. Therefore, we adopt a functional unit that pictures the LIB's life-cycle contribution (i.e. 1 kWh life cycle electricity delivery). Three popular EOL scenarios are assessed and compared, including hydrometallurgical, pyrometallurgical, and direct cathode recycling, which are designed and optimized to recover as many materials and

energy as possible based on state-of-the-art experimental data.[34-40] To be specific, hydrometallurgical recycling recovers metals using aqueous chemistry; direct cathode recycling directly recovers the cathode active materials through electrolyte extraction; pyrometallurgical recycling recovers metals in the form of alloy by a three-stage smelting process. However, the pyrometallurgical recycling of LFP is disregarded due to the lack of cyclable critical metals such as nickel and cobalt. It is worth mentioning that under the baseline case, the whole life cycle of LIBs, including the production and assembly, EV use, repurpose, stationary ESS use, and EOL, are assumed to be placed in the Texas State in 2018 due to the independence of its electric power system. The temporal and spatial variation of the power grid will be considered in the sensitivity analyses. Also, environmental hotspots are identified to gain insights into the potential scale-up of laboratory-scale recycling technologies. Last, sensitivity analyses of temporal and geographical variation in electricity generation are conducted. Key results and insights into experimental work, industry, and policymakers are summarized in the following section.

The major novelties of this work include:

- The first systematic investigation of the environmental and economic benefits of introducing second life to the life cycle of LIBs with different battery chemistries, including LFP, LMO+NMC mixture, NMC, and NCA;
- The first results of identifying environmental hotspots throughout the life cycle of LFP, LMO+NMC, NMC, and NCA LIBs considering three EOL scenarios, including hydrometallurgical, pyrometallurgical, and direct cathode recycling;
- The most comprehensive modeling and analysis of three major EOL recycling approaches (hydrometallurgical, pyrometallurgical, and direct cathode recycling) for LFP, LMO+NMC, NMC, and NCA LIBs based on both state-of-the-art experimental data and estimations to

maximize the material and energy recovery.

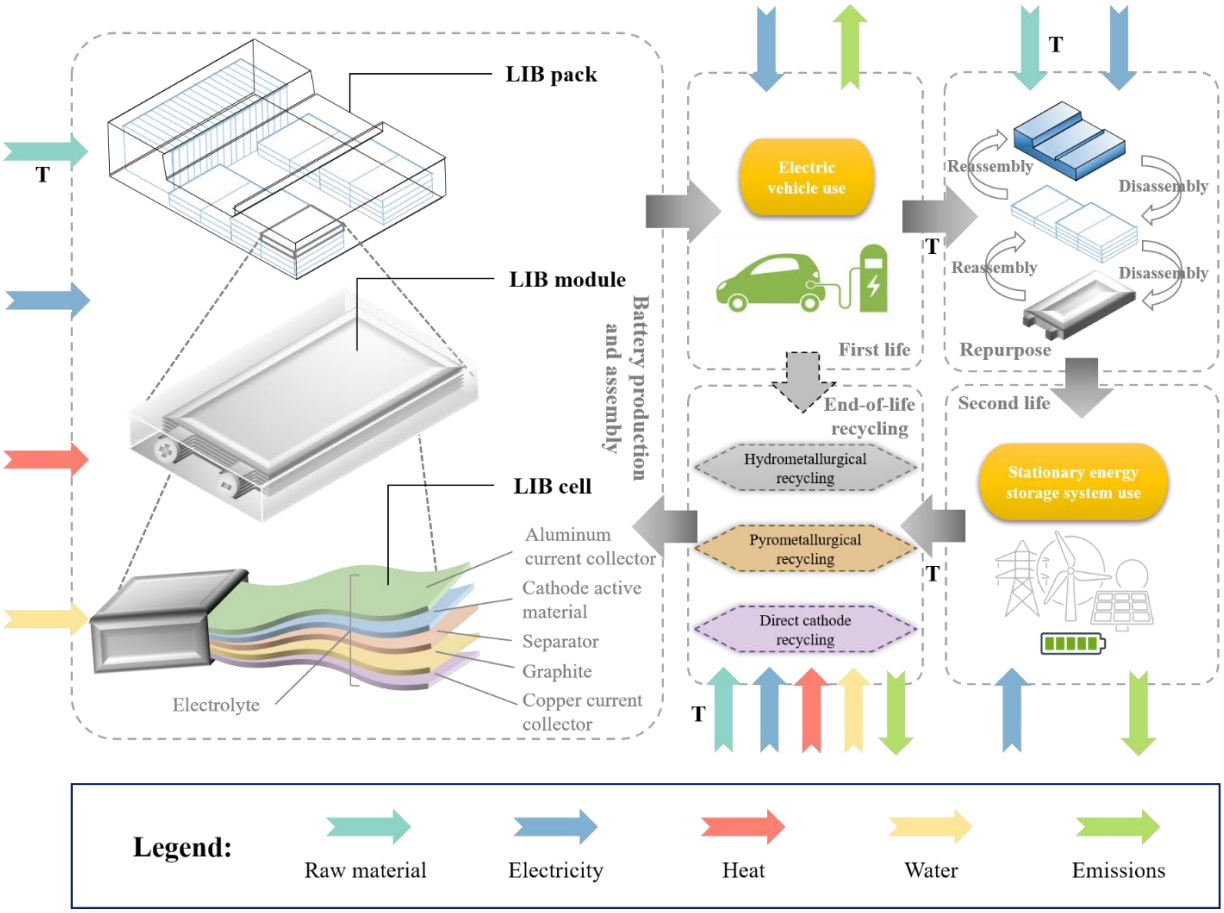

Figure 1. System boundary of LIB life cycle with second life and three EOL alternatives, including hydrometallurgical, pyrometallurgical, and direct cathode recycling.

1.1 Key results and insights to bench work, industry, and policymakers

- Carbon footprint and CED of high-performance LIBs can be reduced by 6% – 11% and 4% – 8% respectively, if second life is introduced to LIBs' life cycle;
- Second life of retired LIBs can reduce the life cycle cost by 60%;
- The heterogeneity in both environmental impact and economics between different types of LIBs and different recycling methods becomes less obvious in the existence of second life.
- Through increasing the level of renewable energy penetration into electric power systems

in the coming three decades, there is a great potential to further reduce the life cycle carbon footprint of reused automotive LIBs in the United States (U.S.) and China by 16% and 27%, respectively;

- Direct cathode recycling is the most competitive technology of future LIB recycling due to its favorable environmental performance and moderate economic cost;
- Since the N-Methyl-2-Pyrrolidone (NMP) production and recovery is highly detrimental to the environment, greener aqueous binders should be further researched and commercialized;
- Carbon-intensive graphite and carbon black should be separated and recycled from the spent LIBs instead of being combusted;
- Energy-intensive processes such as re-lithiation should be coupled with other exothermic processes to reduce energy demand;
- Industrial recycling process flows should be well-designed to avoid excessive use of both environmentally and economically costly chemicals.

CHAPTER 2

MATERIALS AND METHODS

2.1 LCA assumptions

In this study, we conduct a "cradle-to-grave" LCA to estimate the carbon footprint, CED, and full-spectrum environmental impacts associated with the production, consumption, and EOL of seven automotive LIBs, namely LFP, LMO+NMC532, NMC333, NMC532, NMC622, NMC811, and NCA, after second life in stationary ESS. In the absence of second life application, common functional units adopted in previous LCA studies of automotive LIBs, such as 1 kWh energy storage capacity and 1 kg battery, are not suitable for this system and can no longer serve as a proper reference to normalize the life cycle inventory (LCI) data of this study, which focuses on LIB second life and recycling. Therefore, we propose a functional unit of 1 kWh life-cycle electricity delivery to quantify the life-cycle contribution of LIBs. Assumptions of working parameters of LIBs are provided in Table S1. The whole life cycle of the LIBs, including manufacturing, EV use, repurpose, stationary ESS use, and recycling, is assumed to be located in the Texas State in 2018, without consideration of temporal variability in the Texas local power grid. That is to say, the environmental profile of electricity production is determined by the energy sources of the Texas power grid in 2018.

Because one of the primary objectives of this study is to investigate the environmental benefits of second life for different LIBs, two use scenarios are considered as shown in Figure 1. The first one is the EV use scenario, of which the system boundary involves stages of cell materials production and assembly, module accessories production and assembly, pack accessories production and assembly, EV use, and EOL recycling. The other one is the cascaded use scenario, which has a system boundary including stationary ESS use (second use) and repurpose, in addition

to all the stages of the aforementioned automotive use only scenario. Transportations are also included in both system boundaries, and assumptions are provided in Table S26. Another goal of this study is to evaluate the environmental impacts of various recycling methods, so three EOL scenarios including hydrometallurgical, pyrometallurgical, and direct cathode recycling, are systematically analyzed and compared. It is worth mentioning that only hydrometallurgical and direct cathode recycling are adopted for LFP due to the lack of critical metals that are recyclable using pyrometallurgical recycling. More details about use scenarios and EOL scenarios are provided in the next sections and APPENDIX.

To calculate the full-spectrum environmental impacts eighteen ReCiPe midpoint indicators from the hierarchist perspective are adopted to examine the severity of the environmental impact categories.[33] These indicators account for agricultural land occupation, climate change, fossil depletion, freshwater ecotoxicity, freshwater eutrophication, human toxicity, ionizing radiation, marine ecotoxicity, marine eutrophication, metal depletion, natural land transformation, ozone depletion, particulate matter formation, photochemical oxidant formation, terrestrial acidification, terrestrial ecotoxicity, urban land occupation, and water depletion. This ReCiPe model is frequently used in LCA studies on LIBs.[20,24,30,41,42]

2.2 Life cycle inventory analysis

During the LCI analysis phase of LCA, energy, and material flows are quantified and compiled across all life cycle stages of the LIBs. Within the production stages, LCIs of an EV battery pack are presented in Table S2–Table S6. LCIs of a stationary ESS LIB pack after automotive use are provided in Table S7. The EOL stage involves three EOL scenarios that correspond to LCIs summarized in Table S9–Table S10, Table S11–Table S12, and Table S14–Table S15. Because the LCIs of cathode active materials production are unavailable in the existing

LCI database, their manufacturing routes are extracted from the literature as shown in Figure S22. Process diagram of active material production for NMC and NCA LIBs and LCIs are established and compiled by modeling the detailed manufacturing processes, as shown in Table S8 and Table S13.

2.3 Use phase scenarios

Two use phase scenarios are assessed: one is the 9-year EV use only scenario, and the other one is the 11-year second life in stationary ESS after the 9-year EV use. The residual energy storage capacity is assumed to be 80% after EV use and 65% after cascaded use. We modeled the battery fading using a previous aging model.[43,44] EV use is assumed to be 60 km on a daily basis. We assume that EV is charged during the on-peak period. For the stationary ESS use, we assume that the repurposed 450-kWh LIB pack charges during the on-peak period and discharges during the off-peak period to support 10 residential utility customers who consume on average 292.3 kWh electricity on a daily basis.[45] The on-peak period and off-peak period are assumed to be 8-hour and 16-hour long, respectively despite the seasonal variability.[46] The average SOC is 60% during the on-peak period (assume linearly discharged to around 20% DOD) and 100% during the off-peak period. Battery temperature is another important parameter in battery fading modeling and we approximate it using the monthly average temperature of Texas.[47]

2.4 End-of-life scenarios

EOL of LIBs involves dismantling, material production, energy generation, incineration, combustion, waste sludge treatment, and energy and materials recovery. The investigated EOL methods differ in the way they recover energy and materials. To be specific, hydrometallurgical recycling recovers metals using aqueous chemistry, and typically involves leaching, solvent

extraction, and precipitation; direct cathode recycling directly recovers the cathode active materials through electrolyte extraction; pyrometallurgical recycling, as the only commercial recycling method for LIBs, recovers metals in the form of alloy by a three-stage smelting process. Subsequent treatments are needed to obtain ready-to-use battery-grade cathode active materials from intermediate products. Moreover, all three recycling methods are optimized to recover as many cathode active materials as possible using the best-available laboratory-scale recycling procedures and experimental data as depicted in Figure S23–Figure S25.

The environmental impacts associated with energy and material recovery are considered as avoided burdens and are reported as reductions in emissions and CED. Therefore, the system boundary is expanded to a "cradle-to-cradle" counterpart. Due to the lack of information, the waste sludge treatment of the EOL phase of spend LIBs is replaced by treatment of sludge from steel rolling, given that sludge from steel rolling resembles sludge from treatment of spent LIBs.

2.5 Life cycle impact assessment method

In this study, carbon footprint, CED, and ReCiPe impact categories are selected to demonstrate and compare the life cycle greenhouse gas emissions, energy consumption, and full-spectrum environmental impacts, respectively. In the life cycle impact assessment stage of LCA, LCIs are computed based on the functional units through characterization factors to quantify their environmental impacts for each impact category. We collect most of the characterization factors from Ecoinvent.[48] However, other characterization factors, such as LFP, NMC, and NCA production, are inaccessible from the Ecoinvent database. $CoSO_4$ and $Ni(OH)_2$, which are raw materials of cobalt-containing cathode active materials and recovered nickel-containing materials, respectively, do not have readily available LCI data either. Therefore, we need to construct the LCI from either upstream processes (i.e. $Ni(OH)_2$, NCM, and NCA production estimated from

upstream energy and material inputs detailed in APPENDIX) or downstream processes (i.e. $CoSO_4$ production estimated from metallic cobalt production). Since $CoSO_4$ can be considered as an intermediate in the metallic cobalt refining by electrowinning, $CoSO_4$ production can be modified from the metallic cobalt production by eliminating the surplus reduction steps and add an H_2SO_4 production step.[30] Nevertheless, emissions and waste disposal are not modified due to a lack of disaggregated data. Moreover, crude cobalt ionic solution must undergo further processing steps, such as crystallization and dry co-product separation and recrystallization, to produce $CoSO_4$ crystals of high purity. However, these steps are not included in the system boundary of this LCA, because corresponding data are unavailable, and their energy and material requirements are expected to be quite low.

2.6 Sensitivity analysis

Sensitivity analysis is performed to evaluate the key assumptions of electricity generation and EOL scenarios. According to the results shown in Figure 7 and Figure 8, the use phase is the leading factor of life cycle carbon footprint and CED. Moreover, use phase is the main contributor for most of the environmental impact categories as shown in Figure 3 – Figure 6. We also conclude that the full-spectrum environmental impact profiles of LIBs are largely affected by the energy sources of electricity generation and the characteristics of those energy sources. Therefore, the temporal and spatial variation in electricity generation is tested by introducing predicted energy sources of electricity generation from 2020 to 2050 in the U.S. and China.[49,50] The environmental impacts associated with 1 kWh electricity generated in each year are computed as a weighted sum of the unit environmental impacts for electricity production from various energy sources. The weights are the shares of different energy sources. The unit environmental impact for electricity production from each energy source in each location is obtained from the Ecoinvent database.[48]

The electricity generation by energy source from 2020 to 2050 in the U.S. and China is presented on a percentage basis in Figure S30. LIBs are assumed to be produced in any year between 2020 to 2050, and then they are used by EVs for 9 years. After retiring from EV use, LIBs are repurposed to start their second life. After an 11-year second life, LIBs are disposed of and recycled. For example, an LIB can be manufactured in 2020, repurposed in 2029, and recycled in 2039, with the first life in 2020–2028 and the second life in 2029–2039. It is worth mentioning that all of the other assumptions related to battery parameters, LIB production, repurpose, and LIB recycling, remain unchanged. Based on the functional unit of life cycle electricity delivery, life cycle carbon footprint and CED are calculated for LFP, LMO+NMC532, NMC622, and NCA LIBs over the period of 2020–2050. Note that the energy sources of electricity generation vary constantly during the 20-year life cycle of LIBs. Therefore, the environmental impacts associated with electricity consumption in a specific year vary depending on the energy sources of electricity generation of this year.

The investigated parameters regarding EOL scenarios are considered according to the carbon and energy hotspots identified in Figure 9 –Figure 14. In particular, the following parameters are included for all three EOL scenarios: the recovery rate of chromium steel 18/8, aluminum, copper, and graphite. The recovery rate of cathode active materials and NMP are evaluated for hydrometallurgical and direct cathode recycling. Specifically, the recovery rate of $LiPF_6$ is assessed for direct cathode recycling; recovery rate of goethite, cobalt, and $Ni(OH)_2$ are investigated for pyrometallurgical recycling; recovery rate of Mn_2O_3 and citric acid are evaluated exclusively for hydrometallurgical recycling of LMO+NMC532. Ranges of parameters are presented in Table S18–Table S21 and impacts of these parameters are shown in Figure S26–Figure S28. The results of sensitivity analyses are discussed in S6. Sensitivity analysis for

recycling parameters.

2.7 Economic analysis

Economic analysis is performed to assess the economic benefits of introducing second life into LIB's life cycle. Life cycle cost is calculated as a metric of economic performance by summing the cost from production, EV use, repurpose, stationary ESS use, and EOL recycling. The production cost and repurpose cost are obtained from the BatPac model,[51] and the recycling costs of the hydrometallurgical, direct cathode, and pyrometallurgical recycling are calculated from the EverBatt model.[52] In particular, the production costs and the recycling costs are estimated based on plants with annual throughput of 100,000 battery packs. Costs associated with the use phase are residential costs of electricity and are calculated based on the average electricity price of 2020 in the region of study (Texas). Material prices and parameters used in the cost estimation are presented in Table S22–Table S23. The absolute values and breakdowns of life cycle costs are presented in Table S24–Table S25.

2.8 Min-max normalization

To intuitively present the life cycle environmental impacts across each impact category, we adopt the min-max normalization method to process data. For a set of data points X_1, X_2, …, X_n (i.e. environmental impacts of all processes for each category), this normalization method linearly maps each data point to the range of 0 to 1 according to the equation (1), where X', X_a, X_{max}, X_{min} represent each data point after normalization, each data point before normalization, minimum of the data set, and maximum of the data set, respectively.

$$X' = \frac{X_a - X_{min}}{X_{max} - X_{min}} \quad (1)$$

Nevertheless, the environmental impacts associated with the avoided environmental burden in the EOL phase are negatively signed. Hence, the magnitude of both negative and positive values should be shown on the same basis, while the orientation of environmental favorability (i.e. the negative signs) for each process is preserved. However, the equation (1) is not able to preserve negative signs. To address this issue, we first take absolute values of the negative numbers, and then apply min-max normalization according to the equation (1), and finally change the sign of those who were negative to negative.

CHAPTER 3

RESULTS AND DISCUSSION

3.1 Environmental impact reduction benefits of introducing second life

To assess the implications of second life application to LIBs from an environmental perspective, we compare the life cycle environmental impacts of two use scenarios (with and without second life) across LFP, LMO+NMC532, NMC622, and NCA LIBs. The LFP LIB is defined as the reference for normalization for all 18 impact categories. From the perspective of life cycle electricity delivery (Figure 2), the reductions in different impact categories vary substantially, when the second life approach is adopted. In particular, the freshwater ecotoxicity, marine ecotoxicity, and metal depletion of all four types of LIBs reduce by 59%–65%, 61%–67%, and 59%–74%, respectively. This can be attributed to two reasons: (1) compared to the other impact categories, electricity production is much less influential in these three impact categories; (2) the amount of life cycle electricity delivery under the cascaded use scenario is substantially higher than under the EV use scenario. Other than these three impact categories, others achieve a relatively moderate level of reduction (less than 40%) by adopting second life, because their environmental impacts are dominated by electricity production. Owing to the recovery of its less environmentally expensive cathode active materials and its lowest specific energy density (177, 229, 255, and 262 Wh/kg for LFP, LMO+NMC532, NMC622, and NCA, respectively), LFP LIBs perform the worst in most impact categories. It is worth mentioning that lower specific energy density results in the requirement of more material and energy inputs for the production of LIBs with the same battery pack energy storage capacity. NCA LIBs perform the worst in four impact categories: natural land transformation, ozone depletion, particulate matter formation, and terrestrial acidification, due to the highest nickel content. The LMO recovery discards the leached

ionic manganese from the spent cathode active materials and employs Mn_2O_3 as the manganese source of LMO, which deteriorates LMO+NMC532 LIBs' performance in life cycle metal depletion.

The environmental performance of LFP LIBs becomes drastically favorable and comparable with those of LMO+NMC532, NMC622, and NCA LIBs in the presence of second life. This notable reduction in the environmental impacts of LFP LIBs can be mainly attributed to the overwhelming environmental impacts associated with the massive amount of electricity delivery during second life.

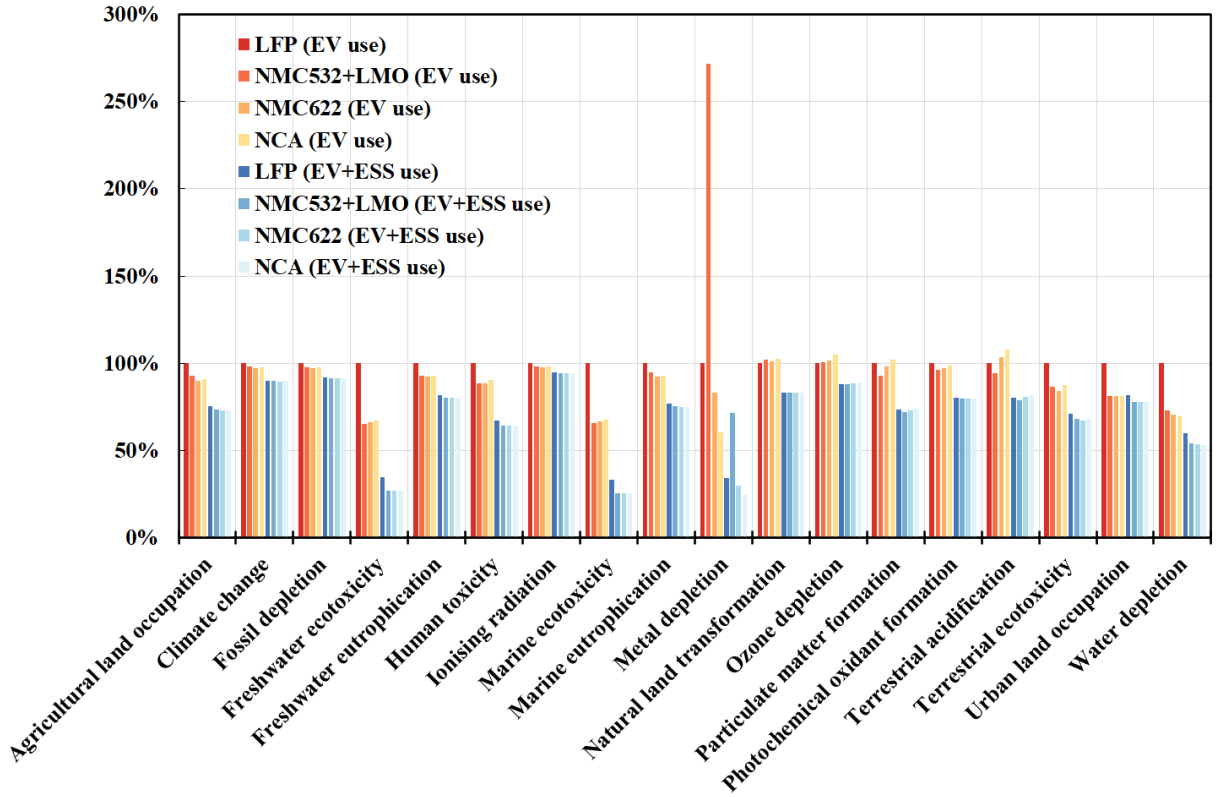

Figure 2. Comparison of environmental impacts between different use scenarios for LFP, LMO+NMC532, NCM622, and NCA LIBs based on the functional unit of life cycle electricity delivery. The environmental impacts of different recycling methods are averaged. Red and blue color indicate life cycle environmental impacts associated with EV use scenario and cascaded use scenario, respectively. Darker color indicates lower pack energy density.

3.2 Environmental impacts of battery recycling methods on second life

Figure 3a–c depicts the environmental profiles of LMO+NMC532 LIBs for all impact categories on a percentage basis. The environmental impacts of each impact category are divided into different life cycle stages. Furthermore, the use phase is disaggregated into EV use and stationary ESS use to better understand their independent environmental impacts. Similarly, the EOL phase is disaggregated into two portions: one includes steps associated with environmental damages, the other is responsible for steps that alleviate environmental burdens. The environmental profiles for other types of LIBs are presented in Figure 4–Figure 6.

Direct cathode recycling is the most environmentally friendly among the three recycling methods, regardless of battery chemistry, for three reasons. First, material recovery of direct cathode recycling and hydrometallurgical recycling avoid comparable environmental impacts, while energy and materials used in hydrometallurgical recycling result in much higher environmental impacts than those used in direct cathode recycling. Second, pyrometallurgical recycling of LMO+NMC532, NMC622, and NCA LIBs recovers much less amount of critical metals (96% of Ni, 62% of Co), generates a large quantity of non-recyclable aluminum and lithium in slag from the smelting process, and utilizes large doses of environmentally expensive reductants. Third, the absence of cobalt and nickel in LMO suggests no recovery of critical metals, and much fewer reductants are needed accordingly. However, the use of citric acid (leachate) and Mn_2O_3 (manganese source) causes notably higher environmental impacts in several impact categories than the LMO avoided from material recovery in hydrometallurgical recycling of LMO+NMC532. Among all the recycling cases, hydrometallurgical and pyrometallurgical recycling of all types of LIBs results in net environmental burdens in natural land occupation and ozone depletion, and direct cathode recycling results in net environmental burdens only in natural land occupation. Due

to the recovery of less environmentally expensive cathode active materials and usage of reagents such as citric acid, Mn_2O_3 (for LMO recovery), and H_3PO_4 (for LFP recovery), hydrometallurgical recycling of LMO+NMC532 and LFP results in net environmental burdens in several other impact categories.

The vast majority of environmental impacts of cell material production and assembly stage are associated with metal consumption and cathode active materials production. Similarly, metal and cathode active materials recovery during battery recycling is the main source for reducing environmental impacts. More details will be provided in the section of 3.4 Environmental hotspots.

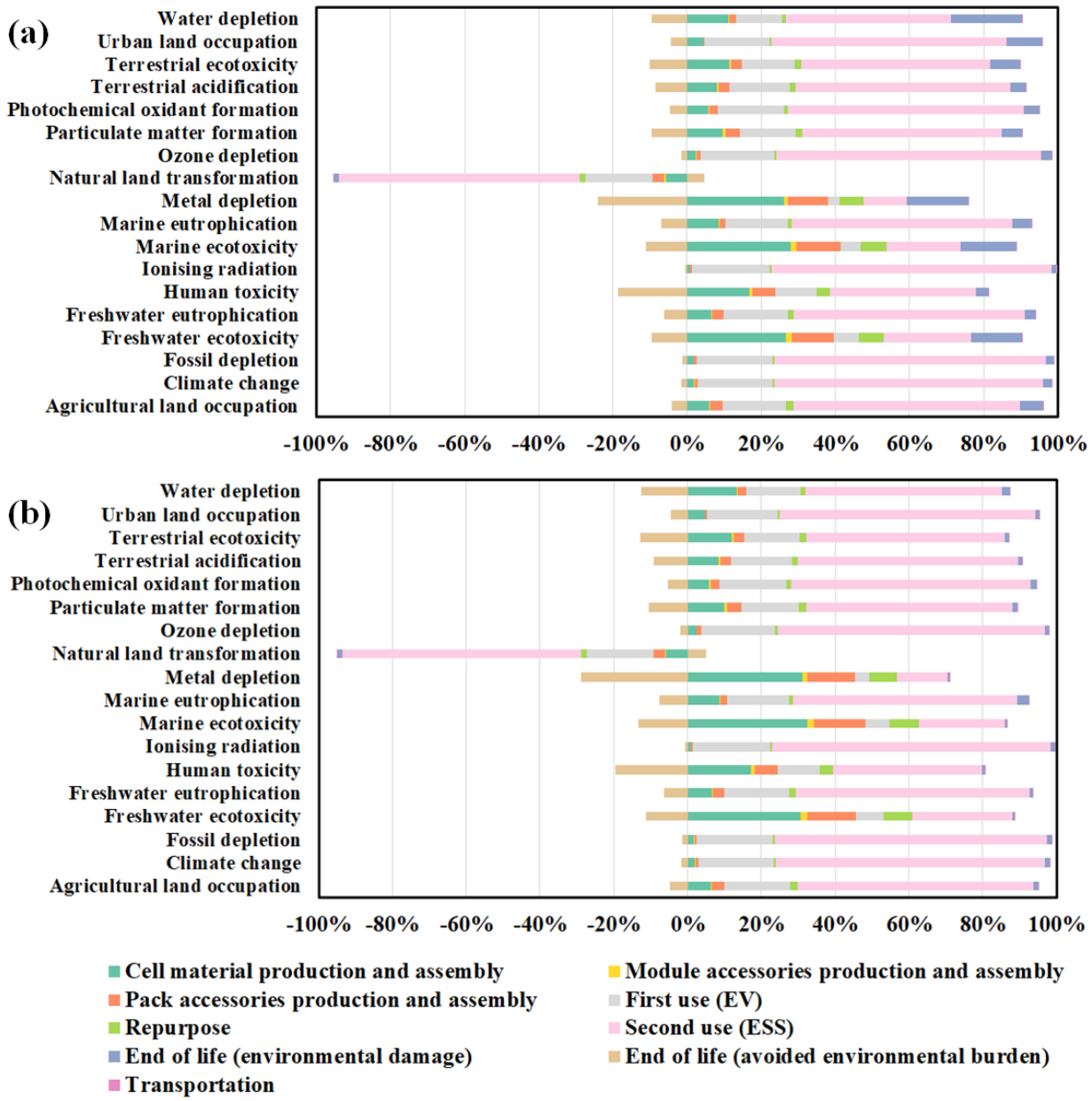

Figure 3. Full-spectrum environmental profiles for LFP LIBs subjected to second life and recycled by (a) hydrometallurgical recycling (b) direct cathode recycling on a percentage scale.

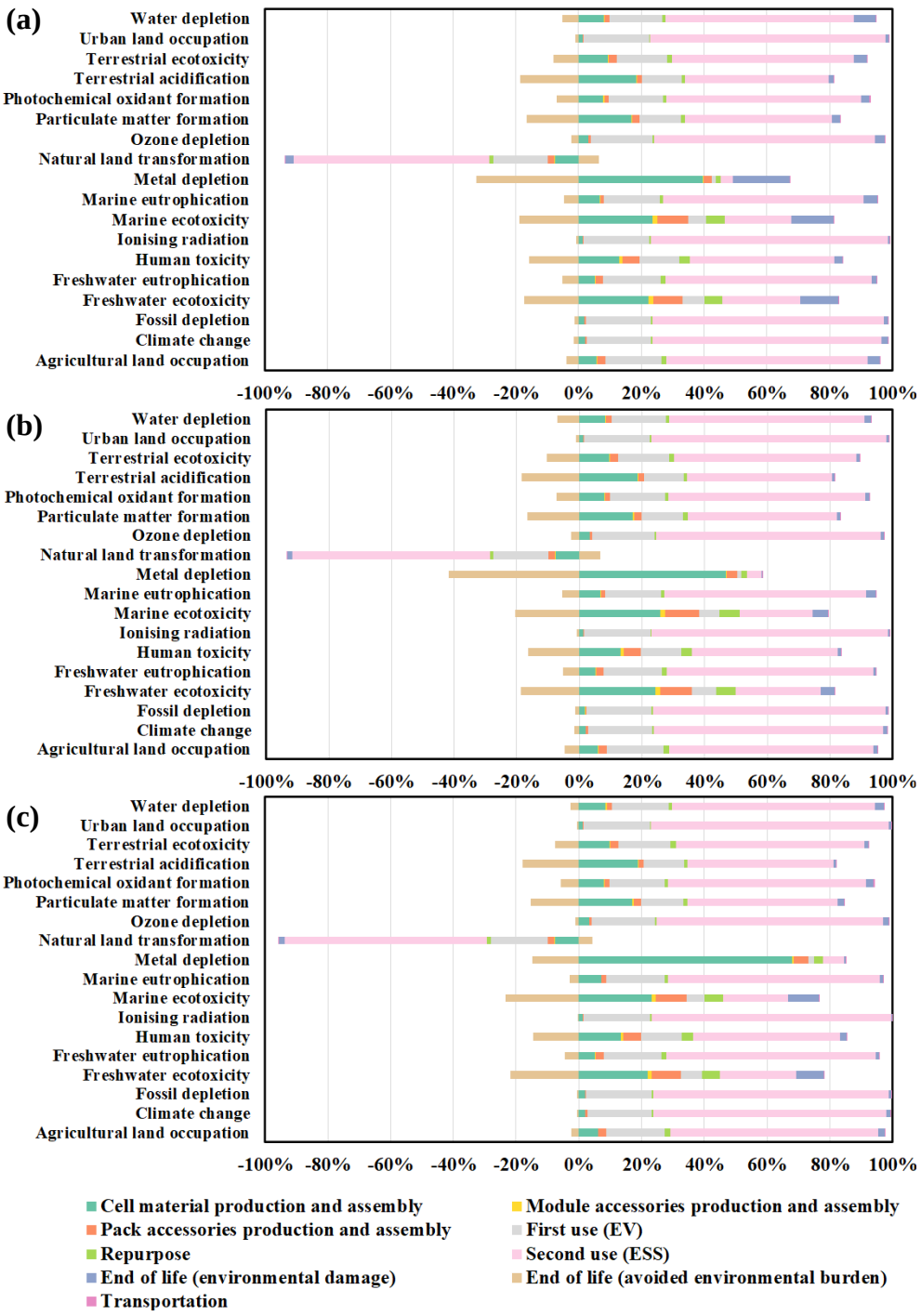

Figure 4. Full-spectrum environmental profiles for LMO+NMC532 LIBs subjected to second life and recycled by (a) hydrometallurgical recycling (b) direct cathode recycling (c) pyrometallurgical recycling on a percentage scale. Different colors in the stacked bars indicate different life cycle stages of LMO+NMC532 LIBs.

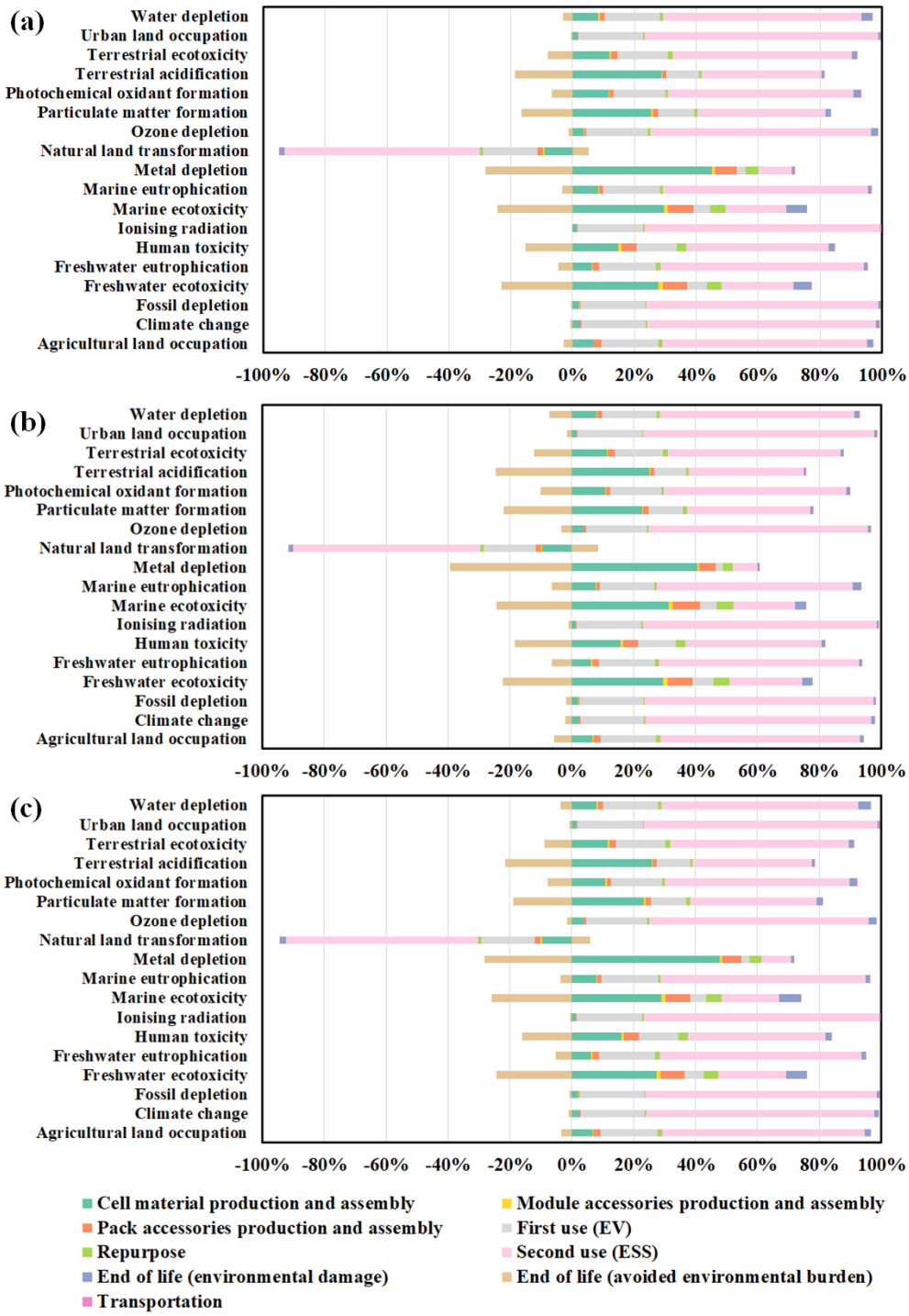

Figure 5. Full-spectrum environmental profiles for NMC622 LIBs subjected to second life and recycled by (a) hydrometallurgical recycling (b) direct cathode recycling (c) pyrometallurgical recycling on a percentage scale.

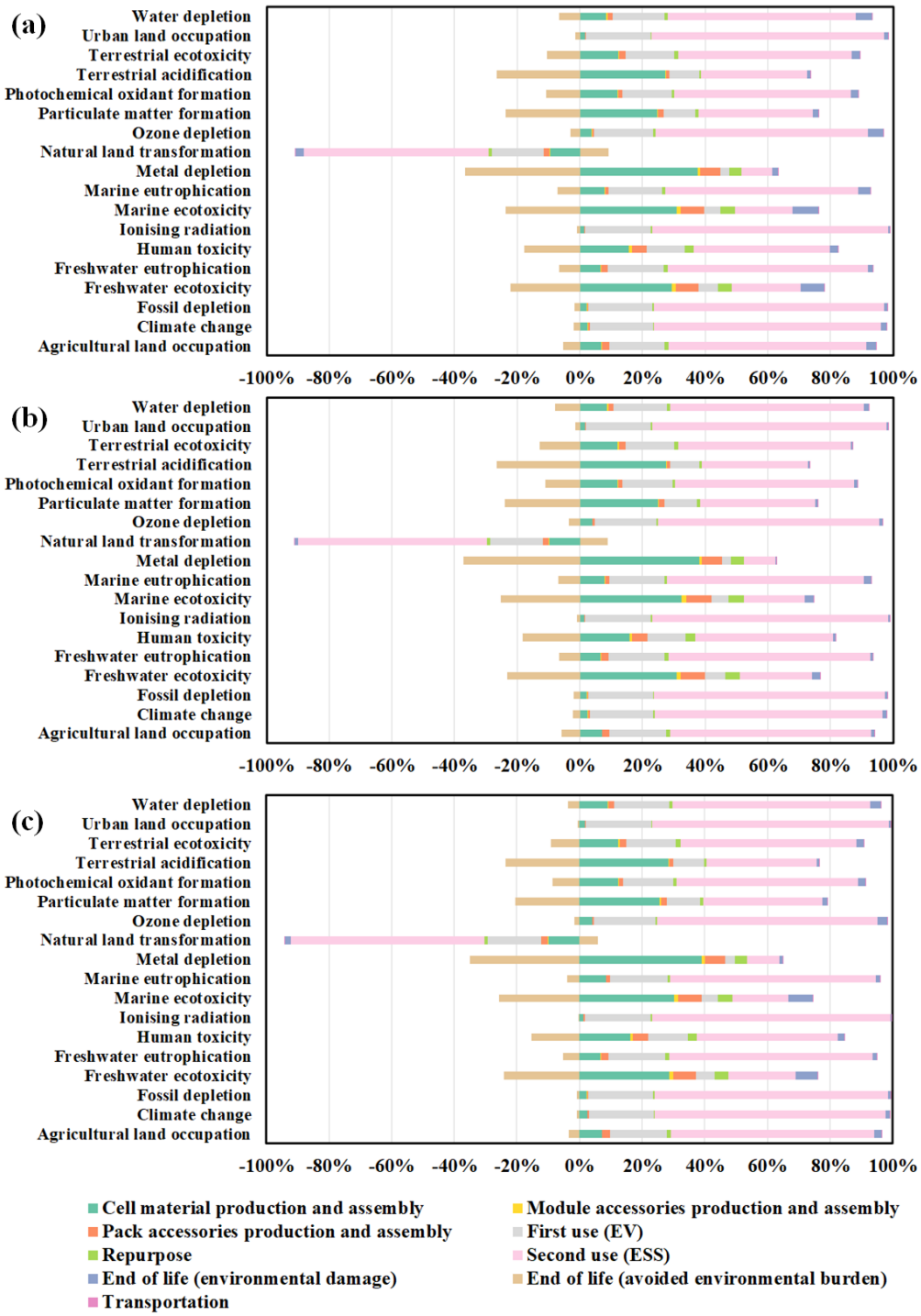

Figure 6. Full-spectrum environmental profiles for NCA LIBs subjected to second life and recycled by (a) hydrometallurgical recycling (b) direct cathode recycling (c) pyrometallurgical recycling on a percentage scale.

3.3 Potential of mitigating climate change and energy consumption

Carbon footprint and CED are two important metrics to evaluate the climate change mitigation potential and energy performance of introducing second life and recycling into batteries' life cycle.

Figure 7a and Figure 8a present the life cycle carbon footprint and CED of all types of LIBs with three recycling methods. Specifically, the average carbon footprint and CED of LFP LIBs without second life are around 2% more than that of the other types of LIBs. Generally, the life cycle carbon footprint and CED of LIBs with higher nickel content and lower cobalt content are lower. This can be attributed to the higher energy density of LIBs with higher nickel content, which requires less material and energy inputs and therefore contributes to a lower carbon footprint and CED. Also, the full material and energy recovery offsets the carbon- and energy-expensive production of high-nickel cathode active materials. The carbon footprint and CED of NMC811 with pyrometallurgical and direct cathode recycling are slightly higher than that of NMC622, mainly due to the employment of around twice the amount of polyvinylidene fluoride (PVDF) used in other LIBs. NCA has the highest nickel content, however, the usage of carbon- and energy-intensive HCl in hydrometallurgical and pyrometallurgical recycling of NCA, instead of H_2SO_4 used for other types of LIBs, leads to increases in both carbon footprint and CED.

Figure 7 shows that second life of retired automotive LIBs results in only moderate carbon mitigation potentials from the perspective of life cycle electricity delivery. Compared to the EV use only scenario, LFP, LMO+NMC532, all types of NMC, and NCA LIBs under the cascaded use scenario achieve 8% – 12%, 6%–11%, 6%–10%, and 6%–11% reduction in carbon footprint, respectively. The reductions in CED are less distinct: 6%–9% for LFP, 5%–7% for LMO+NMC532, 4 – 8% for all types of NMC, and 4%–8% for NCA. This suggests that while LIBs with high nickel content remain to be the less carbon- and energy-intensive ones, the adoption

of second life can pull down the higher carbon and energy burdens of the widely commercialized low-nickel or no-nickel LIBs such as LFP and LMO+NMC mixtures substantially to a level that is comparable to them. In other words, widely commercialized automotive LIB technologies are more carbon- and energy-intensive, and the adoption of second life can relieve their environmental burdens to a comparable level as those greener next-generation LIB technologies.

Due to the massive electricity delivery during the use phase and relatively carbon-intensive electricity production of Texas power grid, cascaded use accounts for a high share in both life cycle carbon footprint) and CED (on average 96% for LFP, 97% for LMO+NMC532, 97% for NMC622 and 97% for NCA). Therefore, the potential for mitigating climate change and energy demand is hindered. Moreover, the EOL phase becomes the second leading contributor to carbon footprint and CED. The comparative results of EOL-related carbon footprint are specific to battery chemistry. Among the three EOL scenarios, direct cathode recycling remains the least carbon-and energy-intensive for all LIBs. Notably, both pyrometallurgical recycling of LMO+NMC532 LIBs and hydrometallurgical recycling of LFP LIBs result in a net positive carbon footprint and CED, mainly due to the adoption of carbon-intensive (or energy-intensive) materials and processes and recovery of relatively less carbon-intensive (or energy-intensive) materials. In addition, hydrometallurgical recycling of LMO+NMC532 LIBs, and pyrometallurgical recycling of NMC622 and NCA LIBs are energy-saving, though they all result in nonnegligible carbon burdens. In other cases of battery recycling, a considerable amount of carbon footprint and CED are avoided by LIBs recycling.

Advanced LIB technologies with high specific energy density do not necessarily demonstrate the better potential of mitigating climate change and energy demand, particularly when the material and energy inputs for the LIB production are highly carbon- and energy-intensive. The

development of green recycling processes with higher material recovery rates, lower energy requirement, and utilization of less environmentally expensive materials, is impactful in improving the potential of mitigating environmental impacts. Moreover, their potentials of mitigating climate change and energy demand are confined by the cleanliness of the local power grid. Therefore, it is essential to penetrate the local power grid with more renewable energy sources. In the next sections, we will discuss how and to what extent we can further reduce the carbon footprint and CED of all types of LIBs with different recycling methods.

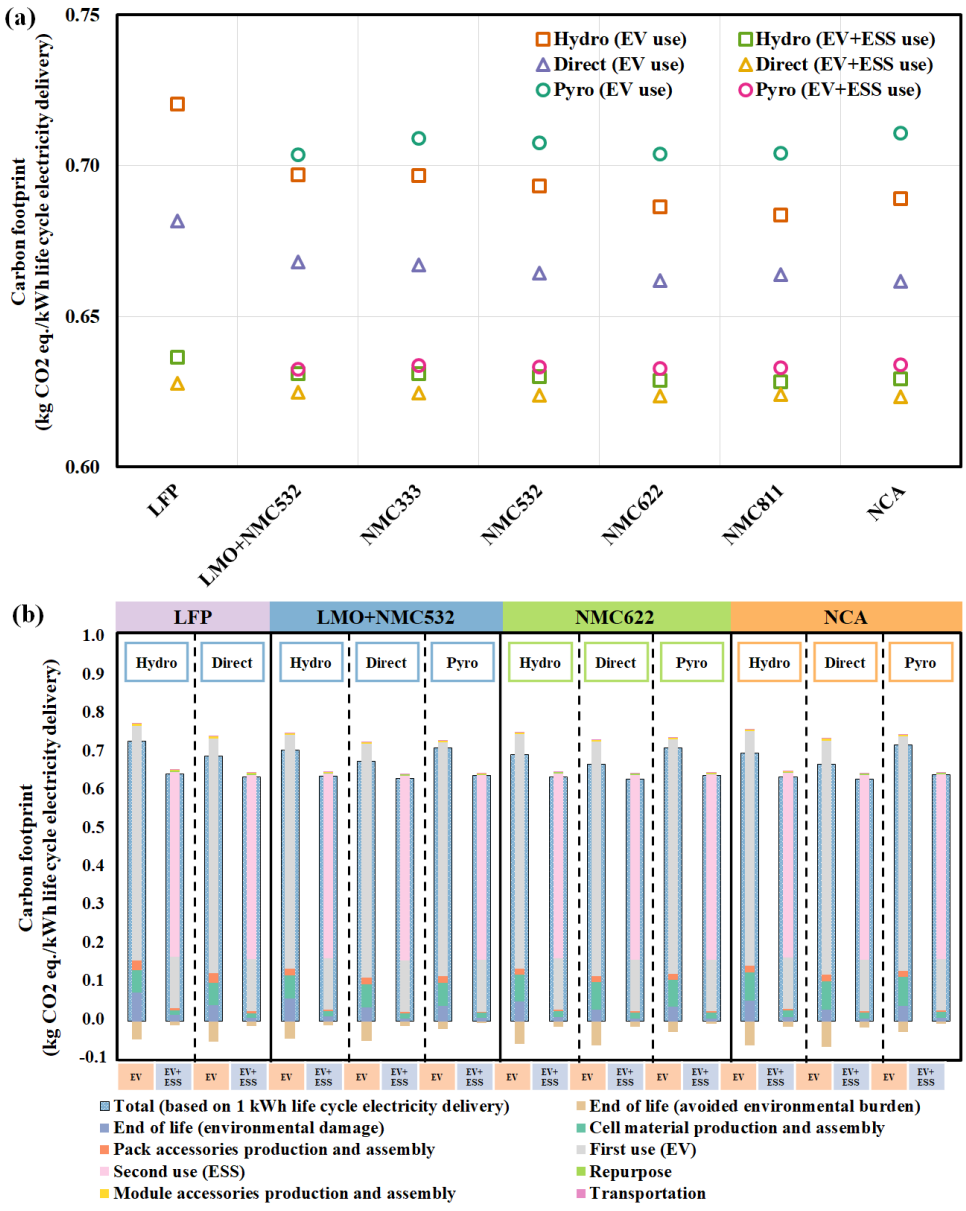

Figure 7. (a) Life cycle carbon footprint of LFP, LMO+NMC532, NMC333, NMC532, NMC622, NMC811, and NCA LIBs with different EOL scenarios. (b) Breakdowns of the carbon footprint for LFP, LMO+NMC532, NMC622, and NCA LIBs with different EOL scenarios. The stacked bar plot represents the breakdowns of carbon footprint per kWh life-cycle electricity delivered to the stage level. Different colors indicate different stages throughout LIB's life cycle as stated in the legend. The hydrometallurgical, direct cathode, and pyrometallurgical recycling are abbreviated as hydro, direct, and pyro.

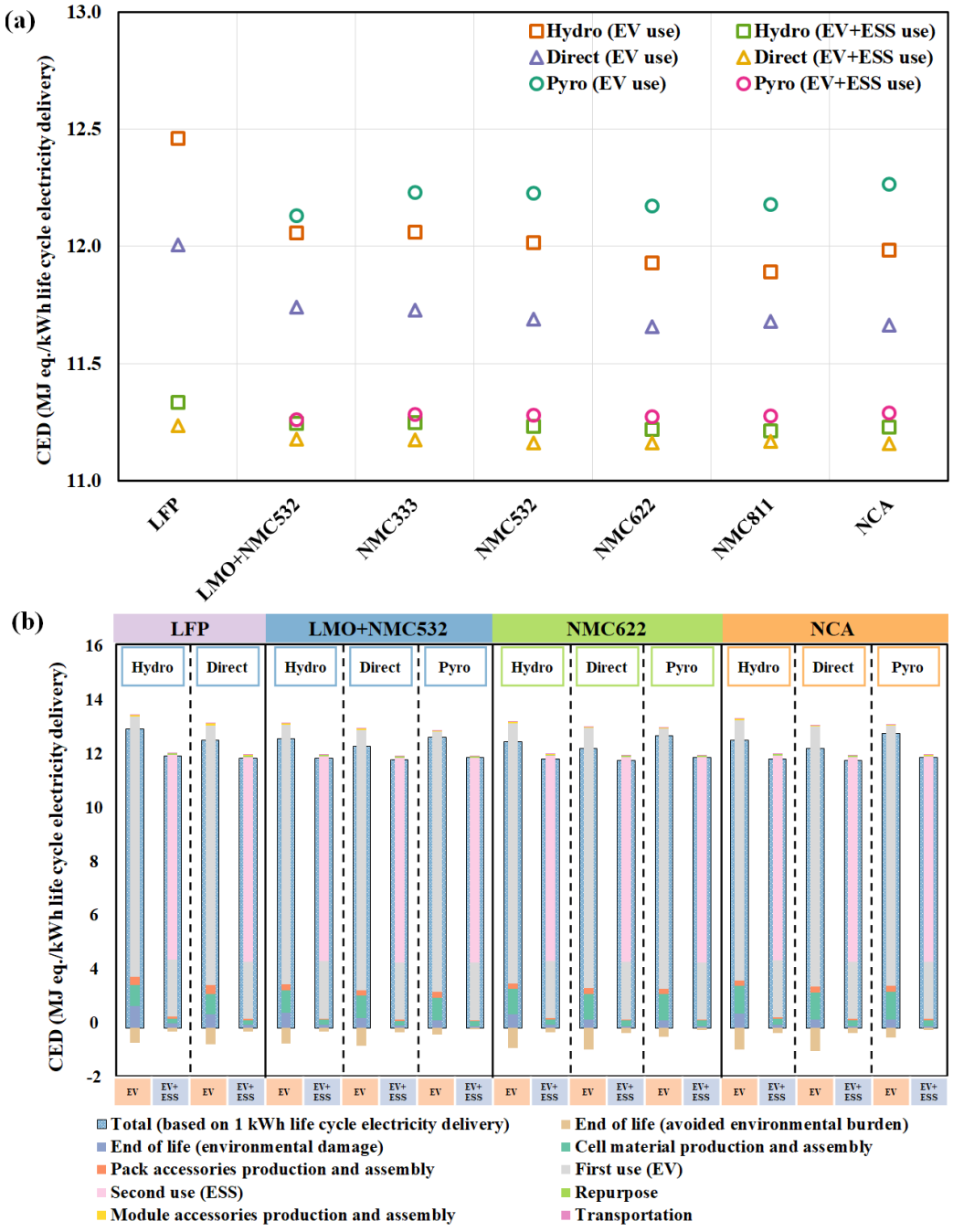

Figure 8. (a) Life cycle CED of LFP, LMO+NMC532, NMC333, NMC532, NMC622, NMC811, and NCA LIBs with different EOL scenarios. (b) Breakdowns of the carbon footprint for LFP, LMO+NMC532, NMC622, and NCA LIBs with different EOL scenarios.

3.4 Environmental hotspots

Impacts of different life cycle stages of reused automotive LIBs on carbon footprint and CED have been explicated in the previous section. To further decipher environmental hotspots embedded in each stage, sunburst charts representing hierarchical results of carbon footprint and CED are depicted in Figure 9–Figure 14. Sunburst charts reveal the contributions of lower-level processes within upper-level life cycle stages. Absolute values of the negative carbon footprint and CED resulted from EOL steps with avoided environmental burden are used for comparison between different life cycle stages. In addition, the use phase is identified as an overriding life cycle stage in terms of carbon footprint and CED, so it is not discussed in this section.

For the cell materials production and assembly stage, cathode active material is the predominant factor that contributes to more than half of the carbon footprint for LMO+NMC532 (62%), NMC622 (68%), and NCA LIBs (69%). On the contrary, LFP production accounts for only 42% of the carbon footprint associated with this stage. This contrast can be attributed to the high climate change footprint associated with $NiSO_4$ and $CoSO_4$ production, high heat and energy demand, and heavy use of the precipitant (NaOH) during the NCM and NCA production.

Battery management system (BMS) production is the main contributor to the carbon footprint of LIB pack accessories production. Production of BMS and other pack accessories, including compression plates and straps, module interconnects and a tri-layer jacket, together are responsible for nearly all of the carbon footprint associated with this stage. The dominant role of BMS and other pack accessories can be attributed to the production of printed wiring boards and aluminum-made outer and inner layer of the battery jackets, respectively.

The roles of EOL steps in carbon footprint depends on the battery chemistry and the specificities of EOL scenarios. First, EOL steps of material and energy recovery during

hydrometallurgical and direct cathode recycling reduce slightly less carbon footprint than the amount added by the cell materials production and assembly stage. On the contrary, material recovery of pyrometallurgical recycling reduces substantially less carbon footprint. Pyrometallurgical recycling is deficient in material recovery since it retrieves nickel as $Ni(OH)_2$ and recovers cobalt in the form of ionic solutions. Moreover, it does not recover cyclable lithium and aluminum. Specifically, in descending order, recovery of cathode active material, aluminum, and $LiPF_6$ constitute the vast majority of carbon footprint reduced by direct cathode recycling; recovery of cathode active material and aluminum dominate the carbon footprint reduction for hydrometallurgical recycling; $Ni(OH)_2$ recovery of pyrometallurgical recycling is the major source to reduce carbon footprint. Second, EOL steps of hydrometallurgical and direct cathode recycling, which emit greenhouse gas emissions, consume materials and deplete energy, produce less greenhouse gas emissions compared to their EOL steps of material and energy recovery. Among these greenhouse gas emitting steps, waste sludge treatment is the most influential one for both hydrometallurgical and pyrometallurgical recycling. This is because they both adopt hydrometallurgical steps, such as leaching, solvent extraction, and precipitation, that eventually discharge a large amount of waste solvent sludge. Instead, liquid CO_2, which consumes plenty of electricity, is much more energy-intensive than other energy-consuming EOL steps for direct cathode recycling. Moreover, graphite combustion remains one of the most influential steps for all three recycling methods, which suggests a need to suppress graphite combustion to further mitigate carbon footprint. Soaking and recovery of the binder solvent NMP is also a major carbon footprint and CED contributor common for both hydrometallurgical and direct cathode recycling. This can be mainly attributed to the need for steam and wastewater treatment for NMP recovery. To further reduce the carbon footprint and CED of battery recycling, especially for hydrometallurgical and

direct cathode recycling, research, and development on skipping the step of binder solvent recovery is highly recommended. Last, according to the battery chemistry, different leaching agents and precipitants with a variety of reaction conditions are selected to recover the cathode active materials for hydrometallurgical and pyrometallurgical recycling, resulting in multiple levels of carbon burden. It is worth mentioning that their contributions to the carbon footprint and CED are relatively comparable, and none of these EOL steps are dominant to the carbon footprint and CED of this stage.

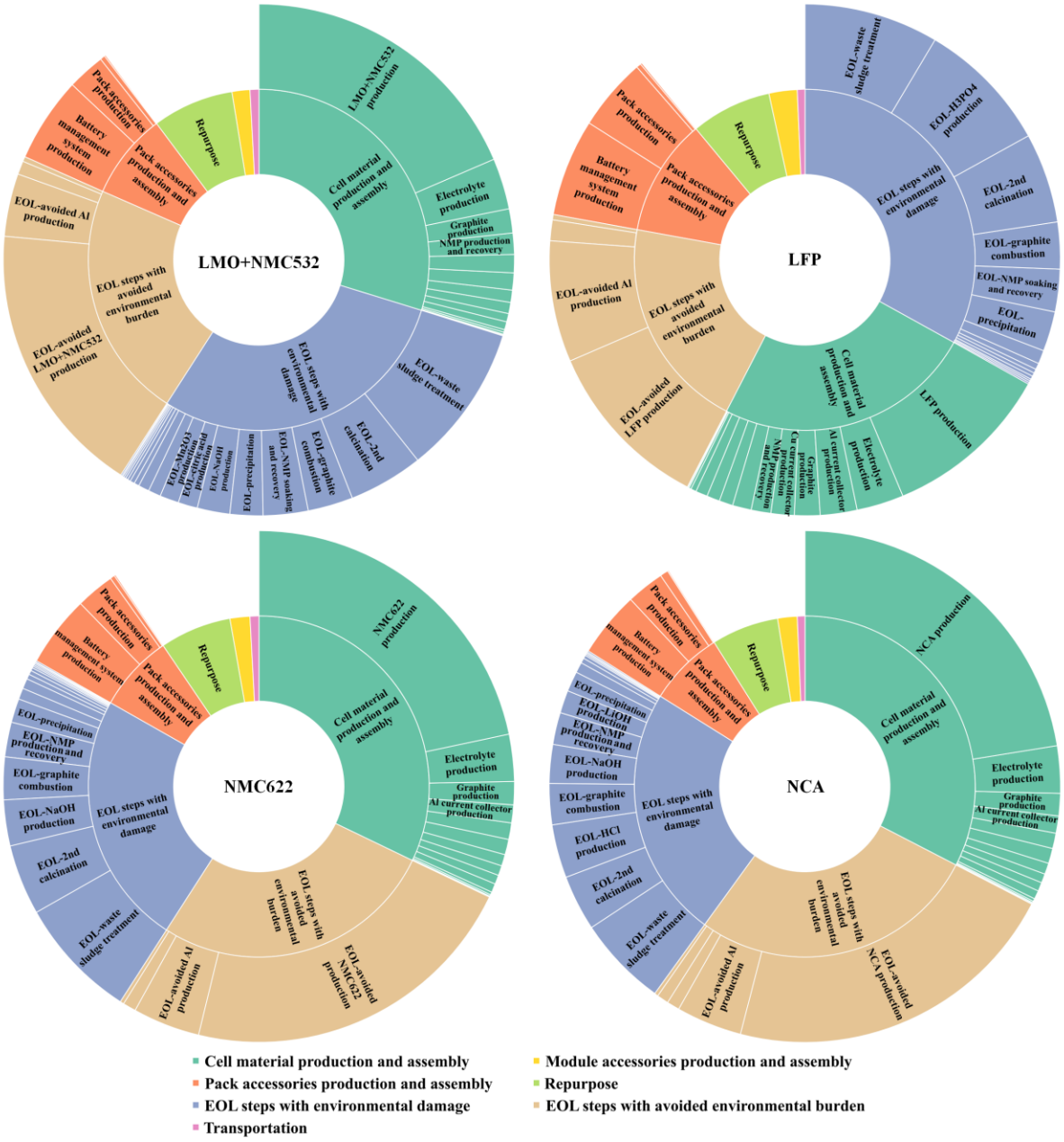

Figure 9. Carbon footprint hotspots of LFP, LMO+NMC532, NMC622, and NCA LIBs with hydrometallurgical recycling. The surrounding sunburst charts represent hierarchical results of the carbon footprint from the life-cycle stages to the process level. The inner circle represents the upper-level stages, while the outer circle represents the lower-level processes of each stage. The colors of stages and their corresponding processes are consistent, and the value of each process and stage is proportional to the angle of concentric circles. Moreover, starting from the top, the shares of the carbon footprint for stages become smaller in a clockwise order; within each stage, the shares of the carbon footprint for lower-level processes become smaller in the same manner.

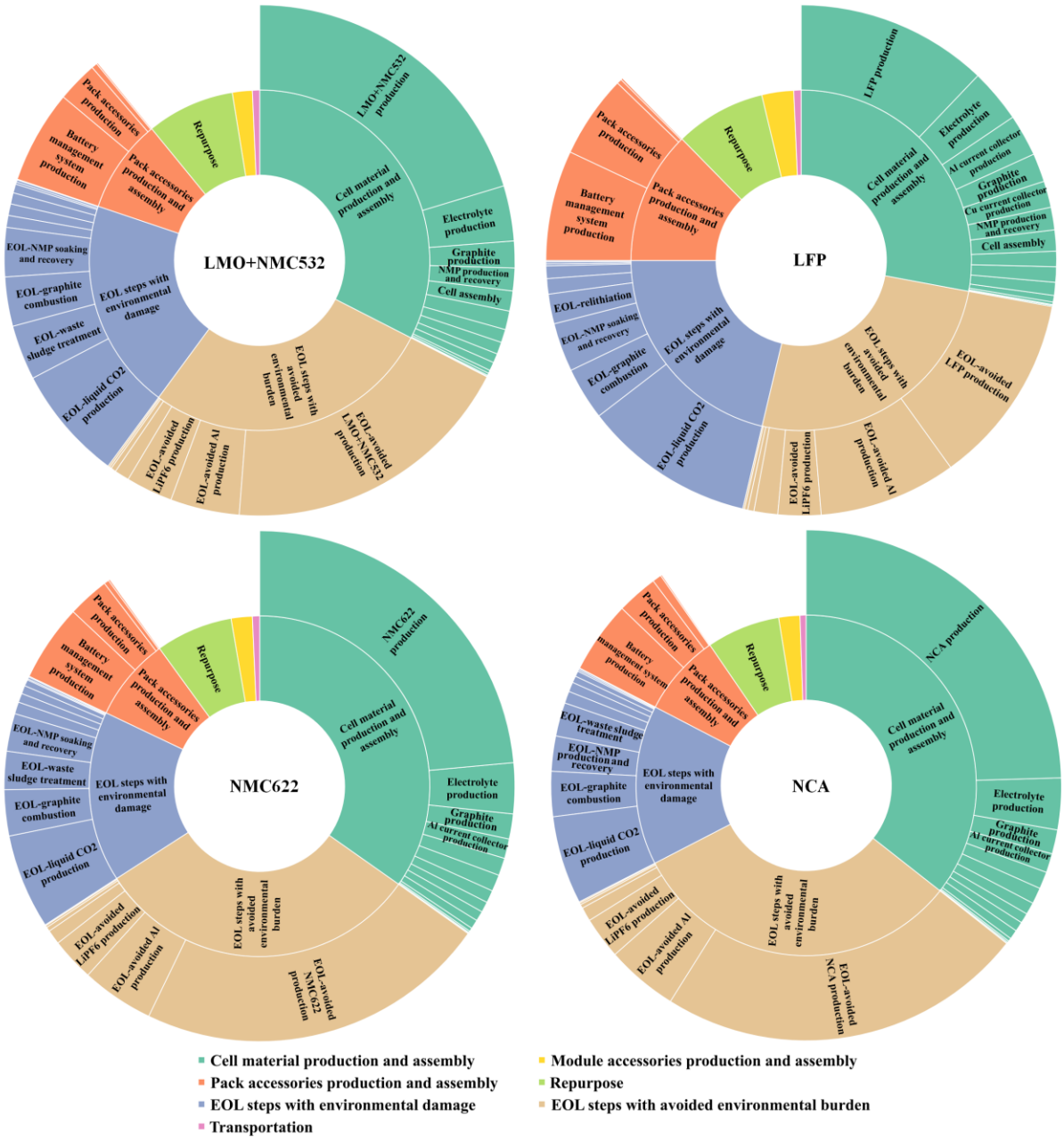

Figure 10. Carbon footprint hotspots of LFP, LMO+NMC532, NMC622, and NCA LIBs with direct cathode recycling.

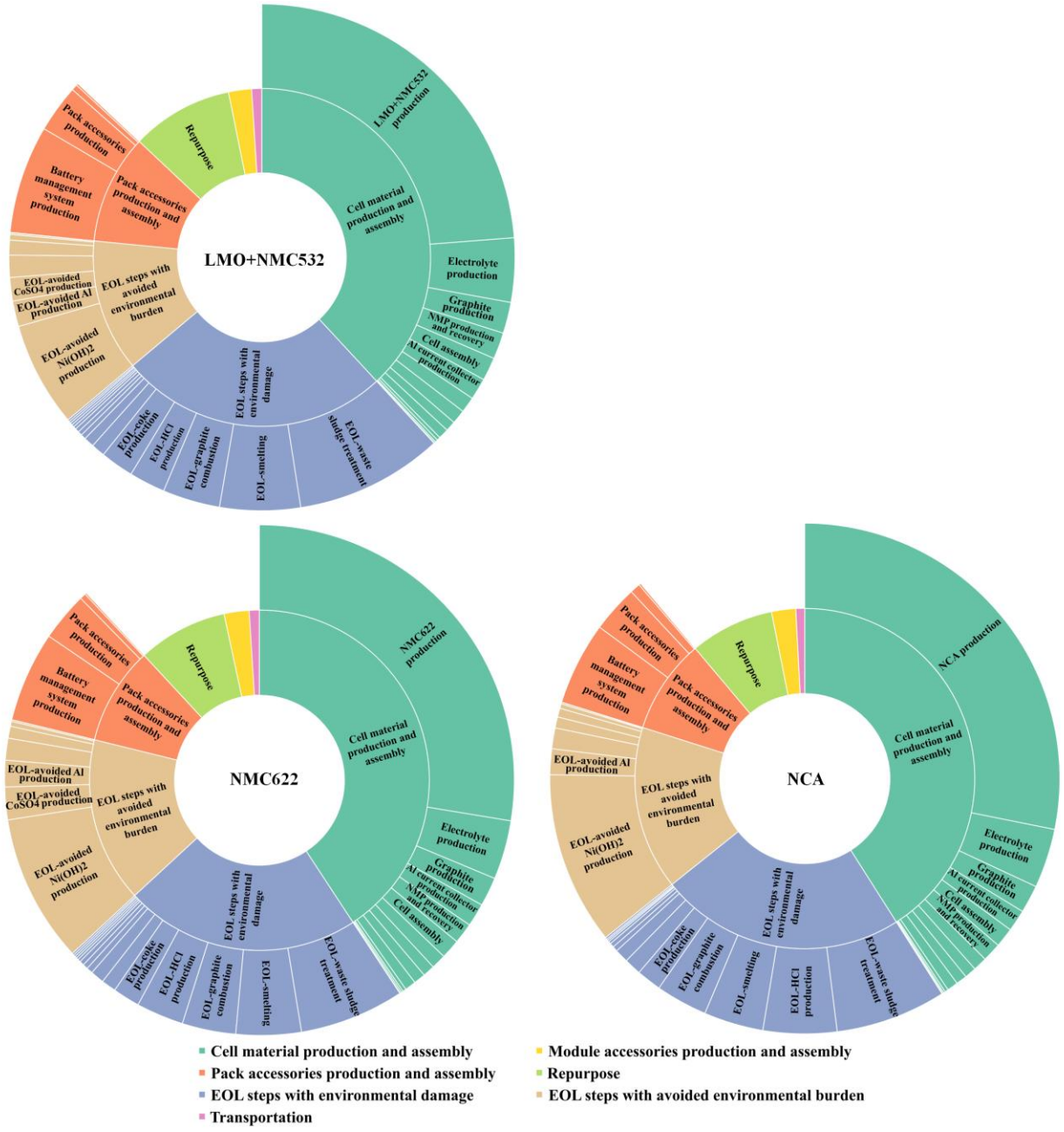

Figure 11. Carbon footprint hotspots of LFP, LMO+NMC532, NMC622, and NCA LIBs with pyrometallurgical recycling.

Figure 12. Energy hotspots of LFP, LMO+NMC532, NMC622, and NCA LIBs with hydrometallurgical recycling.

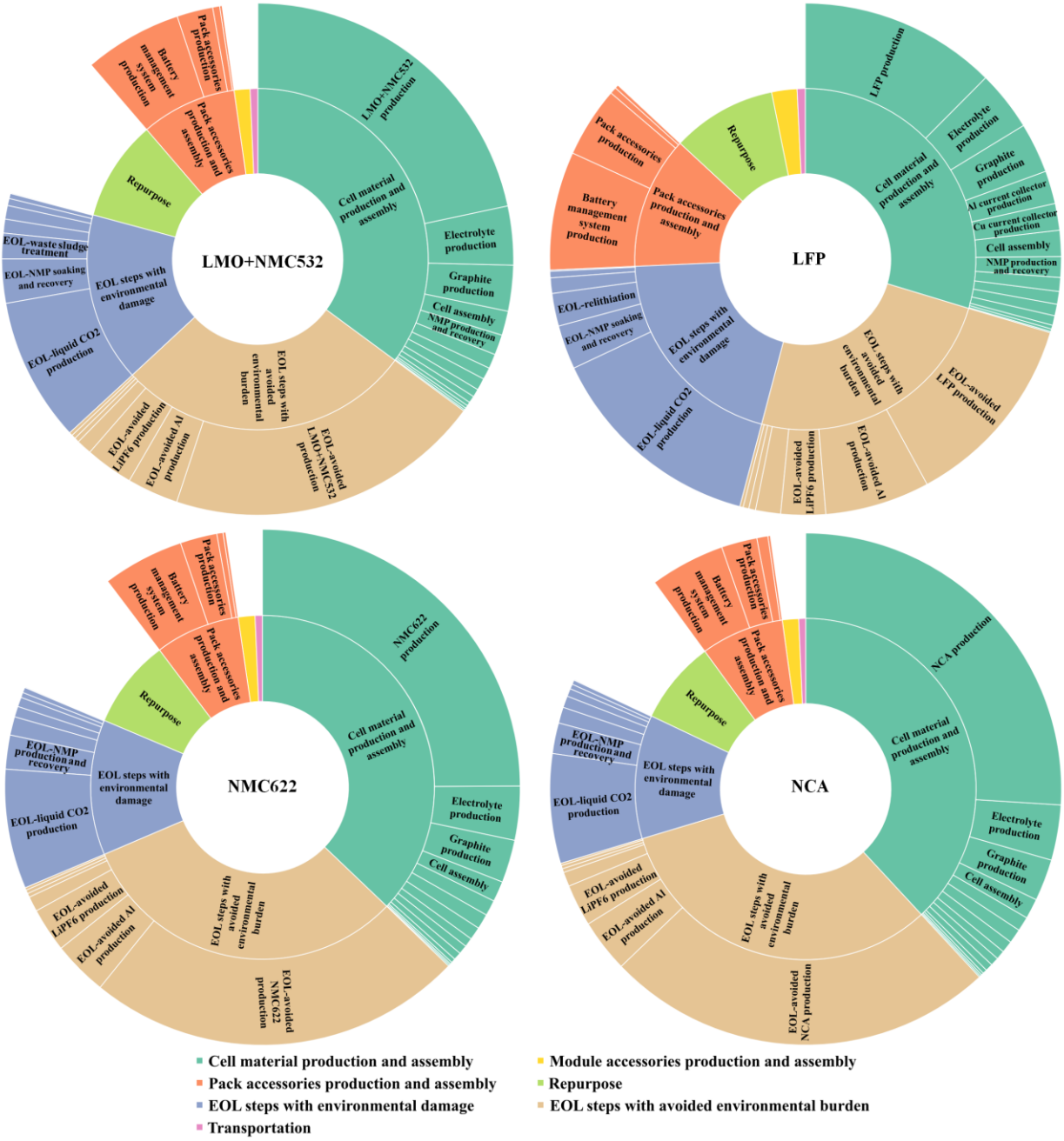

Figure 13. Energy hotspots of LFP, LMO+NMC532, NMC622, and NCA LIBs with direct cathode recycling.

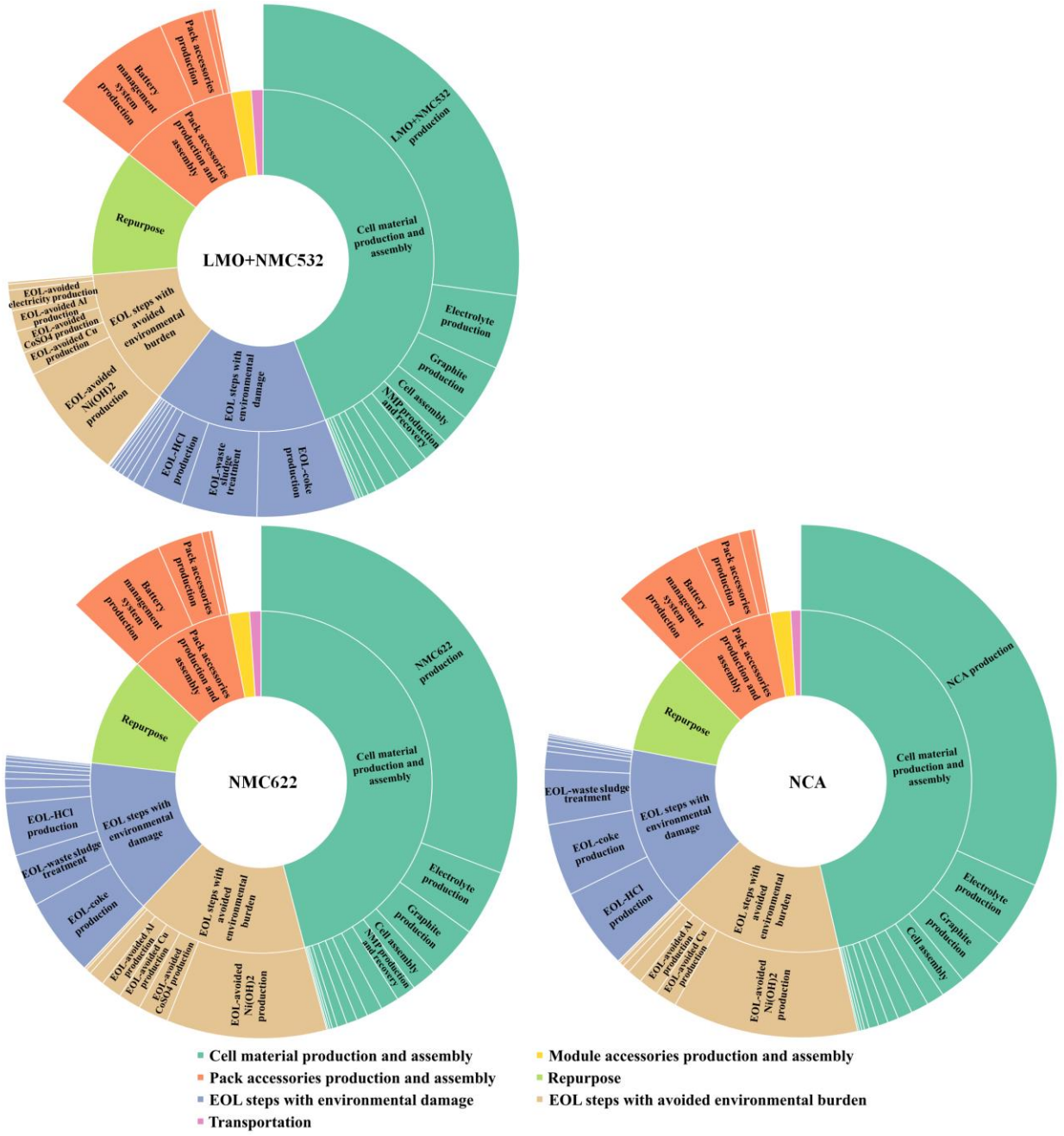

Figure 14. Energy hotspots of LMO+NMC532, NMC622, and NCA LIBs with hydrometallurgical recycling.

To explicitly identify the environmental hotspots across the full spectrum of impact categories, we aggregate the normalized LCI data to process-level and visualize them using a heat map as shown in Figure 15–Figure 17.

We can observe that for all types of LIBs, recovery of cathode active material, $Ni(OH)_2$, and metals are major contributors to alleviate environmental impacts. Notably, LFP, LMO+NMC532, and $Ni(OH)_2$ recovery are not as environmentally valuable as NMC and NCA recovery in all environmental impact categories, suggesting that the attempts to recover NMC and NCA are more important in battery recycling. $LiPF_6$ recovery of direct cathode recycling is another moderate contributor to reduce environmental impacts from the categories of agricultural land occupation, climate change, fossil depletion, ionizing radiation, marine eutrophication, ozone depletion, terrestrial ecotoxicity, and water depletion. The result also suggests that the cathode active material production is the major contributor to environmental impacts.

Environmental hotspots are specific to recycling methods. For both hydrometallurgical and pyrometallurgical recycling of LMO+NMC532, NMC, and NCA, the production of leaching agent and precipitant are more impactful in contributing to ozone depletion, terrestrial ecotoxicity, and water depletion than to other impact categories. However, for hydrometallurgical recycling of LFP, production of H_3PO_4 as a leaching agent accounts for more than 20% of life cycle metal depletion and water depletion. Due to massive electricity usage, liquid CO_2 production of direct cathode recycling contributes to 35% – 50%, 51%–63%, 75%–84%, 39%–53%, and 48% – 74% of climate change, fossil depletion, ionizing radiation, ozone depletion, and urban land occupation associated with the EOL steps causing environmental damages, respectively.

Notably, environmental hotspots are not always extensively distributed across the category list. For example, copper recovery is not comparable with aluminum recovery in terms of climate

change and fossil depletion. However, copper recovery can largely reduce environmental impacts through the categories of freshwater ecotoxicity, freshwater eutrophication, human toxicity, marine ecotoxicity, metal depletion, and terrestrial ecotoxicity; In addition to fossil depletion, aluminum recovery leads to much environmental burden on freshwater and marine ecotoxicity; NMP soaking and recovery makes a minor contribution to most of the impact categories but contributes to a large portion of the marine eutrophication.

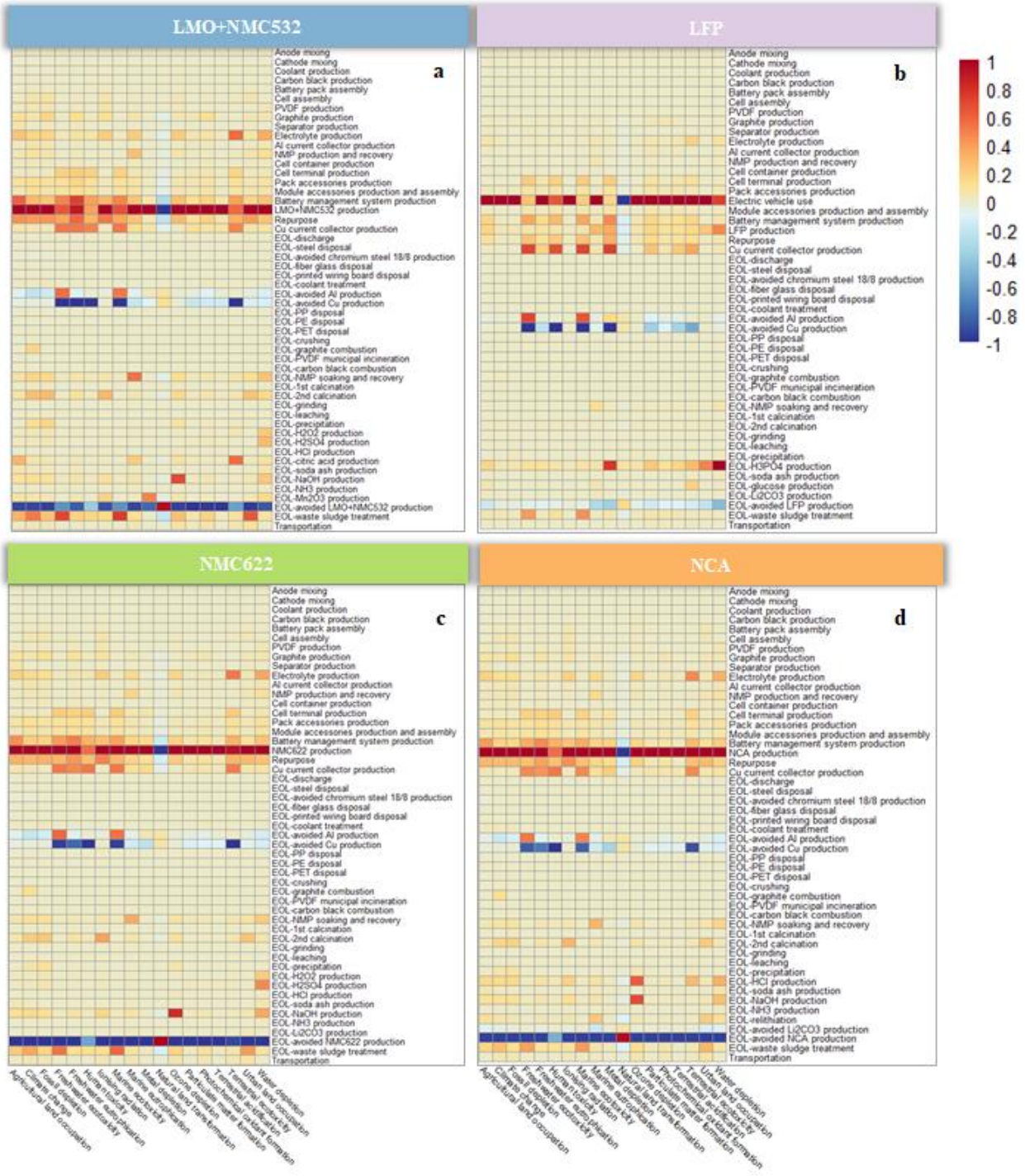

Figure 15. Full-spectrum environmental hotspots for LFP, LMO+NMC532, NMC622, and NCA LIBs with hydrometallurgical recycling. Use phases are excluded from the system boundary. Colors represent values corresponding to the environmental impacts of each process under each impact category. The values are normalized using the min-max normalization method and vary according to the colors presented on the color bar. In particular, red color represents positive values

and suggests damage to the environment; blue color represents negative values and indicates an avoidance of environmental burden. Moreover, the darker color along each column implies more environmental impacts on the corresponding impact category.

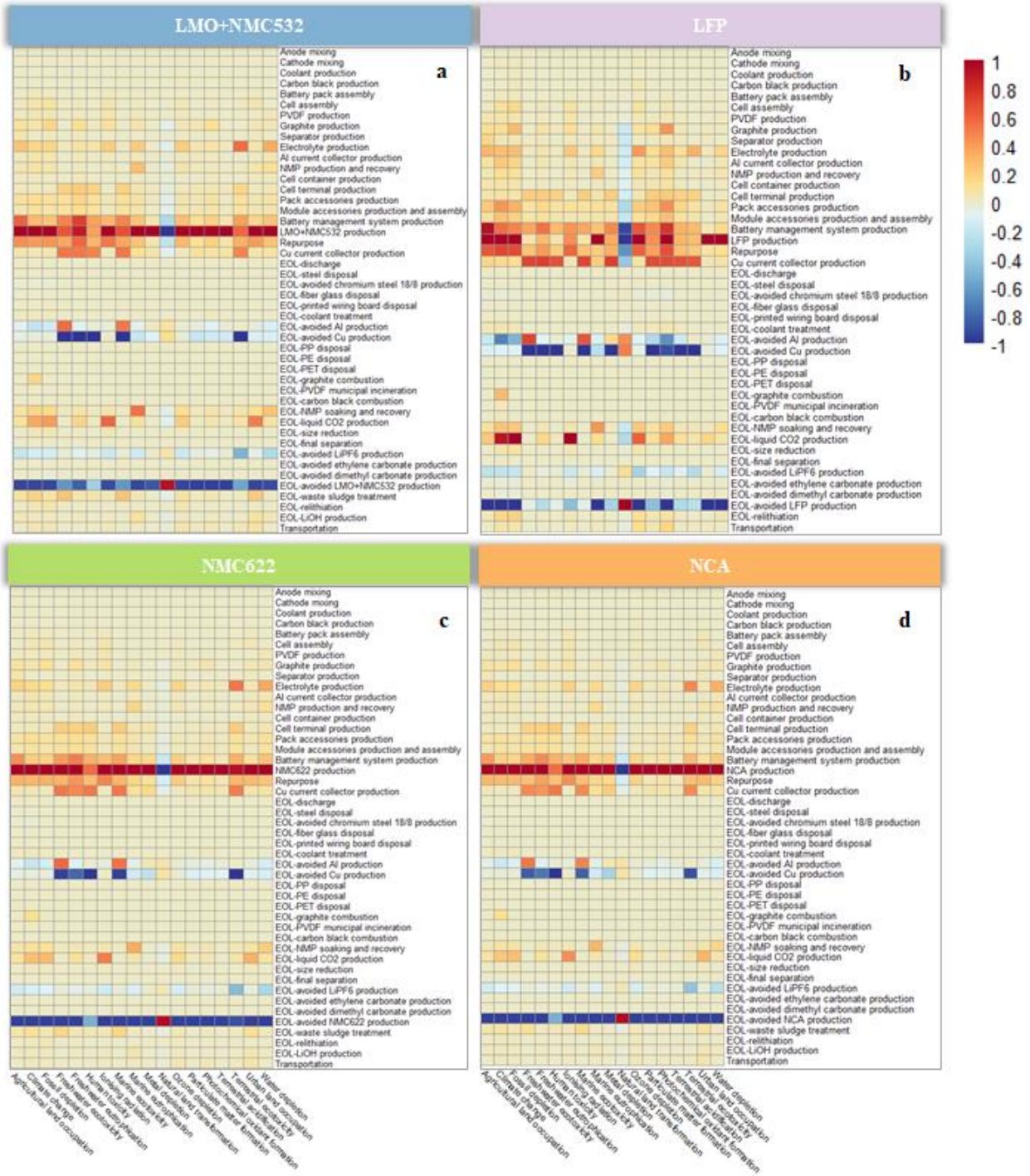

Figure 16. Full-spectral environmental profiles for LFP, LMO+NMC532, NMC622, and NCA

LIBs with direct cathode recycling. Use phases are excluded from the system boundary. Colors represent values corresponding to the environmental impacts of each process under each impact category.

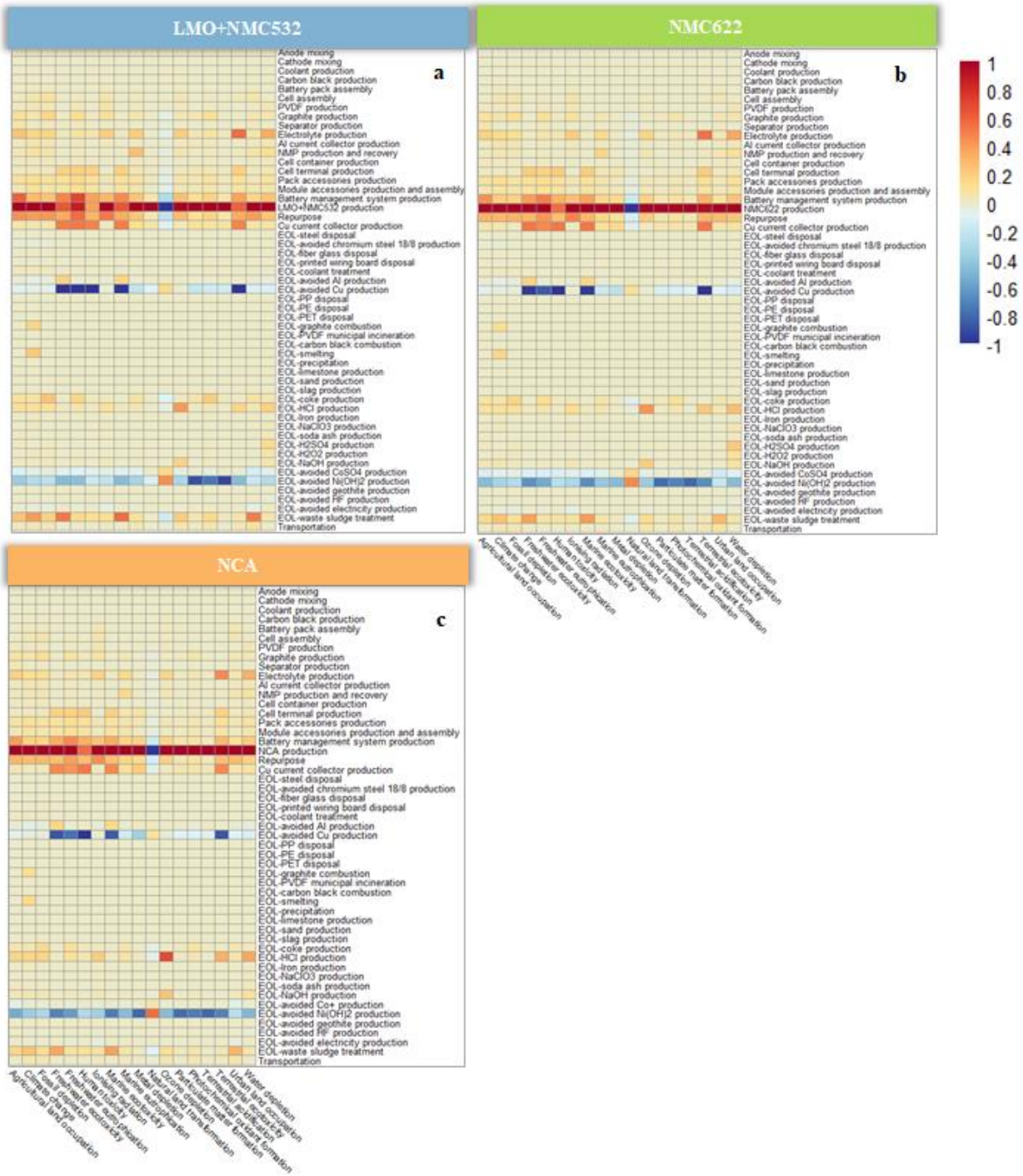

Figure 17. Full-spectral environmental profiles for LMO+NMC532, NMC622, and NCA LIBs

with pyrometallurgical recycling. Use phases are excluded from the system boundary. Colors represent values corresponding to the environmental impacts of each process under each impact category.

3.5 Temporal and geographical variability

Previous results have shown that environmental impacts associated with the use phase are overwhelming and unavoidable. Since electricity consumption is the only process in the use phase that causes damages to the environment, the key action to minimize environmental impacts of the use phase is to make the electricity generation more sustainable and environmentally friendly. To test the sensitivity of LIB's environmental performance to the temporal and spatial variability of electricity generation, we adopt the projection of electricity generation from 2020 to 2050 from the U.S. Energy Information Administration (EIA) and calculate the environmental impacts accordingly.[49,50] The U.S. and China are selected for this sensitivity analyses, because these two countries have the most manufacturing capacity of automotive LIBs in the Eastern and Western Hemisphere, respectively.[53]

Figure 18 demonstrates the results of sensitivity analyses for the LFP, LMO+NMC532, NMC622, and NCA LIBs. Compared to the electricity generation in 2020, we obtain 16%and 27% greenhouse gas emission reduction in 2050 for LIBs produced, consumed, and recycled in the U.S. and China, respectively. This difference in carbon mitigation potential is attributed to the critical difference in energy sources of electricity generation in 2020 for the U.S. and China. To be specific, coal, which is relatively carbon-intensive, accounts for 62% of electricity generation in China in 2020, and it will decrease to 30% in 2050 by projection.[50] On the contrary, coal-fired power generation only accounts for 24% of the total electricity production in the U.S. in 2020, and it will decrease to 12% in 2050.[49] The share of renewable sources in China will increase substantially from 36% in 2020 to 63% in 2050. Similarly, the share of renewable sources in the U.S. increases

from 40% to 56% during 2020–2050. This suggests that for regions without a strong penetration of renewables in the power grid, energy systems decarbonization has a great potential to substantially cut down LIB's life cycle carbon footprint. In fact, natural gas, which is a relatively clean energy source, will remain the leading energy source in the U.S. for the next three decades accounting for 38% to 32% of the electricity generation from 2020 to 2050 according to EIA's projection.[49] Although electricity generation in China shows greater carbon mitigation potential in the next three decades, the life cycle carbon footprint of LIBs produced, consumed, and recycled in China would remain to be higher than that in the U.S. during the period of 2020–2050. Similar results has been found in a previous study that compares the well-to-wheel carbon footprint of EV between China and U.S.'s power grid in 2015 and 2030, despite the carbon footprint estimated from the projection of China's power grid in 2030 by the United States Environmental Protection Agency (USEPA) in this study is around 9% lower than provided in this previous study.[54]

Nevertheless, in terms of CED, we obtain an 8% reduction for LIBs in the U.S and a 6% reduction for LIBs in China during the period of 2020–2050. The results show that LIBs produced, consumed, and recycled in China lead to more energy-saving than those in the U.S. for the next three decades. This is mainly attributed to the higher CED required for coal-fired electricity production in the U.S. CED of generating 1 kWh electricity is directly related to the energy efficiency of the power plants. Existing studies and government data suggest that the average energy efficiency of China's coal-fired power plants surpasses the average energy efficiency of coal-fired power plants in the U.S.[55-57] While the average energy efficiency of other energy sources, including petroleum, natural gas, wind, geothermal, solar photovoltaic, and hydroelectric, in the U.S. are higher than those in China, the resulting decrease in CED cannot offset the increase in CED. As a consequence, the CED for average electricity generation in the U.S. is higher than that

in China.

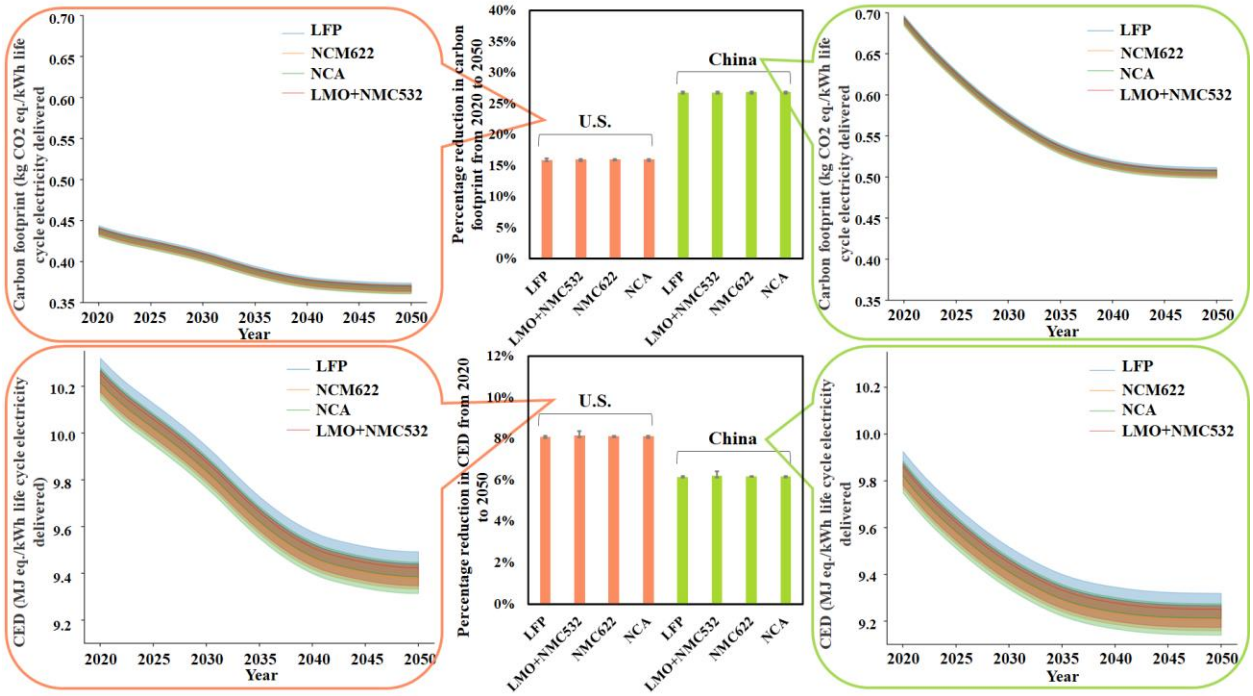

Figure 18. Sensitivity analyses of temporal and spatial variation in electricity generation from the Year 2020 to 2050 in the United State and China.

3.6 Economic benefits of battery second life

To assess the economic benefits of introducing second life to LIB's life cycle, the life cycle costs (costs associated with production, use phase, and recycling are considered) of LFP, LMO+NMC532, NMC622, and NCA LIBs under the two use scenarios are presented and compared in Figure 19. Among all types of LIBs, LFP demonstrates the worst economic performance (on average 37 and 14 cents per kWh life cycle electricity delivery for EV use scenario and cascaded use scenario, respectively). This can be attributed to both its high production cost and its high recycling cost. Despite the lowest cathode active material price ($14/kg versus $15 – 22 per kg for other types of cathode active materials), the inferior specific energy density causes increases in both production and recycling costs due to more demand for materials and

energy. Moreover, relithiation of LFP during direct cathode recycling requires doping with new LFP at the ratio of 3:7, which leads to a substantially higher recycling cost (nearly double other LIB's cost of direct cathode recycling).

As the assumed annual throughput of LIB production and recycling are on the energy storage capacity basis, the weight-based annual capacities for LIBs with higher specific energy density are lower. Due to the economies of scale, an economic advantage can be gained by LIBs with lower specific energy density. On the contrary, LIBs with lower specific energy density could also acquire an economic disadvantage due to the requirement of more material and energy inputs for LIB production on the basis of 1 kWh energy storage capacity. Generally, LIBs with higher nickel content demonstrate better economic performance (i.e. lower life cycle costs). An exception is the LMO+NMC532: Since LMO contains no nickel and cobalt, which can be recovered from the alloy through downstream leaching and precipitation after smelting, less leaching agents and precipitants are required for pyrometallurgical recycling. In combination with the lower production cost of LMO+NMC532, which benefited from the low LMO price ($10/kg), LMO+NMC532 with pyrometallurgical recycling exhibits the lowest life cycle cost; The low production cost of LMO+NMC532 also results in a relatively low life cycle cost for LMO+NMC532 with direct cathode recycling; however, due to the heavy usage of expensive materials such as citric acid and Mn_2O_3, LMO+NMC532 with hydrometallurgical recycling exhibits the higher life cycle cost than other investigated LIBs with hydrometallurgical recycling.

If repurposing and second life are considered, all types of LIBs can achieve a reduction of around 60% in the life cycle costs. Figure 19b also shows that the heterogeneity between different types of LIBs and different recycling methods become less.

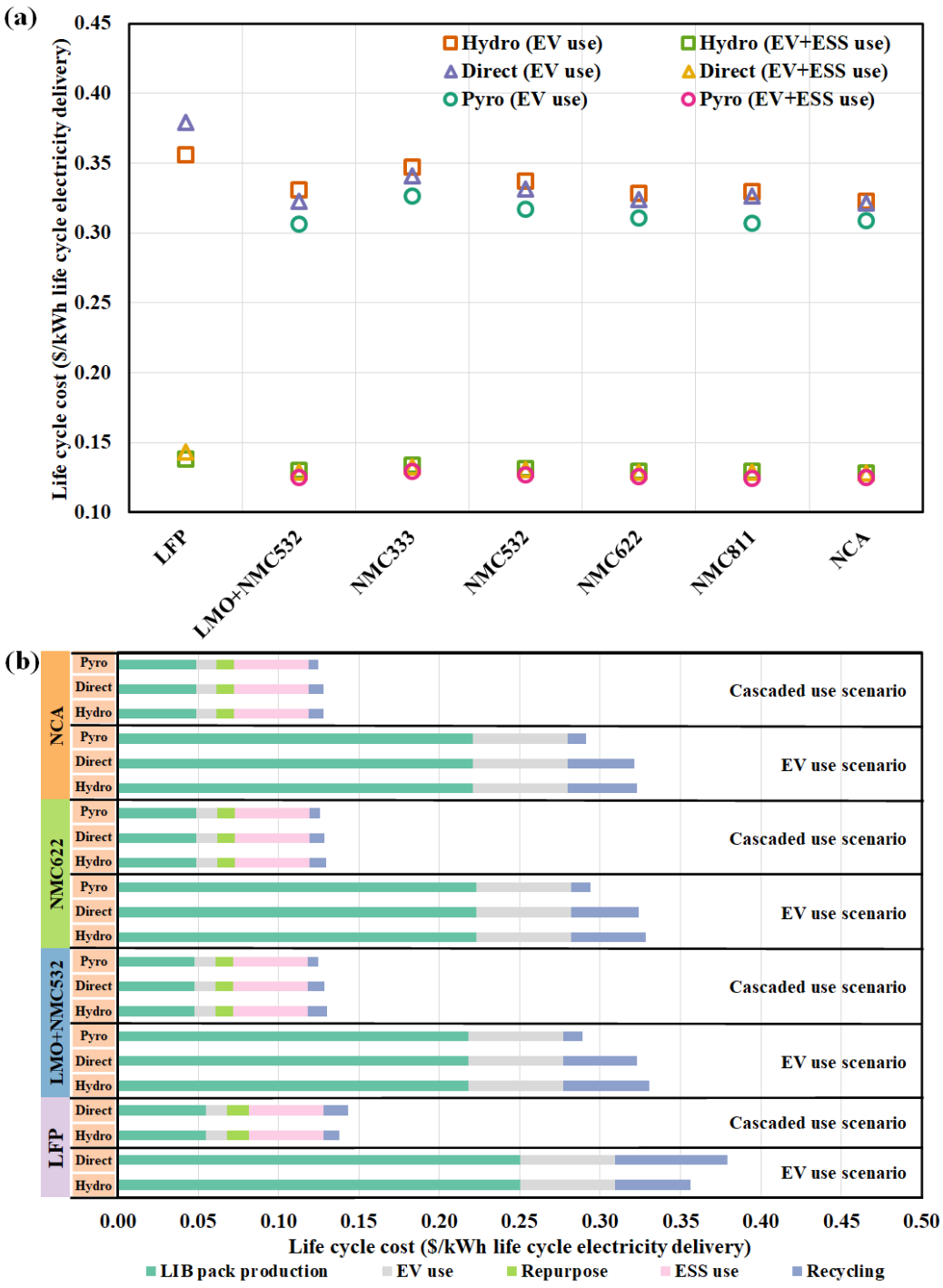

Figure 19. (a) Life cycle cost of LFP, LMO+NMC532, NMC333, NMC532, NMC622, NMC811, and NCA LIBs with different EOL scenarios. (b) Breakdowns of the life cycle costs for LFP, LMO+NMC532, NMC622, and NCA LIBs with different EOL scenarios.

CHAPTER 4

CONCLUSIONS

4.1. Conclusions

In this work, we studied the energy and environmental sustainability of second life and recycling for three types of LIBs, using a "cradle-to-cradle" LCA. Compared to the nickel-free LFP LIBs, the nickel-rich NMC and NCA LIBs with higher specific energy density perform better in terms of carbon footprint and CED, if the second life approach is not adopted. With second life, 6% – 9% of carbon footprint and 4%–8% of CED can be reduced by the high-nickel NMC and NCA, while 8% – 12% and 6%–9% reduction in carbon footprint and CED can be achieved by the widely used LFP, respectively. All types of LIBs can achieve a reduction of around 60% in the life cycle costs. With second life, the heterogeneity between different types of LIBs and different recycling methods become less obvious in terms of both environmental and economic performances. In terms of LIB recycling, direct cathode recycling was identified as the most competitive technology of future LIB recycling due to its favorable environmental performance and moderate economic performance. LIB's potential of mitigating carbon footprint and CED are largely restricted by the cleanliness of the local power grid. With the transition towards more than 50% penetration of renewable energy sources, 16% and 27% of carbon footprint can be achieved by the electricity mix in the U.S. and China, respectively.

4.2 Insights to bench work, industry and policymakers

Towards the urgent need of prolonging the driving-range of EV, the nickel-rich cathode is at the forefront of achieving higher energy density and reducing the supply risk of cobalt.[58,59] Previous studies showed that the increase of nickel content would trigger severe capacity fading

and thermal safety hazards.[60] Nevertheless, a recent study has demonstrated promising performances of single-crystal NMC532: mild capacity fading and outstanding lifetimes (over 1 million miles).[58,61,62] There is still a lot of room to improve for these new-generation single-crystal high-nickel LIBs regarding production cost, specific capacity, and rate capability. Moreover, due to the requirement of high temperature (above 930 ℃ for 12 hours),[62] more inferior environmental performance is expected as compared to the results of the EV use scenario in this study (Figure 2 and Figure 7 – Figure 8). Some high-performance batteries retain a rather high energy storage capacity after their first life in EV, so the resources used for battery production are not fully recovered if the LIBs are sent to EOL directly after EV use. Our results suggest the necessity of introducing second life or even multiple lives to the currently adopted LIBs with relatively low specific energy density for sustainable development, and it is in line with the current trend towards the development of traction LIBs with higher energy density, and longer battery life. Moreover, we conclude that by upgrading the electricity generation to all-renewable energy sources, the life cycle environmental impacts of LIBs can be substantially reduced.

Direct cathode recycling is a strong sustainable candidate for future commercialization due to its outstanding environmental performance and moderate economic performance. Considering the increasing demand for LIBs and potential shortage in cobalt in 30 years,[2,9,63] deployment of direct cathode recycling with a 95% recovery rate of cathode active materials could largely mitigate the risk of metal depletion and relieve the pressure of metal supply on the global market. Therefore, it is crucial to gain more insights into its scalability and potentials for improvement. First, the electrolyte extraction efficiency for liquid CO_2 with additives of propylene carbonate and acetonitrile should be improved. Moreover, the current electrolyte extraction technology can be replaced by less energy-intensive and more environmentally friendly alternatives. The costly

combination of acutely toxic, irritating binder solvent NMP[64] and mutagenic binder polyvinylidene fluoride could be replaced by greener alternatives. For example, the combinations of aqueous binders and corresponding binder solvent (i.e. water) have the properties of fluorine-free, ease of disposal, and availability from renewable resources.[65] Moreover, water is used as the binder solvent that does not need to be recovered, so the economic and environmental burden caused by solvent recovery is avoided. Although the field of aqueous binders is rather unexplored, previous studies show promising results on the enhanced electrochemical performance of LIBs.[66,67] Furthermore, the combustion of graphite and carbon black take a great share of carbon burdens caused by EOL phase. Recycling graphite from waste LIBs at the laboratory scale has been assessed and could be further explored and upgraded to commercial scale.[68,69] Lastly, the energy-intensive hydrothermal and annealing process can be coupled with other exothermic processes to reduce the energy demand. As one of the two carbon avoiding recycling methods, hydrometallurgical recycling could be improved by optimizing the product yields to reduce the use of environmentally detrimental leaching agents and precipitants.

REFERENCES

1 McKinsey & Company. James, E., Alexander, P. & Jasper, v. d. S. *Recharging economies: The EV-battery manufacturing outlook for Europe*, (2019). <https://www.mckinsey.com/industries/oil-and-gas/our-insights/recharging-economies-the-ev-battery-manufacturing-outlook-for-europe> [Accessed 10/28/2020]

2 Department of Energy. *Vehicle Technologies Office's Research Plan to Reduce, Recycle, and Recover Critical Materials in Lithium-Ion Batteries*, (2019). <https://www.energy.gov/sites/prod/files/2019/07/f64/112306-battery-recycling-brochure-June-2019%202-web150.pdf>

3 Tesla. *Introducing Megapack: Utility-Scale Energy Storage*, (2019). <https://www.tesla.com/blog/introducing-megapack-utility-scale-energy-storage> [Accessed 04/18/2020]

4 Harper, G. et al. Recycling lithium-ion batteries from electric vehicles. *Nature* **575**, 75-86, doi:10.1038/s41586-019-1682-5 (2019).

5 Marcelo Azevedo, N. C., Toralf Hagenbruch, Ken Hoffman, Ajay Lala, Oliver Ramsbottom. Lithium and cobalt - a tale of two commodities. (McKinsey&Company, 2018) [Accessed 04/18/2020]

6 Narins, T. P. The battery business: Lithium availability and the growth of the global electric car industry. *Extr. Ind. Soc.* **4**, 321-328, doi:https://doi.org/10.1016/j.exis.2017.01.013 (2017).

7 Gil-Alana, L. A. & Monge, M. Lithium: Production and estimated consumption. Evidence of persistence. *Resour. Policy* **60**, 198-202, doi:https://doi.org/10.1016/j.resourpol.2019.01.006 (2019).

8 van den Brink, S., Kleijn, R., Sprecher, B. & Tukker, A. Identifying supply risks by mapping the cobalt supply chain. *Resour. Conserv. Recycl.* **156**, 104743, doi:https://doi.org/10.1016/j.resconrec.2020.104743 (2020).

9 Olivetti, E. A., Ceder, G., Gaustad, G. G. & Fu, X. Lithium-Ion Battery Supply Chain Considerations: Analysis of Potential Bottlenecks in Critical Metals. *Joule* **1**, 229-243, doi:https://doi.org/10.1016/j.joule.2017.08.019 (2017).

10 Wang, X., Gaustad, G., Babbitt, C. W. & Richa, K. Economies of scale for future lithium-ion battery recycling infrastructure. *Resour. Conserv. Recycl.* **83**, 53-62, doi:https://doi.org/10.1016/j.resconrec.2013.11.009 (2014).

11 Wolfs, P. An economic assessment of "second use" lithium-ion batteries for grid support. *2010 20th Australasian Universities Power Engineering Conference*, 1-6 (2010).

12 Pillot, C. *Lithium ion Battery Raw Material Supply & Demand 2016-2025*, (2017). <http://cii-resource.com/cet/AABE-03-17/Presentations/BRMT/Pillot_Christophe.pdf> [Accessed 04/19/2020]

13 Kamath, D., Arsenault, R., Kim, H. C. & Anctil, A. Economic and Environmental Feasibility of Second-Life Lithium-Ion Batteries as Fast-Charging Energy Storage. *Environ. Sci. Technol.* **54**, 6878-6887, doi:10.1021/acs.est.9b05883 (2020).

14 Neubauer, J. & Pesaran, A. The ability of battery second use strategies to impact plug-in electric vehicle prices and serve utility energy storage applications. *J. Power Sources* **196**, 10351-10358, doi:https://doi.org/10.1016/j.jpowsour.2011.06.053 (2011).

15 Lih, W., Yen, J., Shieh, F. & Liao, Y. Second Use of Retired Lithium-ion Battery Packs from Electric Vehicles: Technological Challenges, Cost Analysis and Optimal Business

Model. *2012 International Symposium on Computer, Consumer and Control*, 381-384, doi:10.1109/IS3C.2012.103 (2012).

16 Bobba, S., Mathieux, F. & Blengini, G. A. How will second-use of batteries affect stocks and flows in the EU? A model for traction Li-ion batteries. *Resour. Conserv. Recycl.* **145**, 279-291, doi:https://doi.org/10.1016/j.resconrec.2019.02.022 (2019).

17 Faria, R. et al. Primary and secondary use of electric mobility batteries from a life cycle perspective. *J. Power Sources* **262**, 169-177, doi:https://doi.org/10.1016/j.jpowsour.2014.03.092 (2014).

18 Ahmadi, L., Yip, A., Fowler, M., Young, S. B. & Fraser, R. A. Environmental feasibility of re-use of electric vehicle batteries. *Sustain. Energy Technol. Assess.* **6**, 64-74, doi:https://doi.org/10.1016/j.seta.2014.01.006 (2014).

19 Ahmadi, L. et al. Energy efficiency of Li-ion battery packs re-used in stationary power applications. *Sustain. Energy Technol. Assess.* **8**, 9-17, doi:https://doi.org/10.1016/j.seta.2014.06.006 (2014).

20 Ahmadi, L., Young, S. B., Fowler, M., Fraser, R. A. & Achachlouei, M. A. A cascaded life cycle: reuse of electric vehicle lithium-ion battery packs in energy storage systems. *Int. J. Life Cycle Assess.* **22**, 111-124, doi:10.1007/s11367-015-0959-7 (2017).

21 Richa, K., Babbitt, C. W., Nenadic, N. G. & Gaustad, G. Environmental trade-offs across cascading lithium-ion battery life cycles. *Int. J. Life Cycle Assess.* **22**, 66-81, doi:10.1007/s11367-015-0942-3 (2017).

22 Casals, L. C., Amante García, B. & Canal, C. Second life batteries lifespan: Rest of useful life and environmental analysis. *Journal of Environmental Management* **232**, 354-363, doi:https://doi.org/10.1016/j.jenvman.2018.11.046 (2019).

23 Casals, L. C., García, B. A., Aguesse, F. & Iturrondobeitia, A. Second life of electric vehicle batteries: relation between materials degradation and environmental impact. *Int. J. Life Cycle Assess.* **22**, 82-93, doi:10.1007/s11367-015-0918-3 (2017).

24 Hiremath, M., Derendorf, K. & Vogt, T. Comparative Life Cycle Assessment of Battery Storage Systems for Stationary Applications. *Environ. Sci. Technol.* **49**, 4825-4833, doi:10.1021/es504572q (2015).

25 Heelan, J. et al. Current and Prospective Li-Ion Battery Recycling and Recovery Processes. *JOM* **68**, 2632-2638, doi:10.1007/s11837-016-1994-y (2016).

26 Elwert, T. et al. Current Developments and Challenges in the Recycling of Key Components of (Hybrid) Electric Vehicles. *Recycling* **1**, 25-60, doi:10.3390/recycling1010025 (2015).

27 Daniel Cheret, S. S. Battery recycling. U.S. patent US7169206B2 (2007).

28 Notter, D. A. et al. Contribution of Li-Ion Batteries to the Environmental Impact of Electric Vehicles. *Environ. Sci. Technol.* **44**, 7744-7744, doi:10.1021/es1029156 (2010).

29 Kim, H. C. et al. Cradle-to-Gate Emissions from a Commercial Electric Vehicle Li-Ion Battery: A Comparative Analysis. *Environ. Sci. Technol.* **50**, 7715-7722, doi:10.1021/acs.est.6b00830 (2016).

30 Majeau-Bettez, G., Hawkins, T. R. & Strømman, A. H. Life Cycle Environmental Assessment of Lithium-Ion and Nickel Metal Hydride Batteries for Plug-In Hybrid and Battery Electric Vehicles. *Environ. Sci. Technol.* **45**, 4548-4554, doi:10.1021/es103607c (2011).

31 United States Environmental Protection Agency. *Application of LCA to Nanoscale Technology: Li-ion Batteries for Electric Vehicles* (2013).

<https://www.epa.gov/sites/production/files/2014-01/documents/lithium_batteries_lca.pdf>

32 Ciez, R. E. & Whitacre, J. F. Examining different recycling processes for lithium-ion batteries. *Nat. Sustain.* **2**, 148-156, doi:10.1038/s41893-019-0222-5 (2019).

33 Goedkoop, M. et al. ReCiPE 2008: A life cycle impact assessment method which comprises harmonised category indicators at the midpoint and the endpoint level. (2008).

34 Muzayanha, U. S. et al. A Fast Metals Recovery Method for the Synthesis of Lithium Nickel Cobalt Aluminum Oxide Material from Cathode Waste. *Metals* **9**, doi:10.3390/met9050615 (2019).

35 Shen, Y., Xue, W. & Niu, W. Recovery of Co(II) and Ni(II) from hydrochloric acid solution of alloy scrap. *Trans. Nonferrous Met. Soc.* **18**, 1262-1268, doi:https://doi.org/10.1016/S1003-6326(08)60214-9 (2008).

36 Shi, Y., Chen, G. & Chen, Z. Effective regeneration of LiCoO2 from spent lithium-ion batteries: a direct approach towards high-performance active particles. *Green Chem.* **20**, 851-862, doi:10.1039/C7GC02831H (2018).

37 Grützke, M. et al. Extraction of lithium-ion battery electrolytes with liquid and supercritical carbon dioxide and additional solvents. *RSC Adv.* **5**, 43209-43217, doi:10.1039/C5RA04451K (2015).

38 Bian, D. et al. A novel process to recycle spent LiFePO4 for synthesizing LiFePO4/C hierarchical microflowers. *Electrochim. Acta* **190**, 134-140, doi:https://doi.org/10.1016/j.electacta.2015.12.114 (2016).

39 Zheng, R. et al. Optimized Li and Fe recovery from spent lithium-ion batteries via a solution-precipitation method. *RSC Adv.* **6**, 43613-43625, doi:10.1039/C6RA05477C (2016).

40 Song, X. et al. Direct regeneration of cathode materials from spent lithium iron phosphate batteries using a solid phase sintering method. *RSC Adv.* **7**, 4783-4790, doi:10.1039/C6RA27210J (2017).

41 Ellingsen, L. A.-W. et al. Life Cycle Assessment of a Lithium-Ion Battery Vehicle Pack. *J. Ind. Ecol.* **18**, 113-124, doi:10.1111/jiec.12072 (2014).

42 Zhao, S. & You, F. Comparative Life-Cycle Assessment of Li-Ion Batteries through Process-Based and Integrated Hybrid Approaches. *ACS Sustain. Chem. Eng.* **7**, 5082-5094, doi:10.1021/acssuschemeng.8b05902 (2019).

43 Yao, J. & You, F. Simulation-based optimization framework for economic operations of autonomous electric taxicab considering battery aging. *Applied Energy* **279**, 115721, doi:https://doi.org/10.1016/j.apenergy.2020.115721 (2020).

44 Schmalstieg, J., Käbitz, S., Ecker, M. & Sauer, D. U. A holistic aging model for Li(NiMnCo)O2 based 18650 lithium-ion batteries. *J. Power Sources* **257**, 325-334, doi:https://doi.org/10.1016/j.jpowsour.2014.02.012 (2014).

45 U.S. Energy Information Administration. *How much electricity does an American home use?*, (2020). <https://www.eia.gov/tools/faqs/faq.php?id=97&t=3> [Accessed 11/16/2020]

46 New York State Energy Research and Development Authority. *Electricity Pricing Strategies to Reduce Grid Impacts from Plug-in Electric Vehicle Charging in New York State*, (2015). <https://www.nyserda.ny.gov/-/media/Files/Publications/Research/Transportation/EV-Pricing.pdf> [Accessed 11/16/2020]

47 National Centers for Environmental Information. *Climate Data Online*, (2020). <https://www.ncdc.noaa.gov/cdo-web/search> [Accessed 11/16/2020]
48 Wernet, G. et al. The ecoinvent database version 3 (part I): overview and methodology. *Int. J. Life Cycle Assess.* **21**, 1218-1230, doi:10.1007/s11367-016-1087-8 (2016).
49 U.S. Energy Information Administration. *Annual Energy Outlook 2020 with projections to 2050*, (2020). <https://www.eia.gov/outlooks/aeo/pdf/aeo2020.pdf> [Accessed 04/18/2020]
50 U.S. Energy Information Administration. *International Energy Outlook 2019 with projections to 2050*, (2019). <https://www.eia.gov/outlooks/ieo/pdf/ieo2019.pdf> [Accessed 04/18/2020]
51 Nelson, P. A., Ahmed, S., Gallagher, K. G. & Dees, D. W. Modeling the Performance and Cost of Lithium-Ion Batteries for Electric-Drive Vehicles, Third Edition. (United States, 2019)
52 Argonne National Laboratory. Dai, Q. et al. *EverBatt: A Closed-loop Battery Recycling Cost and Environmental Impacts Model*, (2019). <https://www.anl.gov/egs/everbatt> [Accessed 04/18/2020]
53 Joint Research Centre, European Commission. Natalia, L., Franco, D. P. & Lois, B.-B. *Lithium ion battery value chain and related opportunities for Europe*, (2016). <https://ec.europa.eu/jrc/sites/jrcsh/files/jrc105010_161214_li-ion_battery_value_chain_jrc105010.pdf> [Accessed 04/18/2020]
54 Shen, W., Han, W., Wallington, T. J. & Winkler, S. L. China Electricity Generation Greenhouse Gas Emission Intensity in 2030: Implications for Electric Vehicles. *Environ. Sci. Technol.* **53**, 6063-6072, doi:10.1021/acs.est.8b05264 (2019).
55 Li, M., Patiño-Echeverri, D. & Zhang, J. Policies to promote energy efficiency and air emissions reductions in China's electric power generation sector during the 11th and 12th five-year plan periods: Achievements, remaining challenges, and opportunities. *Energy Policy* **125**, 429-444, doi:https://doi.org/10.1016/j.enpol.2018.10.008 (2019).
56 Xu, Y., Yang, C.-J. & Xuan, X. Engineering and optimization approaches to enhance the thermal efficiency of coal electricity generation in China. *Energy Policy* **60**, 356-363, doi:https://doi.org/10.1016/j.enpol.2013.05.047 (2013).
57 U.S. Energy Information Administration. *Form EIA-923*, (2020). <https://www.eia.gov/electricity/annual/html/epa_08_01.html> [Accessed 04/18/2020]
58 Li, W., Erickson, E. M. & Manthiram, A. High-nickel layered oxide cathodes for lithium-based automotive batteries. *Nature Energy* **5**, 26-34, doi:10.1038/s41560-019-0513-0 (2020).
59 Myung, S.-T. et al. Nickel-Rich Layered Cathode Materials for Automotive Lithium-Ion Batteries: Achievements and Perspectives. *ACS Energy Letters* **2**, 196-223, doi:10.1021/acsenergylett.6b00594 (2017).
60 Noh, H.-J., Youn, S., Yoon, C. S. & Sun, Y.-K. Comparison of the structural and electrochemical properties of layered Li[NixCoyMnz]O2 (x = 1/3, 0.5, 0.6, 0.7, 0.8 and 0.85) cathode material for lithium-ion batteries. *J. Power Sources* **233**, 121-130, doi:https://doi.org/10.1016/j.jpowsour.2013.01.063 (2013).
61 Harlow, J. E. et al. A Wide Range of Testing Results on an Excellent Lithium-Ion Cell Chemistry to be used as Benchmarks for New Battery Technologies. *J. Electrochem. Soc.* **166**, A3031-A3044, doi:10.1149/2.0981913jes (2019).
62 Li, J. et al. Comparison of Single Crystal and Polycrystalline

LiNi0.5Mn0.3Co0.2O2Positive Electrode Materials for High Voltage Li-Ion Cells. *J. Electrochem. Soc.* **164**, A1534-A1544, doi:10.1149/2.0991707jes (2017).

63 European Commission. *REPORT ON CRITICAL RAW MATERIALS FOR THE EU CRITICAL RAW MATERIALS PROFILES*, (2014). <http://ec.europa.eu/DocsRoom/documents/11911/attachments/1/translations>

64 United States Environmental Protection Agency. *Scope of the Risk Evaluation for N-Methylpyrrolidone (2-Pyrrolidinone, 1-Methyl-)*, (2017). <https://www.epa.gov/sites/production/files/2017-06/documents/nmp_scope_6-22-17_0.pdf>

65 Bresser, D., Buchholz, D., Moretti, A., Varzi, A. & Passerini, S. Alternative binders for sustainable electrochemical energy storage – the transition to aqueous electrode processing and bio-derived polymers. *Energy Environ. Sci.* **11**, 3096-3127, doi:10.1039/C8EE00640G (2018).

66 Wang, R. et al. Effect of Different Binders on the Electrochemical Performance of Metal Oxide Anode for Lithium-Ion Batteries. *Nanoscale Res. Lett.* **12**, 575, doi:10.1186/s11671-017-2348-6 (2017).

67 Chen, Z. et al. Toward greener lithium-ion batteries: Aqueous binder-based LiNi0.4Co0.2Mn0.4O2 cathode material with superior electrochemical performance. *J. Power Sources* **372**, 180-187, doi:https://doi.org/10.1016/j.jpowsour.2017.10.074 (2017).

68 Rothermel, S. et al. Graphite Recycling from Spent Lithium-Ion Batteries. *ChemSusChem* **9**, 3473-3484, doi:10.1002/cssc.201601062 (2016).

69 Yang, Y. et al. A process for combination of recycling lithium and regenerating graphite from spent lithium-ion battery. *Waste Manage.* **85**, 529-537, doi:https://doi.org/10.1016/j.wasman.2019.01.008 (2019).

70 Frischknecht, R. LCI modelling approaches applied on recycling of materials in view of environmental sustainability, risk perception and eco-efficiency. *Int. J. Life Cycle Assess.* **15**, 666-671, doi:10.1007/s11367-010-0201-6 (2010).

71 Dunn, J. B., Gaines, L., Sullivan, J. & Wang, M. Q. Impact of Recycling on Cradle-to-Gate Energy Consumption and Greenhouse Gas Emissions of Automotive Lithium-Ion Batteries. *Environ. Sci. Technol.* **46**, 12704-12710, doi:10.1021/es302420z (2012).

72 Redondo-Iglesias, E., Venet, P. & Pelissier, S. Efficiency Degradation Model of Lithium-Ion Batteries for Electric Vehicles. *IEEE Transactions on Industry Applications* **55**, 1932-1940, doi:10.1109/TIA.2018.2877166 (2019).

73 Pahola Thathiana Benavides, Q. D., Jarod Kelly, Jennifer B. Dunn. Addition of nickel cobalt aluminum (NCA) cathode material to GREET2. (2016) [Accessed 04/14/2020]

74 Q. Dai, J. K., J. Dunn, P. Benavides. Update of Bill-of-materials and Cathode Materials Production for Lithium-ion Batteries in the GREET Model. (2018) [Accessed 04/14/2020]

75 Q. Dai, J. D., J. Kelly, A. Elgowainy. Update of Life Cycle Analysis of Lithium-ion Batteries in the GREET Model. (2017) [Accessed 04/14/2020]

76 Ecoinvent database version 3.6. Hischier, R. *Treatment of scrap printed wiring boards, shredding and separation, RoW, Allocation at the point of substitution*,

77 Dunn, J., Gaines, L., Barnes, M., Wang, M. & Sullivan, J. Material and energy flows in the materials production, assembly, and end-of-life stages of the automotive lithium-ion battery life cycle. doi:10.2172/1044525 (2012).

78 Geisler, G., Hofstetter, T. B. & Hungerbühler, K. Production of fine and speciality chemicals: procedure for the estimation of LCIs. *Int. J. Life Cycle Assess.* **9**, 101-113,

doi:10.1007/BF02978569 (2004).
79 Wood III, D. L. et al. Technical and Economic Analysis of Solvent-based Lithium-ion Electrode Drying with Water and NMP. *Drying Technol.* **36**, 234, 244, doi:10.1080/07373937.2017.1319855 (2018).
80 U.S. Department of Energy, National Energy Technology Laboratory. *Final Environmental Assessment for Compact Power, Inc. Electric Drive Vehicle Battery and Component Manufacturing Initiative Application*, (2010). <http://energy.gov/sites/prod/files/nepapub/nepa_documents/RedDont/EA-1709-FEA-2010.pdf>
81 Zhou, X. et al. in *2010 4th International Conference on Bioinformatics and Biomedical Engineering*. 1-4.
82 Golmohammadzadeh, R., Rashchi, F. & Vahidi, E. Recovery of lithium and cobalt from spent lithium-ion batteries using organic acids: Process optimization and kinetic aspects. *Waste Manage.* **64**, 244-254, doi:https://doi.org/10.1016/j.wasman.2017.03.037 (2017).
83 He, L.-P., Sun, S.-Y., Song, X.-F. & Yu, J.-G. Leaching process for recovering valuable metals from the LiNi1/3Co1/3Mn1/3O2 cathode of lithium-ion batteries. *Waste Manage.* **64**, 171-181, doi:https://doi.org/10.1016/j.wasman.2017.02.011 (2017).
84 Lee, D. et al. Modeling the Effect of the Loss of Cyclable Lithium on the Performance Degradation of a Lithium-Ion Battery. *Energies* **12**, 1-14 (2019).
85 Lee, U. et al. Carbon Dioxide Liquefaction Process for Ship Transportation. *Ind. Eng. Chem. Res.* **51**, 15122-15131, doi:10.1021/ie300431z (2012).
86 Pritzl, D. et al. Editors' Choice—Washing of Nickel-Rich Cathode Materials for Lithium-Ion Batteries: Towards a Mechanistic Understanding. *J. Electrochem. Soc.* **166**, A4056-A4066, doi:10.1149/2.1351915jes (2019).
87 Campion, C. L., Li, W. & Lucht, B. L. Thermal Decomposition of LiPF6-Based Electrolytes for Lithium-Ion Batteries. *J. Electrochem. Soc.* **152**, A2327, doi:10.1149/1.2083267 (2005).
88 Gielen, D. CO2 removal in the iron and steel industry. *Energy Convers. Manage.* **44**, 1027-1037, doi:10.1016/S0196-8904(02)00111-5 (2003).
89 Partnership, U. S. E. P. A. C. H. a. P. Catalog of CHP Technologies. (2017) [Accessed 04/14/2020]
90 International copper association: copper alliance. *Copper Recycling*, (2017). <https://copperalliance.org/wp-content/uploads/2017/03/ica-copper-recycling-201712-A4-HR2.pdf> [Accessed Apr. 18, 2020]
91 NYSERDA. *Monthly Average Retail Price of Electricity - Residential*, (2020). <https://www.nyserda.ny.gov/Researchers-and-Policymakers/Energy-Prices/Electricity/Monthly-Avg-Electricity-Residential> [Accessed Apr. 18, 2020]
92 U.S. Geological Survey. *Mineral commodity summaries 2020: U.S. Geological Survey*, (2020). <https://doi.org/10.3133/mcs2020.> [Accessed 04/18/2020]
93 U.S. Department of Energy, The Energy Information Administration (EIA). *Form EIA-923*, (2018). <https://www.eia.gov/electricity/data/eia923/>
94 Ciez, R. E. & Whitacre, J. F. Comparison between cylindrical and prismatic lithium-ion cell costs using a process based cost model. *J. Power Sources* **340**, 273-281, doi:https://doi.org/10.1016/j.jpowsour.2016.11.054 (2017).

APPENDIX

This supplementary information file covers: (1) Comparison with results from existing literature; (2) Battery parameters; (3) Material and energy inventory for production of LFP, LMO+NMC, NMC and NCA LIBs; (4) Material inventory and energy inventory for NMC and NCA cathode active material; (5) Material inventory and energy inventory for recycling processes; (6) Sensitivity analysis for recycling parameters; (7) Economic Parameters and Breakdowns of Life cycle costs; (8) Additional information and data which includes the electricity generation by energy sources, transportation parameters, and yield rates for battery materials and cells.

S1. Comparison with results from existing literature

Figure S20 summarizes carbon footprint results from existing LCA studies on reused automotive LIBs and compares them with the carbon footprint results from this work. As most existing work on LIB's second life did not assess energy performance or investigate a comprehensive list of impact categories, the results of CED and full-spectrum environmental impacts are not comparable. It is noticeable that there are only a few LCA studies on second life adoption of retired automotive LIBs. Neither of these works included direct cathode recycling as an alternative recycling method nor considered LIBs other than LMO and LFP. And some of them excluded LIB production and EV use from the system boundary.[13,23] Besides, all of the existing literature used average data to estimate the carbon footprint associated with EOL recycling. Hence it could result in large uncertainty in their results.

The life cycle carbon footprint calculated in this study is substantially higher than those from the previous literature (columns in Figure S20). These variabilities can be mainly attributed to differences in the choice of system specifications related to the use phase such as choice of

electricity mix (Ahmadi. et al.[20] and Faria et al.[17]), modeling of life cycle energy consumption or only the energy loss due to battery weight and charge-discharge efficiency (Richa et al.[21]), and amount of electricity delivery during second life (all three studies). Ahmadi. et al.[20] and Faria et al.[17] investigated the life cycle carbon footprint of reusing LFP LIBs, respectively. For example, due to the high penetration of renewable energy sources in the chosen Ontario grid mix[20] and French grid mix[17], the carbon footprint associated with the use phase is only around 0.14 and 0.06 kg CO_2 eq. per life cycle electricity delivery, respectively, which is much lower than that in the baseline scenario of this study (around 0.6 kg CO_2 per life cycle electricity delivery for the Texas grid). If the same assumption of the electricity grid is applied, they should produce a higher life cycle carbon footprint than this study.

Due to the inconsistencies in the assumptions related to the use phase and the substantial impacts of the use phase on the life cycle carbon footprint, we recalculate the life cycle carbon footprint by excluding the use phase from the system boundary (red circles in Figure S20). Besides the difference in battery chemistries, the assumptions for both the LIB use in stationary ESS and the EOL recycling could contribute to the difference in the carbon footprint results. First, Richa et al.[21] assumed a 50% cell conversion rate for the repurposing of retired EV LIB pack, while a 100% cell conversion rate is assumed in this study. Under the same assumption of 100% cell conversion rate, the carbon footprint allocated to the LIB production and recycling in Richa et al.[21] could be reduced by half. Second, the EOL recycling in Faria et al.[17] and Richa et al.[21] were highly simplified. For example, in Richa et al.[21], neither a metallurgical charge comprising iron and slag formers (including limestone, sand, slag, and coke) or leaching agents (such as HCl and H_2SO_4) was used in the pyrometallurgical recycling. With respect to the hydrometallurgical recycling in Richa et al.[21], materials for essential steps, such as NMP, nitrogen, steam, and water for NMP

soaking and recovery, and precipitant for lithium carbonate (Li_2CO_3), are missing. This could lead to an underestimated carbon footprint associated with EOL recycling. On the other hand, Richa et al.[21] only considered the avoided burden from steel, aluminium, and copper recycling and neglected the recovery of critical metals, which could in contrary lead to overestimated carbon footprints. Faria et al.[17] and Ahmadi. et al.[20] estimated the carbon footprint of hydrometallurgical recycling based on data from the Ecoinvent database. Since Faria et al.[17] and Ahmadi. et al.[20] did not provide details about the EOL recycling of LIBs, we will not discuss about its carbon footprint result. Lastly, the assumed life cycle electricity delivery in this study is higher. If all other assumptions are the same, higher life cycle electricity delivery will cause a lower life cycle carbon footprint.

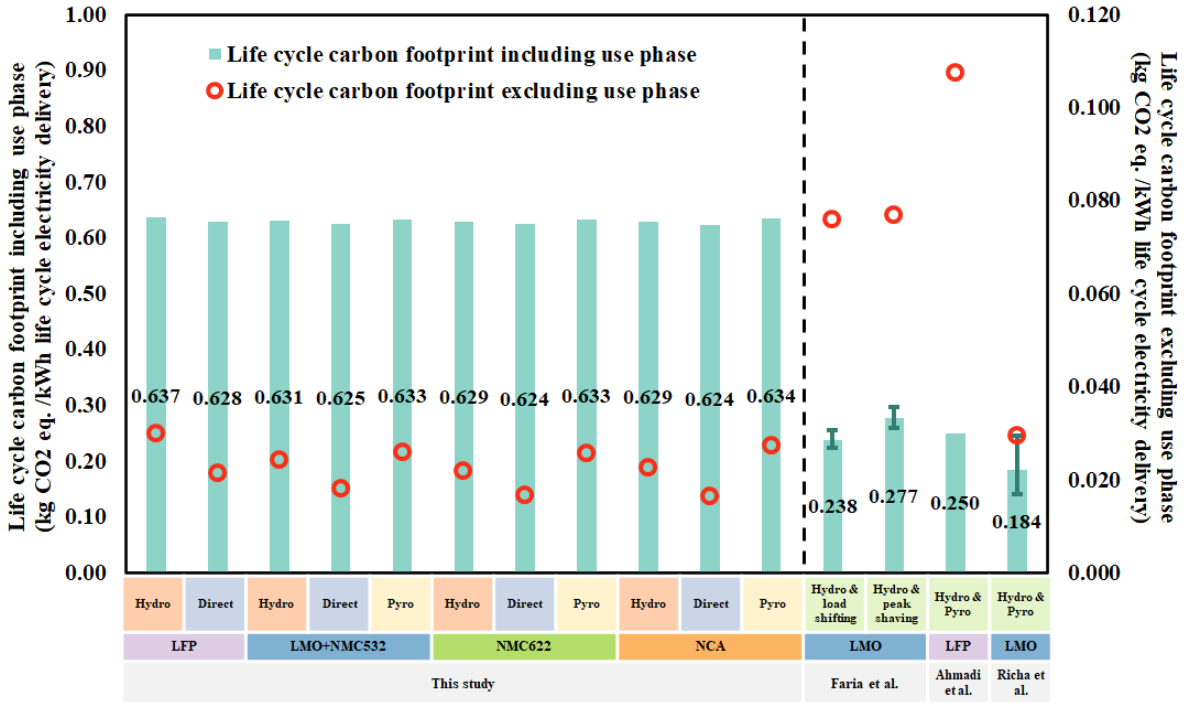

Figure S20. Comparison of LCA studies on LIBs second life adoption of retired automotive LIBs

The carbon footprint and CED resulted from battery recycling methods are summarized and compared in Figure S21. There are two most common approaches used in EOL models: the

avoided burden approach and the recycled content approach.[70] The avoided burden approach assumes that the recycled material or energy can offset the same amount of primary material and energy production. The recycled content approach assumes that no credits are given for material or energy recycling and no burdens are given for secondary material usage. Accordingly, the environmental impacts resulted from the recycled content approach are nonnegative and the environmental impacts resulted from the avoided burden approach can be either negative or positive. Therefore, the results of different EOL models cannot be compared.

Among all studies with the avoided burden assumption, the process designs of recycling in Dunn et al.[71] are obtained from the GREET model which is also the basis of process flows in this analysis. We do not compare our study with Dunn et al.[71] because the battery chemistries are different.

The carbon footprint and energy performance in this work are much worse than that in USEPA[31] for the EOL recycling of LFP, and NMC LIBs. Possible reasons could be their assumptions of higher material recovery rates and the absence of carbon- and energy-intensive materials, compared to this study. Since the USEPA[31] results of hydrometallurgical, pyrometallurgical, and direct cathode recycling are averaged and their recycling processes are modeled based on industrial data that is not accessible by the public, the differences in assumptions and data are unrecognized.

The carbon mitigation potential of hydrometallurgical and direct cathode recycling for NMC622 and NCA LIBs in this study is better than that from Ciez et al.[32] This is because "best-available" laboratory procedures to achieve the maximum material recovery rate were not fully considered by Ciez et al.[32] and other LCA studies on LIB recycling. On the contrary, the carbon footprint of pyrometallurgical recycling for NCA in this study is slightly higher than that from

Ciez et al.[32] A potential reason could be the omission of some essential steps of pyrometallurgical recycling in Ciez et al.[32] and other works. For example, the steps of reducing alloy generated from smelting into recyclable products such as iron, copper, and nickel hydroxide ($Ni(OH)_2$). In addition, the emitted flue gas from electrolyte combustion and blast furnace gas from coking and alloy formation is often neglected by existing LCA studies on battery recycling. Therefore, the environmental benefits of pyrometallurgical recycling are often overestimated.

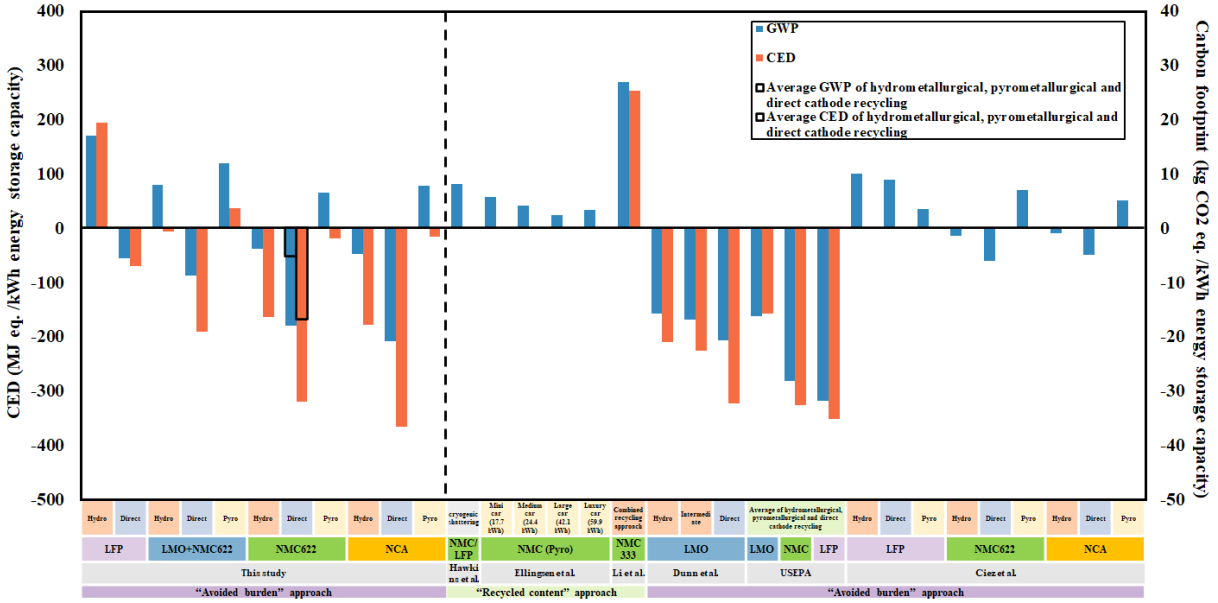

Figure S21. Comparison of LCA studies on carbon footprint and CED resulted from battery recycling

S2. Battery parameters

Battery parameters, such as energy consumption rate in electric vehicles and energy storage capacity, are extracted from the BatPac model.[51] Other battery parameters, including residual battery capacity after electric vehicle use and after stationary ESS use, roundtrip and transmission efficiency for stationary ESS, daily discharge of electricity of single stationary ESS battery packs, EV energy consumption rate, specific energy density, and battery pack energy storage capacity,

are extracted from the previous studies[18,20,21] and presented in Table S1. Electric vehicle use is assumed to be 60 km per day over a 9-year timeframe for both use scenarios of all types of batteries, and the battery capacity decreases from 100% to 80%. Starting from an initial discharging efficiency of 80%, stationary ESS use is assumed to operate one charge/discharge cycle on a daily basis for 11 years with an EOL discharging efficiency of 65%. The lifetime of EV battery packs and stationery ESS battery packs and the number of charge-discharge cycles of EV and stationary ESS battery packs are estimated according to the battery fading. We model the battery fading based on Equation (2) and (3) derived and reformulated from a previous aging model.[43,44] $C_t^{Loss,\ Cycle}$ represents the capacity loss due to cycle aging during time period t and $C_t^{Loss,\ Cal}$ represents the capacity loss due to calendar aging during time period t. ΔQ_t represents the throughput in Ampere hours during time period t, and is approximated from dividing the energy consumption by the open circuit voltage (OCV) at 100% state of charge (SOC) for EV use. For the stationary ESS use, we assume that the repurposed 450-kWh LIB pack charges during the on-peak period and discharges during the off-peak period to support 10 residential utility customers who consume on average 292 kWh electricity on a daily basis.[45] The on-peak period and off-peak period are assumed to be 8-hour and 16-hour long, respectively despite the seasonal variability.[46] The average SOC is 60% during the on-peak period (assume linearly discharged to around 20% depth of discharge (DOD)) and 100% during the off-peak period. ΔQ_t of second life is estimated based on the energy consumption and OCV at the level of SOC during the on-peak period and off-peak period. φV_t denotes the quadratic mean of OCV, and we approximate it using the OCV at their corresponding average level of SOC for EV use and stationary ESS use. ΔDOD_t is the average depth of charge and is calculated as the ratio of electricity delivery to the residual energy storage capacity. V_t^{Bat} is the average battery voltage during time period t, which is also assumed to be the OCV at their

corresponding average level of SOC for EV use and stationary ESS use. T_t^{Bat} is the battery temperature, and we approximate it using the monthly average temperature of Texas.[47] Equation (4) models the energy efficiency (η_t) of batteries during time period t.[72]

$$C_t^{Loss,Cycle} = \beta_t \cdot \left[\left(\frac{C_{t-1}^{Loss,Cycle}}{\beta_t} \right)^2 + \Delta Q_t \right]^{0.5}, \quad (2)$$

$$\text{where } \beta_t = 7.35\times10^{-3} \cdot (\phi V_t - 3.67)^2 + 7.6\times10^{-4} + 4.08\times10^{-3} \cdot \Delta DOD_t$$

$$C_t^{Loss,Cal} = \alpha_t \cdot \left[\left(\frac{C_{t-1}^{Loss,Cal}}{\alpha_t} \right)^{\frac{1}{0.75}} + 1 \right]^{0.75}, \quad (3)$$

$$\text{where } \alpha_t = (7.54 \cdot V_t^{Bat} - 23.75) \cdot 10^6 \cdot e^{-\frac{6976}{T_t^{Bat}}}$$

$$\eta_t = -0.23 \cdot (C_t^{Loss,Cycle} + C_t^{Loss,Cal}) + 0.96 \quad (4)$$

Table S1. Battery parameters of LIBs[18,20,21,51]

Battery parameter	LFP	LMO+ NMC532	NMC 333	NMC 532	NMC 622	NMC 811	NCA
Initial battery capacity				100%			
Residual battery capacity after EV use				80%			
Residual battery capacity after ESS use				65%			
Lifetime of EV battery packs (year)				9			
Lifetime of stationary ESS battery packs (year)				11			
Charge-discharge cycles for EV battery packs (number)				3285			
Charge-discharge cycles for stationary ESS battery packs (number)				4015			
Transmission efficiency				90%			
Daily discharge of electricity of single stationary ESS battery pack (kWh)				292			
Daily traveled distance (km)				60			
EV energy consumption rate (kWh/km)				0.155			
Battery pack energy density (Wh/kg)	177	229	234	243	255	265	262
Roundtrip efficiency after EV use	94.8%	94.7%	94.7%	94.7%	94.7%	94.7%	94.7%
Roundtrip efficiency after ESS use	93.6%	93.5%	93.5%	93.6%	93.4%	93.4%	93.5%
Electricity delivery during EV use	386100	386166	386198	386139	386255	386288	386198
Electricity delivery during ESS use	1383888	1384786	1385032	1384399	1385828	1386327	1384941
Battery pack energy storage capacity (kWh)				52			

S3. Material and energy inventory of LIB packs

The inventory of the battery pack is estimated from the BatPac model and is provided in Table S2–Table S6.[51] The inventory of a stationary ESS battery pack is presented in Table S7. It is worth

mentioning that the environmental impacts associated with cathode active material of LMO are obtainable directly through the Ecoinvent database, where the avoided environmental impacts associated with $Ni(OH)_2$ recovery and cathode active material production for LFP, NMC, and NCA are inaccessible. Instead, the data on upstream materials and energy for producing $Ni(OH)_2$ and LFP are sourced from Majeau-Bettez et al.[30], and the cathode active materials of NMC and NCA are acquired from the GREET model.[73,74] The process model of cathode active materials are detailed in the next section.

Table S2. Material input and output of single LIB cell[51]

Input	Component (g)	LFP	LMO+ NMC532	NMC333	NMC532	NMC622	NMC811	NCA
Cathode	Cathode active material	448.08	430.80	387.67	374.35	326.80	277.40	299.71
	Conductor: Carbon black	9.33	8.98	8.08	7.80	6.81	15.41	6.24
	Binder: Polyvinylidene difluoride (PVDF)	9.33	8.98	8.08	7.80	6.81	15.41	6.24
	Binder solvent: NMP	223.92	215.52	193.92	187.20	163.44	369.84	149.76
	Current collector: Aluminium foil	29.04	11.75	13.73	12.43	13.32	12.35	13.32
Anode	Anode active material: Graphite	235.14	200.34	210.14	201.21	201.36	208.67	204.73
	Binder: PVDF	4.80	4.09	4.20	4.11	4.11	4.26	4.18
	Binder solvent: NMP	115.20	98.16	100.80	98.64	98.64	102.24	100.32
	Current collector: copper foil	68.28	28.49	32.97	29.93	31.99	29.66	31.99
Electrolyte	Electrolyte salt: $LiPF_6$	37.03	37.03	37.03	37.03	37.03	37.03	37.03
	Electrolyte solvent: Ethylene carbonate (EC)	51.57	24.27	22.95	20.43	19.59	19.23	18.33
	Electrolyte solvent: Dimethyl carbonate (DMC)	51.57	24.27	22.95	20.43	19.59	19.23	18.33
Separator	Microporous membrane: Polypropylene (PP)	7.36	2.91	3.42	3.84	3.32	3.75	3.33
	Microporous membrane: Polyethylene (PE)	1.84	0.73	0.86	0.96	0.83	0.94	0.83
Positive terminal assembly	Tab: aluminium	6.30	3.40	3.90	3.70	4.00	3.90	4.20
Negative terminal assembly	Tab: copper	20.70	11.10	13.00	12.30	13.30	12.80	13.90
Cell container	Aluminium	10.30	5.38	6.20	5.83	6.36	6.15	6.62
	Polyethylene terephthalate (PET)	1.60	0.84	0.96	0.91	0.99	0.96	1.03
	PP	0.69	0.36	0.41	0.39	0.42	0.41	0.44
Output	Single LIB cell	999.72	809.97	782.43	749.14	701.86	676.99	675.45
	Recovered NMP	-332.34	-307.41	-288.83	-280.12	-256.84	-462.64	-245.08

Table S3. Energy input and output of single LIB cell production[21,28]

Process	Energy component	LFP	LMO+ NMC532	NMC333	NMC532	NMC622	NMC811	NCA
Cathode mixing, coating, and coiling	Electricity (kWh)	7.47E-04	6.94E-04	6.29E-04	6.06E-04	5.33E-04	4.90E-04	4.90E-04
Cathode drying	Heat (MJ)	4.25E-01	3.81E-01	3.65E-01	3.52E-01	3.08E-01	5.83E-01	2.82E-01
Anode mixing, coating, and coiling	Electricity (kWh)	5.44E-04	4.12E-04	4.37E-04	4.16E-04	4.21E-04	4.29E-04	4.26E-04
Anode drying	Heat (MJ)	2.17E-01	1.81E-01	1.88E-01	1.82E-01	1.83E-01	1.89E-01	1.86E-01
Drying of cathode, anode, and separator	Heat (MJ)	1.11E-01	6.64E-02	9.21E-02	8.87E-02	8.17E-02	7.99E-02	7.81E-02
Calendaring of cathode, anode, and separator	Electricity (kWh)	2.08E-03	1.79E-03	1.72E-03	1.65E-03	1.53E-03	1.47E-03	1.46E-03
Charging	Electricity (kWh)	1.52E-01	1.52E-01	1.52E-01	1.52E-01	1.52E-01	1.52E-01	1.52E-01
Dry room operation	Electricity (kWh)	2.44E-01	1.98E-01	1.91E-01	1.83E-01	1.71E-01	1.65E-01	1.65E-01
	Heat (MJ)	1.65E+00	1.33E+00	1.29E+00	1.23E+00	1.16E+00	1.11E+00	1.11E+00
Output	Single LIB cell (g)	999.72	809.97	782.43	749.14	701.86	676.99	675.45

Table S4. Material input and output of recovering 1 kg NMP[21]

Input		Amount
Material	NMP (g)	1020.41
	Decarbonised water (g)	83297.91
	Nitrogen (g)	14.70
Energy	Steam (g)	1528.84
	Electricity (kWh)	0.05
Output	NMP (g)	1000.00

Table S5. Material input and output of single LIB module[51]

Input	Component	LFP	LMO+NMC532	NMC333	NMC532	NMC622	NMC811	NCA
Module	LIB cells (Number)	12	12	12	12	12	12	12
	Module casing: Aluminium (kg)	0.22	0.14	0.15	0.15	0.16	0.15	0.16
	Cooling plates: Aluminium (kg)	0.22	0.10	0.12	0.11	0.13	0.12	0.13
	Module terminals: Copper (kg)	0.06	0.053	0.056	0.055	0.055	0.055	0.055
Output	Single LIB module (kg)	12.49	10.01	9.72	9.31	8.76	8.45	8.45

S3.1 Material input and output of single Electric Vehicle LIB pack

The BMS is assumed to be 3% of the total mass of one battery pack.[30] The energy input and output of the battery pack assembling processes, including material mixing, drying, NMP recovery, calendering, dry room operation, single-cell charge, welding, and testing, are estimated from Richa et al.[21]

Table S6. Material input and output of single EV LIB pack[21,28,30,41,51]

Input	Component	LFP	LMO+ NMC532	NMC333	NMC532	NMC622	NMC811	NCA
Module	LIB module (Number)	20	20	20	20	20	20	20
Battery pack accessories	Outer layer of battery jacket: Aluminium (kg)	11.69	4.53	4.93	4.77	4.99	4.89	5.12
	Sandwiched layer of battery jacket: Fibre glass (kg)	17.23	10.42	11.35	10.98	11.50	11.25	11.78
	Module compression plates: Steel (kg) Straps: Steel (kg)	1.24	0.57	0.68	0.63	0.70	0.66	0.73
	Module interconnects: Copper (kg)	1.46	1.28	1.34	1.32	1.32	1.32	1.32
BMS	Performance monitoring: Printed wiring board (kg)	0.89	0.69	0.67	0.65	0.62	0.60	0.60
	Wire: Copper (kg)	4.46	3.43	3.37	3.23	3.08	2.98	2.99
	Corrosion resistance: Chromium steel 18/8 (kg)	3.57	2.75	2.70	2.59	2.46	2.38	2.39
Coolant	Ethylene glycol (kg)	3.60	2.46	2.68	2.59	2.71	2.65	2.78
	Deionised water (kg)	3.60	2.46	2.68	2.59	2.71	2.65	2.78
Energy	Welding: Electricity (kWh)	0.12	0.092	0.09	0.086	0.082	0.079	0.08
	Test and activation: Electricity (kWh)	36.37	36.37	36.39	36.37	36.40	36.40	36.38
Output	Single EV LIB pack (kg)	297.59	228.82	224.81	215.44	205.25	198.34	199.52

S3.2 Material input and output of single Stationary Energy Storage Systems LIB pack

After retiring from the electric vehicle, battery cells will be tested to validate their residual energy capacity and this process consumes electricity.[21] Life-extending battery cells are assumed to be repurposed into new battery packs with an energy storage capacity of 450 kWh, aiming for their second use in stationary ESS.[21] All battery module components and part of battery pack components such as module compression plates and steep straps are reused, while coolant, BMS, module interconnects and a tri-layer battery jacket is replaced. The replaced components will be sent to the EOL phase. Notably, BMS is assumed to be 1.5% of the total mass of one repurposed battery pack, based on the fact that BMS of battery packs designed for stationary ESS is not as demanding as those for EV, and thus less advanced printed wiring board design and less complicated wiring will be applied.[21] Lastly, a cabinet made of mild steel sheet is used as the pack casing, instead of using the tri-layer jacket.

Table S7. Material input and output of single 450 kWh stationary ESS LIB pack[21,30,51]

Input		Component	LFP	LMO+ NMC532	NMC 333	NMC 532	NMC 622	NMC 811	NCA
EV LIB pack	Module	LIB cell (Number)	2596	2596	2596	2596	2596	2596	2596
		Module casing: Aluminium (kg)	47.16	29.85	33.10	31.80	33.75	32.67	34.61
		Cooling plates: Aluminium (kg)	47.16	22.07	26.39	24.66	27.04	25.74	28.34
		Module terminals: Copper (kg)	12.98	11.47	12.11	11.90	11.90	11.90	11.90
	Battery pack accessories	Outer layer of battery jacket: Aluminium (kg)	126.39	48.95	53.35	51.58	54.03	52.84	55.36
		Sandwiched layer of battery jacket: Fiber glass (kg)	186.42	112.69	122.82	118.73	124.37	121.64	127.43
		Module compression plates: Steel (kg) Straps: Steel (kg)	13.37	6.11	7.32	6.83	7.52	7.18	7.92
		Module interconnects: Copper (kg)	15.79	13.85	14.49	14.28	14.28	14.28	14.28
	BMS	Performance monitoring: Printed wiring board (kg)	9.66	7.43	7.30	6.99	6.66	6.44	6.47
		Wire: Copper (kg)	48.28	37.13	36.48	34.96	33.30	32.18	32.37
		Corrosion resistance: Chromium steel 18/8 (kg)	38.63	29.70	29.18	27.96	26.64	25.74	25.90
	Coolant	Ethylene glycol (kg)	38.89	26.55	28.99	27.96	29.31	28.66	30.07
		Deionised water (kg)	38.89	26.55	28.99	27.96	29.31	28.66	30.07
Battery pack accessories		Module interconnects: Copper (kg)	15.79	13.85	14.49	14.28	14.28	14.28	14.28
		Steel cabinet: Mild steel (kg)	232.11	184.99	180.32	172.68	163.18	157.51	157.85
BMS		Performance monitoring: Printed wiring board (kg)	4.63	3.69	3.60	3.45	3.26	3.14	3.15
		Wire: Copper (kg)	23.16	18.46	17.99	17.23	16.28	15.72	15.75
		Corrosion resistance: Chromium steel 18/8 (kg)	18.53	14.77	14.39	13.78	13.03	12.57	12.60
Coolant		Ethylene glycol (kg)	38.89	26.55	28.99	27.96	29.31	28.66	30.07
		Deionised water (kg)	38.89	26.55	28.99	27.96	29.31	28.66	30.07
Energy		Welding: Electricity (kWh)	1.24	0.98	0.96	0.92	0.87	0.84	0.84
		Test and activation: Electricity (kWh)	4811.96	4811.96	4811.96	4811.96	4811.96	4811.96	4811.96
Output		ESS LIB pack (kg)	3087.93	2461.03	2398.90	2297.31	2170.89	2095.49	2100.00
Output waste		Outer layer of battery jacket: Aluminium (kg)	126.39	48.95	53.35	51.58	54.03	52.84	55.36
		Sandwiched layer of battery jacket: Fibre glass (kg)	186.42	112.69	122.82	118.73	124.37	121.64	127.43
		Module interconnects: Copper (kg)	15.79	13.85	14.49	14.28	14.28	14.28	14.28
		Performance monitoring: Printed wiring board (kg)	9.66	7.43	7.30	6.99	6.66	6.44	6.47
		Wire: Copper (kg)	48.28	37.13	36.48	34.96	33.30	32.18	32.37
		Corrosion resistance: Chromium steel 18/8 (kg)	38.63	29.70	29.18	27.96	26.64	25.74	25.90
		Coolant (kg)	77.77	53.11	57.98	55.92	58.63	57.33	60.14

S4. Material and energy inventory of cathode active material

The production of cathode active material for NMC and NCA LIBs requires material inputs of lithium source, transit metal sources, deionized water, ammonium hydroxide (NH_4OH), and sodium hydroxide (NaOH), energy inputs, and waste sludge treatment. In addition to the main

products of NMC and NCA, sodium sulphate (Na_2SO_4) crystal is produced.

Figure S22 depicts the process flow for NMC or NCA cathode active material production: First, nickel sulfate ($NiSO_4$), cobalt sulfate ($CoSO_4$), manganese sulfate ($MnSO_4$), or aluminium sulfate ($Al_2(SO_4)_3$) solutions in the case of NCA production, are dissolved and mixed. Then, 20% NH_4OH and 48% NaOH are added to the mixed solution and heated to 50 ℃, and the NMC or NCA precursor ($Ni_xMn_yCo_z(OH)_2$ or $Ni_{0.8}Co_{0.15}Al_{0.05}(OH)_2$) are subsequently precipitated as shown in equation (5)–(9). Next, the NMC and NCA precursors are filtered out, washed with deionized water, and dried. The yields of products are assumed as 100% given that the amount of NH_4OH and NaOH are slightly more than the amount calculated based on stoichiometry. The filtrate is further processed in an ammonia stripping tower to recover excess ammonia. After ammonia stripping, the processed filtrate is evaporated to recover Na_2SO_4 crystal (i.e. sodium and sulfate removal) and effluent is sent to the waste sludge treatment. Next, the assumed lithium source which is Li_2CO_3 for NMC33, NMC532, and NMC622, and lithium hydroxide (LiOH) for NMC811 and NCA as shown in equation (7), (8), and (9), respectively, are mixed with the dried cathode active material precursors and go through a two-stage calcination (over 1000 ℃) together over 12 hours to produce the cathode active materials. Particularly, the calcination process for NCA production requires oxygen input, while air ventilation is sufficient in the case of NMC production.[73,74] Later, the product is crushed and sieved. In the end, the production is finalized with metal detection and demagnetization processes and preparation of ready-to-use NMC or NCA powder.[74] Hydrothermal synthesis under 150–200 ℃ for 5 hours is assumed to be used to synthesize LFP.[30]

Heat and electricity are exclusively consumed to power the precursor production and the calcination process, respectively. Heat production from natural gas burned at the industrial furnace

is required for precipitation, ammonia stripping, and evaporation, among which the most demanding process is precipitation, followed by evaporation. Since energy demand for calcination of materials rich in nickel (Ni) is the most intensive, calcination for NCA and NMC811 is assumed to consume more electricity (8 kWh/kg cathode active materials produced) compared to that of the less Ni-containing NMC622, NMC532, and NMC333 (7 kWh/kg cathode active materials produced). Table S8 details the bill of materials and energy.

$$xNiSO_4 + yMnSO_4 + zCoSO_4 + 2NaOH \rightarrow Ni_xMn_yCo_z(OH)_2 + Na_2SO_4 \quad (5)$$

$$NiSO_4 + CoSO_4 + Al_2(SO_4)_3 + NaOH \rightarrow Ni_{0.8}Co_{0.15}Al_{0.05}(OH)_2 + Na_2SO_4 \quad (6)$$

$$Ni_xMn_yCo_z(OH)_2 + 0.5Li_2CO_3 + 0.25O_2 + H_2O \rightarrow LiNi_xMn_yCo_zO_2 + 2H_2O + 0.5CO_2 \quad (7)$$

$$Ni_{0.8}Mn_{0.1}Co_{0.1}(OH)_2 + LiOH \cdot H_2O + 0.25O_2 \rightarrow LiNi_{0.8}Mn_{0.1}Co_{0.1}O_2 + 2.5H_2O \quad (8)$$

$$Ni_{0.8}Co_{0.15}Al_{0.05}(OH)_2 + LiOH \cdot H_2O + 0.25O_2 \rightarrow LiNi_{0.8}Co_{0.15}Al_{0.05}O_2 + 2.5H_2O \quad (9)$$

$$3LiOH + H_3PO_4 + FeSO_4 \rightarrow LiFePO_4 + Li_2SO_4 + 3H_2O \quad (10)$$

Table S8. Material input and output of cathode active material production for LFP, NMC333, NMC532, NMC622, NMC811, and NCA LIBs[30,73-75]

Input	Component	LFP	NMC333	NMC532	NMC622	NMC811	NCA
Lithium source	Li_2CO_3 (kg)	-	0.38	0.38	0.38	-	-
	LiOH (kg)	0.46	-	-	-	0.25	0.25
Precursor	$MnSO_4$ (kg)	-	0.50	0.49	0.33	0.15	-
	$NiSO_4$ (kg)	-	0.51	0.84	1.01	1.27	1.29
	$CoSO_4$ (kg)	-	0.51	0.34	0.34	0.16	0.25
	$Al_2(SO_4)_3$ (kg)	-	-	-	-	-	0.086
	$FeSO_4$ (kg)	0.96	-	-	-	-	-
	H_3PO_4 (kg)	0.62	-	-	-	-	-
	NaOH (kg)	-	0.87	0.87	0.87	0.87	0.84
	Ammonia (NH_3)	-	0.06	0.06	0.06	0.06	0.35
Oxygen	Oxygen (kg)	-	-	-	-	-	0.04
Water	Decarbonised Water (kg)	46	0.64	0.64	0.64	0.64	0.64
Energy	Electricity (kWh)	-	6.35	6.35	6.35	7.26	7.26
	Heat (MJ)	15	38.67	38.67	38.67	38.67	38.67
Output	Cathode active material (kg)	1.00	1.00	1.00	1.00	1.00	1.00
Emitted (kg)	CO_2	-	0.23	0.23	0.23	-	-
Avoided	Na_2SO_4 (kg)	-	1.55	1.55	1.54	1.54	1.48

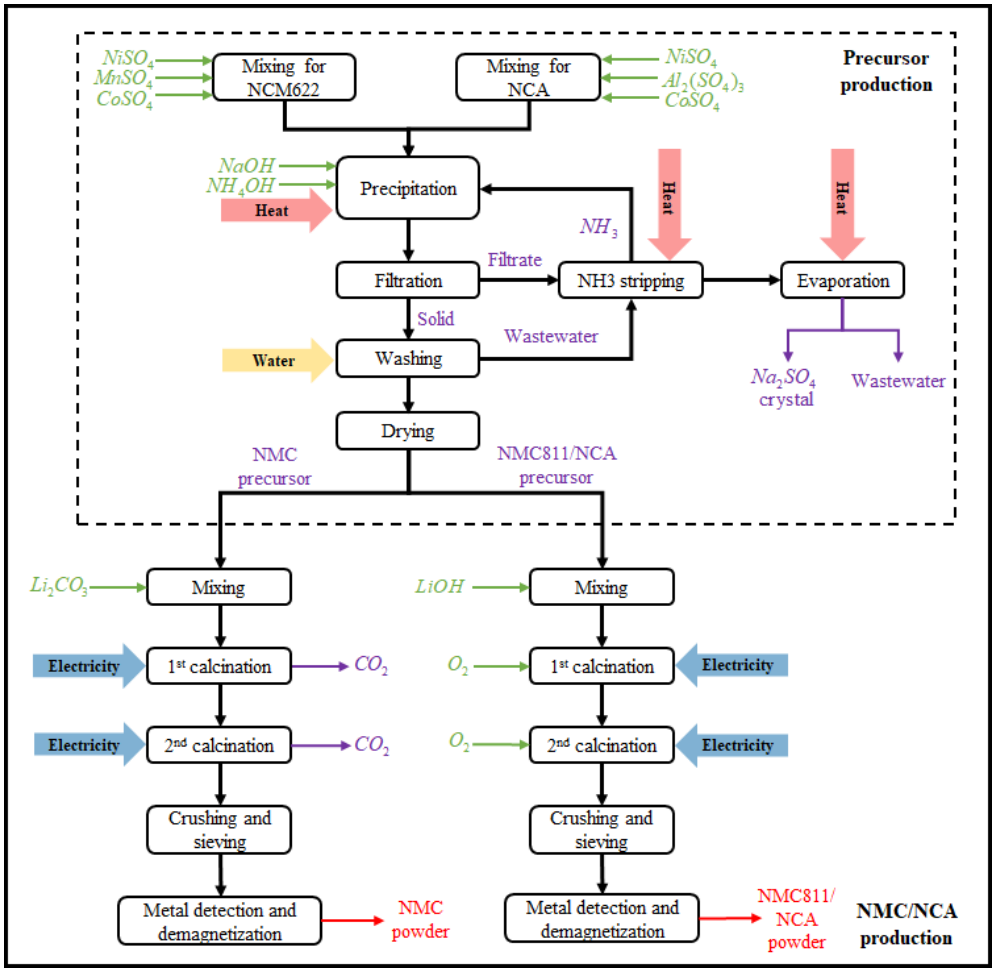

Figure S22. Process diagram of active material production for NMC and NCA LIBs

S5. Material and energy inventory of recycling processes

Three EOL scenarios, namely hydrometallurgical, pyrometallurgical and direct cathode recycling, are investigated and the processes are depicted in Figure S23–Figure S25. Notably, for the EOL scenarios of hydrometallurgical recycling and direct cathode recycling, the spent LIB pack is first discharged and dismantled to the cell level (i.e. all battery module and pack components, including BMS, coolant, terminals, interconnects, thermal systems, and casing were manually disassembled and disposed accordingly), while the spent LIB pack is dismantled to the

module level for pyrometallurgical recycling. Then, the battery cells are further dismantled to cathode, anode, electrolyte, separator, positive and negative terminal assemblies, and cell container. In this step, the plastics (PP, PE, and PET) constituting the separator and cell container are landfilled. The metals such as aluminium (composing current collector for the cathode, positive terminal assembly, cell container, inner and outer layer of battery pack jacket, module casing, and cooling plate) and copper (composing current collector for the anode, negative terminal assembly, interconnects, module terminals, the wires in BMS) are assumed to be recycled to produce (including collection, sorting, cleaning, pressing and re-melting for aluminium, and collection, refining and wastewater management for copper, respectively) with a loss rate of 5%, 1.3%, and 8%, respectively. The waste steel is landfilled, waste chromium steel is recycled, and waste fiber glass is sent to the municipal incinerator. The printed wiring boards are weighted, separated, and shredded into electronic scraps that are ready for further metallurgical treatment.[76] The coolant is incinerated as hazardous waste. After disassembly, cathode, anode, and electrolyte are left for all three EOL scenarios. In addition, plastics (PP, PE, and PET), aluminium and copper, are left for the scenario of pyrometallurgical recycling.

S5.1 Hydrometallurgical recycling

Hydrometallurgical recycling aims at recovering metals using aqueous chemistry, which involves steps of leaching, solvent extraction, and precipitation. Figure S23 depicts the process design of hydrometallurgical recycling. Table S9–Table S10 detail the bill of materials and energy.

Under this scenario, the leftovers are soaked in NMP at 100 ℃ for one hour and crushed in a planetary ball mill to dissolve the binder PVDF and separate the active materials from the current collectors in cathode and anode, respectively.[77] The NMP soaking needs inputs of NMP, deionized water, nitrogen, and heat. The crushing step requires electricity input. The amount of NMP needed

is assumed to be the same as the sum of the weight of active materials, graphite, carbon black, and PVDF.[77] The heat needed to support NMP soaking ($Q_{soaking}$) is calculated as shown in equation (11), where eff_{ng}, c_p^i, m_i and ΔT represent the efficiency of natural gas boilers (60%), the specific heat for each soaked material i (2100, 900, 385 J/(kg·℃) for NMP, aluminium, and copper, active materials for both cathode and anode), the mass of each soaked material i, and the elevated temperature (75 ℃ in premise of an assumed room temperature of 25 ℃).

$$Q_{soaking} = \frac{\sum_i c_p^i \cdot m_i \cdot \Delta T}{eff_{ng}}, i \in \{Al, Cu, NMP, PVDF, graphite, carbon\ black\} \quad (11)$$

Later, solids such as graphite, carbon black, copper, and aluminium are filtered out. The carbon black and graphite are completely combusted to CO_2. The copper and aluminium are recycled, and the filtrate is calcined at around 700 ℃ with inputs of electricity and heat. During the calcination, NMP vapor is recovered for the following reasons: (1) large environmental impacts if NMP vapor is emitted (2) costly expense of NMP (3) easy NMP recovery approach by cooling down to or below room temperature due to its high boiling point (204 ℃) and low vapor pressure. To be specific, the NMP vapor can be cooled down using deionized water paired up with a nitrogen stripping system to remove the dissolved oxygen.[21,78] The high boiling point and low vapor pressure ensure the stability of NMP at room temperature.[79] A recovery rate of 98% is assumed for NMP recovery.[80] The PVDF is burned out and is assumed to be treated the same as municipal incineration. Next, the cathode active material is ground, and the leaching process is used to extract the valuable metals from the aged lithium-metal-oxides using heat, hydrogen peroxide (H_2O_2), and a variety of acids. Specifically, H_2O_2 and citric acid (10% more input than calculated based on stoichiometry and a recovery rate of 90%) are used for leaching lithium (Li) ions from aged LMO; 1 vol.% H_2O_2, 1 M sulfuric acid (H_2SO_4) is used for leaching Ni, cobalt (Co), and manganese (Mn)

ions from aged NMC at 40 ℃ with a stirring speed of 400 rpm and solid-to-liquid (S:L) ratio of 40 g/L for one hour. Moreover, a minor amount of hydrochloric acid (HCl) is added. H_2O_2 and 4 M HCl are used for leaching Ni, Co, and aluminium (Al) ions from aged NCA at 80 ℃ with an S:L ratio of 100 g/L for 80 minutes. 0.5 M phosphoric acid solution is used for leaching $FePO_4$ and Li at room temperature with an S:L ratio of 25 g/L under continuous stirring for 1 hour. The leaching efficiency is 95% of $FePO_4$ for LFP, 95% of Li for LMO, 99.7% of Li, Ni, Co, Mn for NMC, and 80% of Li, 99.8% of Ni, 95.6% of Co, and 99.5% of Al for NCA, respectively. After leaching, filtration and reflux heating at 85 ℃ for 9 hours are performed to obtain $FePO_4 \cdot 2H_2O$.

In the precipitation step, sodium carbonate (Na_2CO_3) is added to the leachate of aged cathode active materials to recover Li_2CO_3. In addition to Na_2CO_3, NaOH and NH_4OH are added to the leachate of aged LMO+NMC532, NMC, or NCA to precipitate their precursors and Li_2CO_3. Inputs of heat, electricity, and deionized water are required for precipitation. Then, manganese (III) oxide (Mn_2O_3) goes through the second calcination together with Li_2CO_3 to produce cathode active materials of LMO and emit CO_2. Flows of oxygen and nitrogen are also introduced to the kiln. NMC and NCA go through the second calcination with Li_2CO_3 and LiOH, respectively. $FePO_4 \cdot 2H_2O$ is mixed with Li_2CO_3 (molar ratio of 1:1.05) and glucose (20 wt.% of LFP product) in water. The slurry is dried, milled, and heated at 350 ℃ for 4 hours and at 650 ℃ for 9 hours in a nitrogen atmosphere. The second calcination of NMC emits CO_2. In the final step, the cathode active materials are crushed, sieved, and undergone metal detection and demagnetization to produce cathode active material powder.

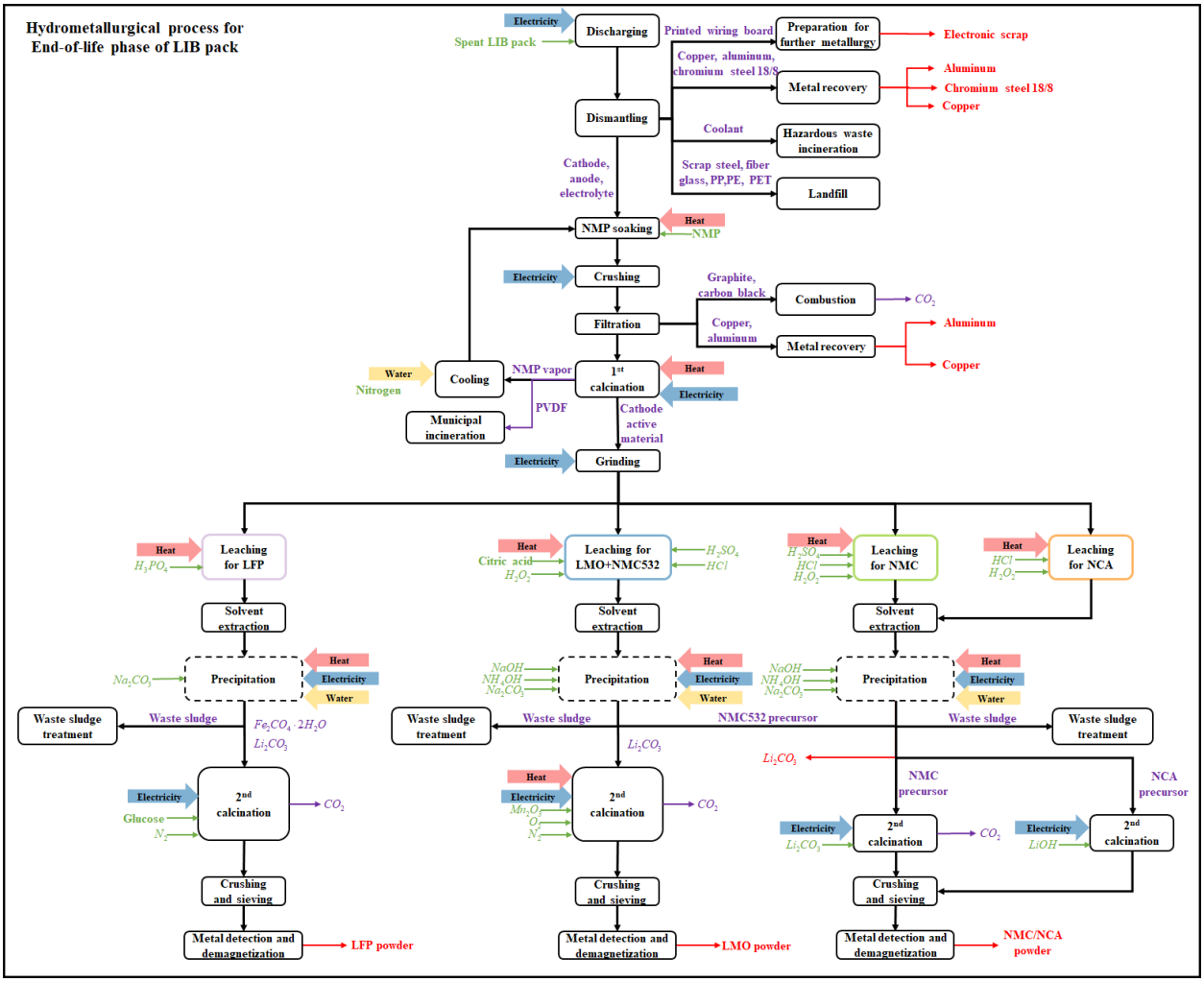

Figure S23. Process diagram of the hydrometallurgical recycling

Table S9. Material input and output of hydrometallurgical recycling for EOL LIB packs with an initial energy storage capacity of 562.5 kWh (LFP, LMO+NMC532, NMC622, NCA)[21,32,34,38,39,75,77,81-83]

		After EV use				After cascaded use			
		LFP	LMO+ NMC	NMC622	NCA	LFP	LMO+ NMC	NMC622	NCA
Material input (kg)	EV LIB pack	3218.89	2475.02	2220.15	2158.19	-	-	-	-
	ESS LIB pack	-	-	-	-	3087.93	2461.03	2170.89	2100.00
	Waste aluminium	-	-	-	-	126.39	48.95	54.03	55.36
	Waste fibre glass	-	-	-	-	186.42	112.69	124.37	127.43
	Waste copper	-	-	-	-	64.08	50.97	47.58	46.65
	Waste printed wiring board	-	-	-	-	9.66	7.43	6.66	6.47
	Waste steel	-	-	-	-	38.63	29.70	26.64	25.90
	Waste coolant	-	-	-	-	77.77	53.11	58.63	60.14
	NMP	1834.54	1695.68	1417.13	1352.78	1834.54	1695.68	1417.13	1352.78
	Decarbonised water	148165.86	136951.84	114454.37	109256.35	148165.86	136951.84	114454.37	109256.35
	Nitrogen	31.01	28.66	23.95	22.86	31.01	28.66	23.95	22.86
	Steam	2728.60	2522.08	2107.77	2012.05	2728.60	2522.08	2107.77	2012.05
	Citric acid	-	1297.29	-	-	-	1297.29	-	-
	Mn_2O_3	-	416.55	-	-	-	416.55	-	-
	O_2	-	324.44	-	-	-	324.44	-	-
	N2	934.63	356.66	-	-	934.63	356.66	-	-
	H_2SO_4	-	1369.99	2070.03	-	-	1369.99	2070.03	-
	HCl	-	43.37	33.71	1711.70	-	43.37	33.71	1711.70
	H3PO4	2279.90	-	-	-	2279.90	-	-	-
	H_2O_2	-	357.87	313.90	-	-	357.87	313.90	-
	NH_3	-	28.29	42.92	37.74	-	28.29	42.92	37.74
	NaOH	-	1042.79	1582.10	1391.29	-	1042.79	1582.10	1391.29
	Sodium carbonate (Na_2CO_3)	389.75	470.68	463.89	468.58	389.75	470.68	463.89	468.58
	Li_2CO_3	271.65	322.23	340.87	-	271.65	322.23	340.87	-
	LiOH	-	-	-	185.95	-	-	-	-
	Glucose	237.82	-	-	-	237.82	-	-	-
	Deionised water	15243.83	14290.55	11944.59	8996.73	15243.83	14290.55	11944.59	8996.73
Energy input (kg)	Electricity: Discharging (kWh)	47.37	34.88	34.38	31.70	47.37	34.88	34.38	31.70
	Electricity: Anode crushing (kWh)	26.87	20.33	20.72	21.43	26.87	20.33	20.72	21.43
	Electricity: Cathode crushing (kWh)	43.29	40.22	30.89	28.99	43.29	40.22	30.89	28.99
	Heat: NMP soaking (MJ)	439.51	401.00	336.36	321.30	439.51	401.00	336.36	321.30
	Electricity: Calcination (kWh)	29.13	27.97	21.28	67.00	29.13	27.97	21.28	67.00
	Heat: Calcination (MJ)	2634.01	2529.67	1924.47	1767.13	2634.01	2529.67	1924.47	1767.13

	Electricity: Grinding (kWh)	4.52	4.35	3.30	3.02	4.52	4.35	3.30	3.02
	Heat: Leaching (MJ)	16.29	15.66	11.88	10.87	16.29	15.66	11.88	10.87
	Electricity: Precipitation (kWh)	87.43	80.86	62.85	55.27	87.43	80.86	62.85	55.27
	Heat: Precipitation (MJ)	20827.97	19261.32	14972.86	13166.99	20827.97	19261.32	14972.86	13166.99
	Electricity: 2nd calcination (kWh)	8093.73	3837.31	5818.44	5116.68	8093.73	3837.31	5818.44	5116.68
	Heat: 2nd calcination (MJ)	-	6942.53	-	-	-	6942.53	-	-
Output waste (kg)	Waste copper	2.41	1.48	1.55	1.56	2.92	1.90	1.95	1.95
	Waste aluminium	16.96	7.71	8.82	9.05	16.96	7.71	8.82	9.05
	Waste printed wiring board	9.66	7.43	6.66	6.47	14.29	11.12	9.92	9.62
	Waste chromium steel 18/8	3.09	2.38	2.13	2.07	4.57	3.56	3.17	3.08
	Waste coolant	77.77	53.11	58.63	60.14	155.54	106.22	117.25	120.28
	Waste fibre glass	186.42	112.69	124.37	127.43	186.42	112.69	124.37	127.43
	Waste steel	13.37	6.11	7.52	7.92	245.48	191.10	170.70	165.77
	Waste PP	20.88	8.47	9.71	9.78	20.88	8.47	9.71	9.78
	Waste PE	4.77	1.89	2.15	2.16	4.77	1.89	2.15	2.16
	Waste PET	4.16	2.17	2.57	2.67	4.16	2.17	2.57	2.67
	Waste sludge	18573.66	19141.90	16644.99	12906.23	19508.29	19141.90	16644.99	12906.23
	Waste PVDF	36.68	33.93	28.35	27.05	36.68	33.93	28.35	27.05
Avoided material (kg)	Chromium steel 18/8	35.54	27.32	24.51	23.83	52.58	40.91	36.49	35.42
	Aluminium	322.23	146.45	167.49	171.95	322.23	146.45	167.49	171.95
	Copper	305.63	163.74	175.49	176.11	344.07	195.62	205.65	205.75
	Cathode active material	1189.10	-	845.83	743.81	1189.10	-	845.83	743.81
	NMC532 (from LMO+NMC532)	-	557.50	-	-	-	557.50	-	-
	LMO (from LMO+NMC532)	-	453.76	-	-	-	453.76	-	-
	Citric acid	-	1167.56	-	-	-	1167.56	-	-
	Li_2CO_3	204.25	322.23	322.87	261.70	204.25	322.23	322.87	261.70
	NMP	1815.11	1677.73	1402.12	1338.44	1815.11	1677.73	1402.12	1338.44
Emitted (kg)	CO_2	2488.81	2165.35	2155.70	2008.15	2488.81	2165.35	2155.70	2008.15
	N_2	934.63	356.66	-	-	934.63	356.66	-	-

Table S10. Material input and output of hydrometallurgical recycling for EOL LIB packs with an initial energy storage capacity of 562.5 kWh (NMC333, NMC532, NMC811)[21,32,34,75,77,81-83]

		After EV use			After cascaded use		
		NMC333	NMC532	NMC811	NMC333	NMC532	NMC811
Material input (kg)	EV LIB pack	2431.72	2330.39	2145.40	-	-	-
	ESS LIB pack	-	-	-	2398.90	2297.31	2095.49
	Waste aluminium	-	-	-	53.35	51.58	52.84
	Waste fibre glass	-	-	-	122.82	118.73	121.64
	Waste copper	-	-	-	50.97	49.23	46.46
	Waste printed wiring board	-	-	-	7.30	6.99	6.44
	Waste steel	-	-	-	29.18	27.96	25.74
	Waste coolant	-	-	-	57.98	55.92	57.33
	NMP	1604.77	1545.32	1352.91	1604.77	1545.32	1352.91
	Decarbonised water	129600.44	124807.87	110188.79	129600.44	124807.87	110188.79
	Nitrogen	27.12	26.12	23.06	27.12	26.12	23.06
	Steam	2386.70	2298.44	2029.22	2386.70	2298.44	2029.22
	Citric acid	-	-	-	-	-	-
	Mn_2O_3	-	-	-	-	-	-
	O_2	-	-	-	-	-	-
	N2	-	-	-	-	-	-
	H_2SO_4	2465.66	2380.94	1749.92	2465.66	2380.94	1749.92
	HCl	39.99	38.62	28.62	39.99	38.62	28.62
	H3PO4	-	-	-	-	-	-
	H_2O_2	372.36	359.57	266.45	372.36	359.57	266.45
	NH_3	50.91	49.16	36.43	50.91	49.16	36.43
	NaOH	1876.79	1812.30	1342.95	1876.79	1812.30	1342.95
	Sodium carbonate (Na_2CO_3)	552.96	533.45	392.10	552.96	533.45	392.10
	Li_2CO_3	404.36	390.47	289.34	404.36	390.47	289.34
	LiOH	-	-	-	-	-	-
	Glucose	-	-	-	-	-	-
	Deionised water	14169.39	13682.55	10139.01	14169.39	13682.55	10139.01
Energy input (kg)	Electricity: Discharging (kWh)	40.98	39.53	28.98	40.98	39.53	28.98
	Electricity: Anode crushing (kWh)	21.58	20.53	21.17	21.58	20.53	21.17
	Electricity: Cathode crushing (kWh)	36.47	35.14	28.38	36.47	35.14	28.38
	Heat: NMP soaking (MJ)	380.40	366.05	322.80	380.40	366.05	322.80
	Electricity: Calcination (kWh)	25.21	24.34	19.30	25.21	24.34	19.30
	Heat: Calcination (MJ)	2279.72	2201.19	1745.39	2279.72	2201.19	1745.39
	Electricity: Grinding (kWh)	3.91	3.78	2.80	3.91	3.78	2.80
	Heat: Leaching (MJ)	14.09	13.61	10.08	14.09	13.61	10.08
	Electricity: Precipitation (kWh)	74.56	72.00	53.35	74.56	72.00	53.35
	Heat: Precipitation (MJ)	17761.71	17151.44	12709.52	17761.71	17151.44	12709.52
	Electricity: 2^{nd} calcination (kWh)	6902.19	6665.03	4938.91	6902.19	6665.03	4938.91
	Heat: 2^{nd} calcination (MJ)	-	-	-	-	-	-
Output waste (kg)	Waste copper	1.60	1.52	1.50	2.02	1.93	1.89
	Waste aluminium	8.73	8.25	8.47	8.73	8.25	8.47
	Waste printed wiring board	7.30	6.99	6.44	10.89	10.44	9.58
	Waste chromium steel 18/8	2.33	2.24	2.06	3.49	3.34	3.07
	Waste coolant	57.98	55.92	57.33	115.95	111.84	114.66
	Waste fibre glass	122.82	118.73	121.64	122.82	118.73	121.64
	Waste steel	7.32	6.83	7.18	183.80	179.51	164.69
	Waste PP	9.95	10.97	10.80	9.95	10.97	10.80
	Waste PE	2.22	2.49	2.43	2.22	2.49	2.43
	Waste PET	2.50	2.35	2.48	2.50	2.35	2.48
	Waste sludge	19717.95	19033.48	14175.13	19717.95	19033.48	14175.13

	Waste PVDF	31.88	30.92	51.06	31.88	30.92	51.06
Avoided material (kg)	Chromium steel 18/8	26.85	25.73	23.69	40.09	38.41	35.25
	Aluminium	165.96	156.80	160.94	165.96	156.80	160.94
	Copper	180.83	169.23	167.08	212.89	200.33	196.68
	Cathode active material	1003.37	968.90	717.97	1003.37	968.90	717.97
	NMC532 (from LMO+NMC532)	-	-	-	-	-	-
	LMO (from LMO+NMC532)	-	-	-	-	-	-
	Citric acid	-	-	-	-	-	-
	Li_2CO_3	384.87	371.29	272.91	384.87	371.29	272.91
	NMP	1587.67	1528.96	1349.87	1587.67	1528.96	1349.87
Emitted (kg)	CO_2	2283.81	2189.05	2280.81	2283.81	2189.05	2280.81
	N_2	-	-	-	-	-	-

S5.2 Direct cathode recycling

Figure S24 depicts the process design of direct cathode recycling and Table S11–Table S12 details the bill of materials and energy. The direct cathode recycling process focuses on recovering the cathode active material and electrolyte with limited processing. The discharging and dismantling are assumed to be the same as described in that of hydrometallurgical recycling. After dismantling, cathode, anode, and electrolyte are crushed first. Electricity is used in this step. Then the electrolyte is extracted by liquid CO_2 at 25 ℃ and 60 bar with a flow rate of 15 L/min, additional solvent, namely acetonitrile (ACN) and propylene carbonate (PC) (3:1), are added to the liquid CO_2 stream with a flow rate of 0.5 mL/min.[37] This process is assumed to be operated in a dry room supported by both heat and electricity.[37,77] Experiment showed that the recovery rate of lithium hexafluorophosphate ($LiPF_6$), EC, and DMC were 100%, 75.76%, and 81.71%, respectively. The extraction time varies according to the amount of electrolyte and the ratio of $LiPF_6$, EC, and EMC.[37] We assume no loss for ACN, PC, and CO_2. After the electrolyte is extracted and recovered, the residues undergo steps of size reduction and final separation which both require electricity.[77] Then, they are soaked in NMP to dissolve PVDF as described in the hydrometallurgical recycling, so do the NMP recovery, the combustion of graphite and carbon

black, the recovery of copper and aluminium, and the municipal incineration of PVDF. The next steps for aged cathode active material of LMO+NMC532, NMC, and NCA are hydrothermal treatment with LiOH and annealing process. During the hydrothermal process, the aged cathode active material is put in LiOH solution at 220 °C for four hours with a volume ratio of solid to liquid equals 1:1.[36] The amount of LiOH depends on the cyclable lithium ion loss, which is assumed to be 10% after first use and 20% after cascaded use.[84] A 5% (molar) excess of lithium ions than needed is assumed to be applied. The residues are washed, dried, and annealed at 800 °C for four hours. The energy input for hydrothermal treatment and annealing is assumed to be 1.59 MJ/kg and 4.29 MJ/kg aged cathode active material.[36] For LFP, this step is called solid-phase sintering which directly regenerates LFP at 700 °C with doping of new LFP at a ratio of 3:7.[40]

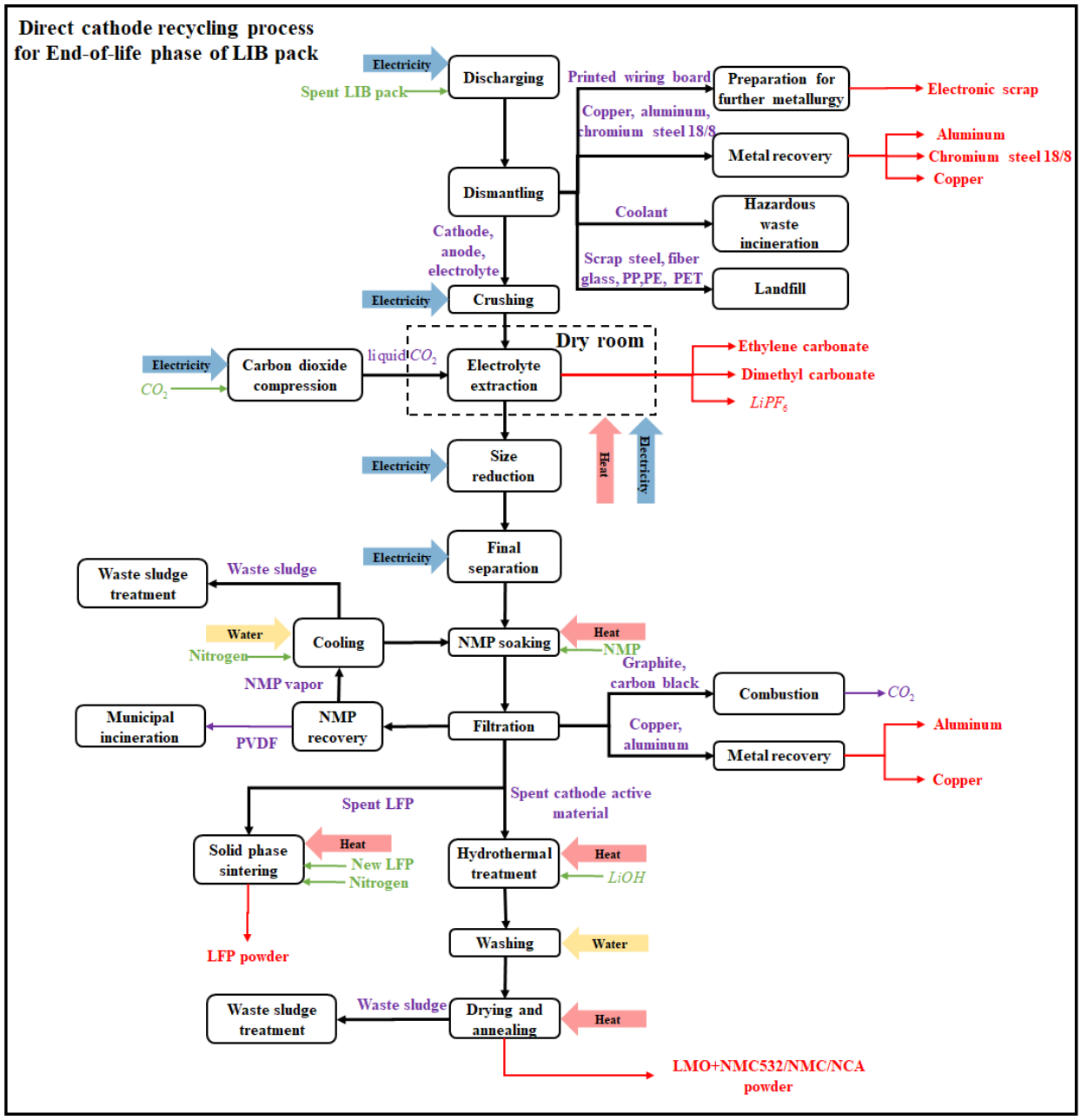

Figure S24. Process diagram of the direct cathode recycling

Table S11. Material input and output of direct cathode recycling for EOL LIB packs with an initial energy storage capacity of 562.5 kWh (LFP, LMO+NMC532, NMC622, NCA)[21,37,40,77,81,85,86]

		After EV use				After cascaded use			
		LFP	LMO+ NMC	NMC622	NCA	LFP	LMO+ NMC	NMC622	NCA
Material input (kg)	EV LIB pack	3218.89	2475.02	2220.15	2158.19	-	-	-	-
	ESS LIB pack	-	-	-	-	3087.93	2461.03	2170.89	2100.00
	Waste aluminium	-	-	-	-	126.39	48.95	54.03	55.36
	Waste fibre glass	-	-	-	-	186.42	112.69	124.37	127.43
	Waste copper	-	-	-	-	64.08	50.97	47.58	46.65
	Waste printed wiring board	-	-	-	-	9.66	7.43	6.66	6.47
	Waste steel	-	-	-	-	38.63	29.70	26.64	25.90
	Waste coolant	-	-	-	-	77.77	53.11	58.63	60.14
	NMP	1834.54	1695.68	1417.13	1352.78	1834.54	1695.68	1417.13	1352.78
	Decarbonised water	148165.86	136951.84	114454.37	109256.35	148165.86	136951.84	114454.37	109256.35
	Nitrogen	31.01	28.66	23.95	22.86	31.01	28.66	23.95	22.86
	Steam	2728.60	2522.08	2107.77	2012.05	2728.60	2522.08	2107.77	2012.05
	LiOH	-	29.08	22.06	20.23	-	58.15	44.12	40.46
	LFP	498.52	-	-	-	498.52	-	-	
	Deionised water	-	5893.74	4470.92	4102.25	-	6195.70	4699.99	4314.27
	N_2	1306.13	-	-	-	1306.13	-	-	-
	CO_2	144086.72	87957.05	78334.82	75744.22	144086.72	87957.05	78334.82	75744.22
	Acetonitrile (ACN)	857.97	523.74	466.45	451.02	857.97	523.74	466.45	451.02
	Propylene carbonate (PC)	438.45	267.65	238.37	230.48	438.45	267.65	238.37	230.48
Energy input (kg)	Electricity: Discharging (kWh)	47.37	34.88	34.38	31.70	47.37	34.88	34.38	31.70
	Electricity: Liquid CO_2 compression (kWh)	14120.50	8619.79	7676.81	7422.93	14120.50	8619.79	7676.81	7422.93
	Electricity: Size reduction (kWh)	167.25	135.51	117.42	113.00	167.25	135.51	117.42	113.00
	Electricity: Final separation (kWh)	14.42	11.68	10.12	9.74	14.42	11.68	10.12	9.74
	Electricity: Dry room operation (kWh)	456.36	369.74	320.40	369.27	456.36	369.74	320.40	369.27
	Heat: Dry room operation (MJ)	3011.99	2440.31	2114.60	2437.20	3011.99	2440.31	2114.60	2437.20
	Heat: NMP soaking (MJ)	439.51	401.00	336.36	321.30	439.51	401.00	336.36	321.30
	Heat: Hydrothermal process (MJ)	-	1778.19	1348.91	1003.68	-	1778.19	1348.91	1003.68

	Heat: Annealing process (MJ)	9980.39	4797.75	3639.52	3337.82	9980.39	4797.75	3639.52	3337.82
Output waste (kg)	Waste copper	2.41	1.48	1.55	1.56	2.92	1.90	1.95	1.95
	Waste aluminium	16.96	7.71	8.82	9.05	16.96	7.71	8.82	9.05
	Waste printed wiring board	9.66	7.43	6.66	6.47	14.29	11.12	9.92	9.62
	Waste chromium steel 18/8	3.09	2.38	2.13	2.07	4.57	3.56	3.17	3.08
	Waste coolant	77.77	53.11	58.63	60.14	155.54	106.22	117.25	120.28
	Waste fibre glass	186.42	112.69	124.37	127.43	186.42	112.69	124.37	127.43
	Waste steel	13.37	6.11	7.52	7.92	245.48	191.10	170.70	165.77
	Waste PP	20.88	8.47	9.71	9.78	20.88	8.47	9.71	9.78
	Waste PE	4.77	1.89	2.15	2.16	4.77	1.89	2.15	2.16
	Waste PET	4.16	2.17	2.57	2.67	4.16	2.17	2.57	2.67
	Waste sludge	-	6039.70	4585.59	4208.89	-	6370.74	4836.71	4441.13
	Waste PVDF	36.68	33.93	28.35	27.05	36.68	33.93	28.35	27.05
Avoided material (kg)	Chromium steel 18/8	35.54	27.32	24.51	23.83	52.58	40.91	36.49	35.42
	Aluminium	322.23	146.45	167.49	171.95	322.23	146.45	167.49	171.95
	Copper	305.63	163.74	175.49	176.11	344.07	195.62	205.65	205.75
	Cathode active material	1661.74	1062.44	805.95	739.14	1661.74	1062.44	805.95	739.14
	$LiPF_6$	96.13	96.13	96.13	96.13	96.13	96.13	96.13	96.13
	EC	101.42	47.72	38.52	36.04	101.42	47.72	38.52	36.04
	DMC	109.51	51.54	41.60	38.92	109.51	51.54	41.60	38.92
	CO_2	144086.72	87957.05	78334.82	75744.22	144086.72	87957.05	78334.82	75744.22
	ACN	857.97	523.74	466.45	451.02	857.97	523.74	466.45	451.02
	PC	438.45	267.65	238.37	230.48	438.45	267.65	238.37	230.48
Emitted (kg)	CO_2	2488.81	2165.35	2155.70	2008.15	2488.81	2165.35	2155.70	2008.15
	N_2	1306.13	-	-	-	1306.13	-	-	-

Table S12. Material input and output of direct cathode recycling for EOL LIB packs with an initial energy storage capacity of 562.5 kWh (NMC333, NMC532, NMC811) [21,37,77,81,85,86]

		After EV use			After cascaded use		
		NMC333	NMC532	NMC811	NMC333	NMC532	NMC811
Material input (kg)	EV LIB pack	2431.72	2330.39	2145.40	-	-	-
	ESS LIB pack	-	-	-	2398.90	2297.31	2095.49
	Waste aluminium	-	-	-	53.35	51.58	52.84
	Waste fibre glass	-	-	-	122.82	118.73	121.64
	Waste copper	-	-	-	50.97	49.23	46.46
	Waste printed wiring board	-	-	-	7.30	6.99	6.44
	Waste steel	-	-	-	29.18	27.96	25.74
	Waste coolant	-	-	-	57.98	55.92	57.33
	NMP	1604.77	1545.32	1352.91	1604.77	1545.32	1352.91
	Decarbonised water	129600.44	124807.87	110188.79	129600.44	124807.87	110188.79
	Nitrogen	27.12	26.12	23.06	27.12	26.12	23.06
	Steam	2386.70	2298.44	2029.22	2386.70	2298.44	2029.22
	LiOH	26.17	25.27	18.72	52.33	50.53	37.45
	LFP	-	-	-	-	-	-
	Deionised water	5303.68	5121.45	3795.09	5575.41	5383.84	3989.52
	N_2	-	-	-	-	-	-

	CO_2	85243.09	80061.89	77594.65	85243.09	80061.89	77594.65
	Acetonitrile (ACN)	507.58	476.73	462.04	507.58	476.73	462.04
	Propylene carbonate (PC)	259.39	243.62	236.12	259.39	243.62	236.12
Energy input (kg)	Electricity: Discharging (kWh)	40.98	39.53	28.98	40.98	39.53	28.98
	Electricity: Liquid CO_2 compression (kWh)	8353.82	7846.06	7604.28	8353.82	7846.06	7604.28
	Electricity: Size reduction (kWh)	130.90	125.33	113.26	130.90	125.33	113.26
	Electricity: Final separation (kWh)	11.28	10.80	9.76	11.28	10.80	9.76
	Electricity: Dry room operation (kWh)	357.17	341.98	309.04	357.17	341.98	309.04
	Heat: Dry room operation (MJ)	2357.35	2257.05	2039.65	2357.35	2257.05	2039.65
	Heat: NMP soaking (MJ)	380.40	366.05	322.80	380.40	366.05	322.80
	Heat: Hydrothermal process (MJ)	1600.16	1545.18	1145.01	1600.16	1545.18	1145.01
	Heat: Annealing process (MJ)	4317.42	4169.08	3089.36	4317.42	4169.08	3089.36
Output waste (kg)	Waste copper	1.60	1.52	1.50	2.02	1.93	1.89
	Waste aluminium	8.73	8.25	8.47	8.73	8.25	8.47
	Waste printed wiring board	7.30	6.99	6.44	10.89	10.44	9.58
	Waste chromium steel 18/8	2.33	2.24	2.06	3.49	3.34	3.07
	Waste coolant	57.98	55.92	57.33	115.95	111.84	114.66
	Waste fibre glass	122.82	118.73	121.64	122.82	118.73	121.64
	Waste steel	7.32	6.83	7.18	183.80	179.51	164.69
	Waste PP	9.95	10.97	10.80	9.95	10.97	10.80
	Waste PE	2.22	2.49	2.43	2.22	2.49	2.43
	Waste PET	2.50	2.35	2.48	2.50	2.35	2.48
	Waste sludge	5437.84	5249.01	3898.54	5735.74	5536.67	4111.70
	Waste PVDF	31.88	30.92	51.06	31.88	30.92	51.06
Avoided material (kg)	Chromium steel 18/8	26.85	25.73	23.69	40.09	38.41	35.25
	Aluminium	165.96	156.80	160.94	165.96	156.80	160.94
	Copper	180.83	169.23	167.08	212.89	200.33	196.68
	Cathode active material	956.07	923.22	684.12	956.07	923.22	684.12
	$LiPF_6$	96.13	96.13	96.13	96.13	96.13	96.13
	EC	45.13	40.17	37.81	45.13	40.17	37.81
	DMC	48.73	43.38	40.83	48.73	43.38	40.83
	CO_2	85243.09	80061.89	77594.65	85243.09	80061.89	77594.65
	ACN	507.58	476.73	462.04	507.58	476.73	462.04
	PC	259.39	243.62	236.12	259.39	243.62	236.12
Emitted (kg)	CO_2	2283.81	2189.05	2280.81	2283.81	2189.05	2280.81
	N_2	-	-	-	-	-	-

S5.3 Pyrometallurgical recycling

Figure S25 depicts the process design of pyrometallurgical recycling. Table S14–Table S15 details the bill of materials and energy. Pyrometallurgical recycling is developed by Umicore and is designed to recover Ni and Co by forming an alloy through a three-stage smelting. The spent LIB pack is disassembled to the module level and disposed as described in that of the hydrometallurgical recycling. After disassembly, the left spent LIB modules are fed directly into the smelting furnace together with slag-forming materials such as limestone, sand, and slag and a

commonly used reducing agent in metal smelting, namely, coke. The furnace can be divided into three zones: the preheating zone (under 300 ℃), the plastics pyrolyzing zone (700 ℃), and the metal melting and reducing zone (ranged from 1200 to 1450 ℃). The preheating zone and plastics pyrolyzing zone is where the electrolyte is evaporated and where the plastics are melted. Heated air is injected into the last zone where blast furnace slag and alloy are subsequently formed.[27] Flue gas containing CO_2, carbon monoxide (CO), formaldehyde, ethylene, acetylene, soot, hydrogen fluoride (HF), and a negligible amount of silicon tetrafluoride, as well as hydrocarbons, is formed from the electrolyte evaporation.[87] Moreover, blast furnace gas containing CO_2, CO, hydrogen, and nitrogen, is formed during alloy formation.[88] The content of the gaseous phase is given in Table S16–Table S17. The gaseous phase is post-combusted in a combined heat and power generation (CHP) facility and complete combustion is assumed. The total CHP efficiency is assumed to be 69%, of which, heat and electricity are generated with efficiencies of 33% and 36%, respectively.[89] During CHP, CO_2, and HF are formed, where CO_2 is emitted, and HF is assumed to be recovered by water. Plastics are assumed to be treated the same as if it is sent to the municipal incineration. The slag containing 100% of Li and Al, 7.2% of copper (Cu), and 35.5% of iron (Fe) from the input are assumed to be granulated blast furnace slag and can be used as strength-enhancing compound for concrete. The alloy consists of 92.8% Cu, 64.5% Fe, 99% Ni, and 94% Co from the input and can be treated to recover metals.[27] The alloy is first leached by 6 M HCl at 95 ℃ with an S:L ratio of 100 g/L for three hours. The leaching efficiencies are 62%, 96%, 99%, and 98% for Co, Ni, Fe, and Cu.[35] By adding iron scraps to the leachate, the copper ions are replaced by iron and precipitated at 80 ℃. Next, Na_2CO_3 and sodium chlorate ($NaClO_3$) are added to precipitate goethite according to Equation (12).

$$6FeCl_2 + NaClO_3 + 3H_2O + 6Na_2CO_3 \rightleftharpoons 6FeOOH\downarrow + 13NaCl \quad (12)$$

After copper and goethite precipitation, NaOH is added to the solution to precipitate $Ni(OH)_2$. The avoided $Ni(OH)_2$ is assumed to be precipitated from the reaction of NaOH and $NiSO_4$ as shown in Equation (13). The bill of materials for producing $Ni(OH)_2$ is given in Table S13. The by-product of sodium sulfate is excluded from the system boundary using the concept of "recycled content" approach. The energy demand for this reaction is assumed to be negligible.

$$NiSO_{4\,(aq)} + 2NaOH_{(aq)} \rightarrow Ni(OH)_{2\,(s)} + Na_2SO_{4\,(aq)} \quad (13)$$

In the end, only Co ions are left in the solution. We assume that the precipitates are washed and recovered. In addition, the cobalt ion solution is also assumed to be recovered.

Table S13. Material input and output of $Ni(OH)_2$ production[30]

Input		Amount
Material	$NiSO_4$ (kg)	1.67
	NaOH (kg)	0.86
Transport	Rail (t·km)	1.50
	Road (t·km)	0.25
Infrastructure	Chemical plant construction (unit)	4.6E-10
Output	$Ni(OH)_2$ (kg)	1.00

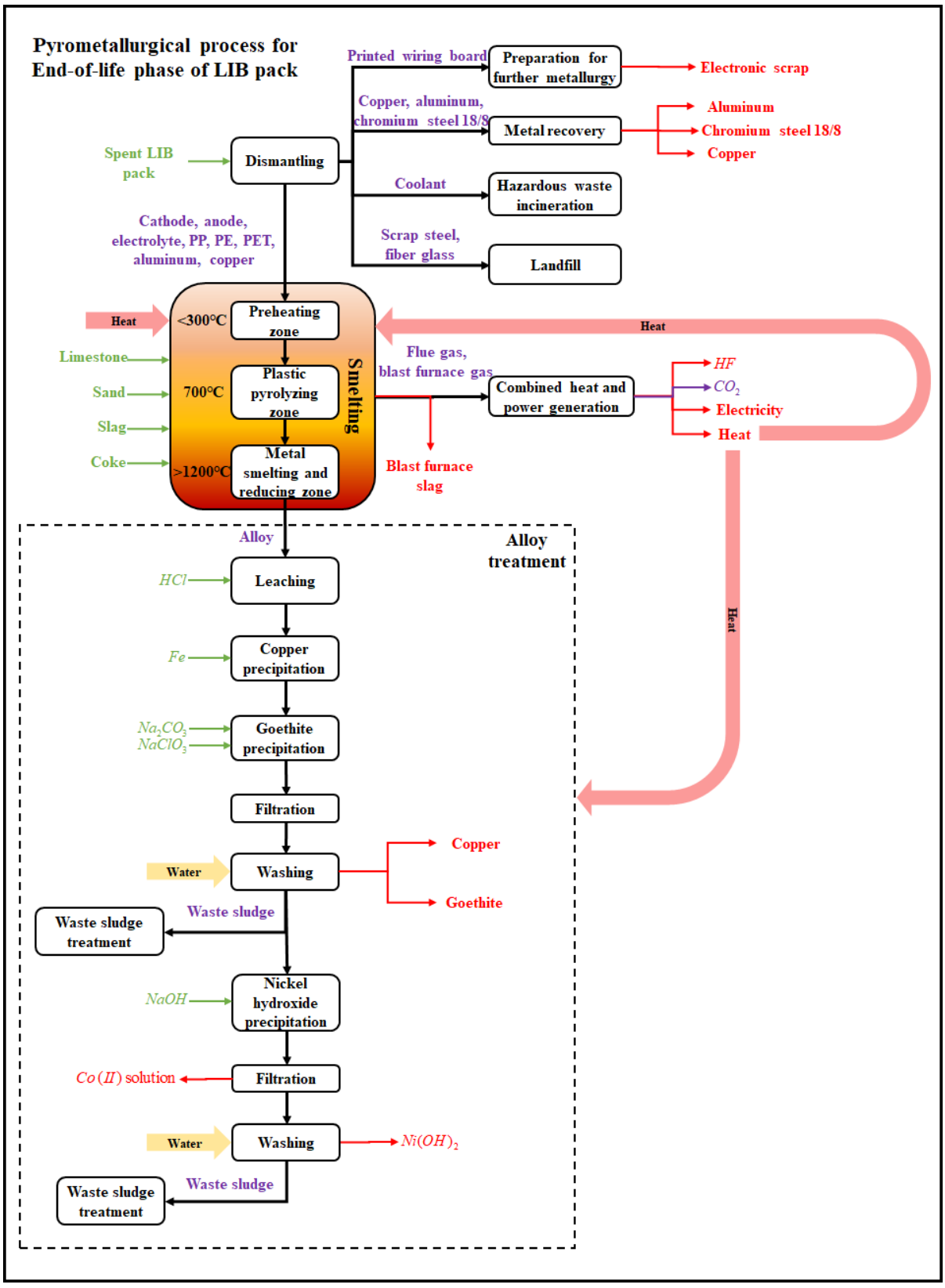

Figure S25. Process diagram of the pyrometallurgical recycling

Table S14. Material input and output of pyrometallurgical recycling for EOL LIB packs with an initial energy storage capacity of 562.5 kWh (LMO+NMC532, NMC622, NCA)[27,32,34,35,83,87-89]

		After EV use			After cascaded use		
		LMO+NMC	NMC622	NCA	LMO+NMC	NMC622	NCA
Material input (kg)	EV LIB pack	2475.02	2220.15	2158.19	-	-	-
	ESS LIB pack	-	-	-	2461.03	2170.89	2100.00
	Waste aluminium	-	-	-	48.95	54.03	55.36
	Waste fibre glass	-	-	-	112.69	124.37	127.43
	Waste copper	-	-	-	50.97	47.58	46.65
	Waste printed wiring board	-	-	-	7.43	6.66	6.47
	Waste steel	-	-	-	29.70	26.64	25.90
	Waste coolant	-	-	-	53.11	58.63	60.14
	Limestone	180.51	157.89	152.36	195.92	171.49	165.51
	Sand	198.56	173.68	167.60	215.51	188.64	182.06
	Slag	361.01	315.79	304.72	391.84	342.98	331.03
	Coke	722.02	631.58	609.44	783.68	685.97	662.05
	HCl	817.82	1148.43	1890.20	818.26	1148.81	1890.57
	Iron	93.50	105.95	107.23	93.50	105.95	107.23
	$NaClO_3$	30.36	34.21	34.59	30.42	34.27	34.64
	Na_2CO_3	181.39	204.41	206.69	181.77	204.74	207.01
	H_2SO_4	643.92	976.94	-	643.92	976.94	-
	H_2O_2	96.22	145.98	-	96.22	145.98	-
	NaOH	261.58	396.87	489.83	261.58	396.87	489.83
	Deionised water	13186.72	9057.55	10405.03	13194.10	9060.89	10408.26
Energy input	Heat: Smelting (MJ)	1447.37	1266.07	1221.69	1570.98	1375.10	1327.16
	Heat: Leaching (MJ)	47.32	66.45	71.89	47.35	66.48	71.91
Output waste (kg)	Waste copper	0.66	0.62	0.61	1.08	1.02	1.00
	Waste aluminium	2.45	2.70	2.77	2.45	2.70	2.77
	Waste printed wiring board	7.43	6.66	6.47	14.29	10.44	9.58
	Waste chromium steel 18/8	2.38	2.13	2.07	4.57	3.34	3.07
	Waste coolant	53.11	58.63	60.14	155.54	111.84	114.66
	Waste fibre glass	112.69	124.37	127.43	186.42	118.73	121.64
	Waste steel	6.11	7.52	7.92	245.48	179.51	164.69
	Waste sludge	15021.97	11687.50	12752.65	14845.12	11298.66	12598.67
	Incinerated PVDF	33.93	28.35	27.05	36.68	30.92	51.06
	Evaporated NMP	16.29	13.61	12.98	16.29	13.61	12.98
	Incinerated PP	8.47	9.71	9.78	20.88	10.97	10.80
	Incinerated PE	1.89	2.15	2.16	4.77	2.49	2.43
	Incinerated PET	2.17	2.57	2.67	4.16	2.35	2.48
Avoided material (kg)	Chromium steel 18/8	27.32	24.51	23.83	40.91	36.49	35.42
	Aluminium	46.50	51.33	52.59	46.50	51.33	52.59
	Copper	153.98	164.44	164.93	185.86	194.60	194.57
	Slag	1704.10	1222.61	1091.55	1952.10	1441.36	1303.16
	Hydrogen fluoride (HF)	44.38	44.38	44.38	44.38	44.38	44.38
	$Ni(OH)_2$	304.17	461.47	569.57	304.17	461.47	569.57
	$CoSO_4$	104.72	158.88	-	104.72	158.88	-
	$CoCl_2$	-	-	88.51	-	-	88.51
	Goethite	150.76	169.89	171.79	151.07		172.05
Avoided energy	Heat (MJ)	2912.08	2545.57	2436.67	3158.61	2763.03	2666.10
	Electricity (kWh)	882.45	771.39	738.39	957.15	837.28	807.91
Emitted	Heat (MJ)	1417.39	1213.05	1143.09	1540.27	1321.45	1267.02
	CO_2 (kg)	4481.63	4146.30	4092.68	4678.33	4319.81	4260.52
	N_2 (kg)	2012.64	1760.52	1698.81	2184.52	1912.14	1845.48

Table S15. Material input and output of pyrometallurgical recycling for EOL LIB packs with an initial energy storage capacity of 562.5 kWh (NMC333, NMC532, NMC811) [27,32,34,35,83,87-89]

		After EV use			After cascaded use		
		NMC333	NMC532	NMC811	NMC333	NMC532	NMC811
Material input (kg)	EV LIB pack	2431.72	2330.39	2145.40	-	-	-
	ESS LIB pack	-	-	-	2398.90	2297.31	2095.49
	Waste aluminium	-	-	-	53.35	51.58	52.84
	Waste fibre glass	-	-	-	122.82	118.73	121.64
	Waste copper	-	-	-	50.97	49.23	46.46
	Waste printed wiring board	-	-	-	7.30	6.99	6.44
	Waste steel	-	-	-	29.18	27.96	25.74
	Waste coolant	-	-	-	57.98	55.92	57.33
	Limestone	175.23	167.76	152.31	190.26	182.15	165.44
	Sand	192.76	184.54	167.54	209.29	200.37	181.98
	Slag	350.47	335.52	304.63	380.52	364.30	330.88
	Coke	700.93	671.05	609.25	761.04	728.61	661.76
	HCl	1317.09	1260.78	1000.17	1317.51	1261.18	1000.54
	Iron	107.59	99.45	99.94	107.59	99.45	99.94
	$NaClO_3$	34.80	32.19	32.28	34.86	32.25	32.34
	Na_2CO_3	207.92	192.34	192.89	208.29	192.69	193.21
	H_2SO_4	1158.91	1119.09	829.27	1158.91	1119.09	829.27
	H_2O_2	173.17	167.22	123.91	173.17	167.22	123.91
	NaOH	470.79	454.61	336.88	470.79	454.61	336.88
	Deionised water	10154.46	9661.18	8017.42	10158.15	9664.71	8020.64
Energy input	Heat: Smelting (MJ)	1405.10	1345.19	1221.32	1525.59	1460.58	1326.57
	Heat: Leaching (MJ)	76.21	72.95	57.87	76.24	72.98	57.90
Output waste (kg)	Waste copper	0.66	0.64	0.60	1.08	1.05	0.99
	Waste aluminium	2.67	2.58	2.64	2.67	2.58	2.64
	Waste printed wiring board	7.30	6.99	6.44	11.12	10.89	9.92
	Waste chromium steel 18/8	2.33	2.24	2.06	3.56	3.49	3.17
	Waste coolant	57.98	55.92	57.33	106.22	115.95	117.25
	Waste fibre glass	122.82	118.73	121.64	112.69	122.82	124.37
	Waste steel	7.32	6.83	7.18	191.10	183.80	170.70
	Waste sludge	13198.68	12582.33	10292.16	12739.69	12137.92	9949.55
	Incinerated PVDF	31.88	30.92	51.06	33.93	31.88	28.35
	Evaporated NMP	15.30	14.84	24.51	15.30	14.84	24.51
	Incinerated PP	9.95	10.97	10.80	8.47	9.95	9.71
	Incinerated PE	2.22	2.49	2.43	1.89	2.22	2.15
	Incinerated PET	2.50	2.35	2.48	2.17	2.50	2.57
Avoided material (kg)	Chromium steel 18/8	26.85	25.73	23.69	40.09	38.41	35.25
	Aluminium	50.68	49.00	50.20	50.68	49.00	50.20
	Copper	169.59	158.86	156.66	201.66	189.96	186.27
	Slag	1375.69	1318.40	1126.19	1617.42	1549.90	1337.34
	Hydrogen fluoride (HF)	44.38	44.38	44.38	44.38	44.38	44.38
	$Ni(OH)_2$	547.43	528.62	391.72	547.43	528.62	391.72
	$CoSO_4$	188.48	182.00	134.87	188.48	182.00	134.87
	$CoCl_2$	-	-	-	-	-	-
	Goethite	172.81	159.86	160.32	173.12	160.15	160.59
Avoided energy	Heat (MJ)	2826.39	2704.26	2455.95	3066.69	2934.38	2665.86
	Electricity (kWh)	856.48	819.47	744.23	929.30	889.21	807.84
Emitted	Heat (MJ)	1345.08	1286.11	1176.76	1464.86	1400.82	1281.39
	CO_2 (kg)	4488.96	4286.64	4223.78	4680.70	4470.26	4391.26
	N_2 (kg)	1953.86	1870.55	1698.30	2121.40	2031.00	1844.65

Table S16. Composition of gaseous phase from electrolyte combustion[87]

	Gas Component	Amount (kg)
Input	Electrolyte	1
Output	CO_2	1.11
	CO	4.90E-03
	Formaldehyde	3.56E-04
	Ethene	8.91E-05
	Ethyne	7.13E-04
	Total hydrocarbon	6.06E-03
	Soot	0.012
	HF	0.099

Table S17. Composition of blast furnace gas from Coking[21,88]

Gas Component	Percentage (w %)
CO_2	28.93
CO	19.33
H_2	0.2
N_2	51.54

S6. Sensitivity analysis for recycling parameters

In addition to electricity generation, LIB recycling affects the most on the life cycle environmental impacts. In this section, we assess the variability in life cycle environmental impacts of LIBs to recycling parameters, including recovery rate of cathode active materials, $Ni(OH)_2$, Co ion solution, other metals, graphite, $LiPF_6$, and chemical agents, as listed in Table S18–Table S21. The upper and lower bound of these recycling parameters are extracted from previous LCA studies and experimental literature.[31,81] Since direct cathode recycling of LFP adopts a solid phase sintering method, which involves no washing, filtration, or separation steps, the recovery rate of LFP is assumed to be 100% and is not investigated in this sensitivity analyses. It is worth mentioning that there are three baseline values for copper recovery. To be specific, 98.7%, 98.3%, and 97.8% represent the recovery rates of copper dismantled from the LIB pack, LIB modules and negative terminals of LIB cells, copper sieved from the anode of LIB cells, and copper recovered from alloy leaching and precipitation following smelting process of pyrometallurgical recycling, respectively.[35,81,90]

Results of sensitivity analyses for recycling parameters are shown in Figure S26–Figure S28. The results suggest that the recovery rate of cathode active materials, aluminium, and NMP is crucial to both the carbon footprint and energy performances of these LIBs. Besides these, improving the recovery rate of citric acid is important to reduce the carbon footprint and CED of hydrometallurgical recycling. The recovery rate of $Ni(OH)_2$ is also an influential recycling parameter to both carbon footprint and CED of LIBs. Moreover, graphite recovery instead of combustion can largely reduce the carbon footprint of hydrometallurgical and direct cathode recycling for all types of LIBs. Notably, even under the best-case scenarios, the carbon footprint mitigation potential of pyrometallurgical and hydrometallurgical recycling is not as good as that of direct cathode recycling under the worst-case scenarios. The results highlight the need to achieve high recovery rates of these parameters during up-scaled recycling.

Table S18. Sensitivity analyses on recycling parameters of LFP[31,81]

Recycling method	Parameter	Baseline	Low	High
Hydrometallurgical recycling	Recovery rate of chromium steel 18/8	92%	90%	99.9%
	Recovery rate of aluminium	95%	70%	99.9%
	Recovery rate of copper	98.7%98.3%	80%	99.9%
	Recovery rate of graphite	0%	-	76.9%
	Recovery rate of LFP	95%	60%	99.9%
	Recovery rate of NMP	98%	80%	99.9%
Direct cathode recycling	Recovery rate of chromium steel 18/8	92%	90%	99.9%
	Recovery rate of aluminium	95%	70%	99.9%
	Recovery rate of copper	98.7%/98.3%	80%	99.9%
	Recovery rate of graphite	0%	-	76.9%
	Recovery rate of $LiPF_6$	100%	70%	-
	Recovery rate of NMP	98%	80%	99.9%

Table S19. Sensitivity analyses on recycling parameters of LMO+NMC532[31,81]

Recycling method	Parameter	Baseline	Low	High
Hydrometallurgical recycling	Recovery rate of chromium steel 18/8	92%	90%	99.9%
	Recovery rate of aluminium	95%	70%	99.9%
	Recovery rate of copper	98.7%98.3%	80%	99.9%
	Recovery rate of graphite	0%	-	76.9%
	Recovery rate of NMC532	90.33%	60%	99.9%
	Conversion efficiency of Mn_2O_3	100%	90%	-
	Recovery rate of citric acid	90%	80%	99.9%
	Recovery rate of NMP	98%	80%	99.9%
Direct cathode recycling	Recovery rate of chromium steel 18/8	92%	90%	99.9%
	Recovery rate of aluminium	95%	70%	99.9%
	Recovery rate of copper	98.7%/98.3%	80%	99.9%
	Recovery rate of graphite	0%	-	76.9%
	Recovery rate of NMC532	95%	60%	99.9%
	Recovery rate of $LiPF_6$	100%	70%	-
	Recovery rate of NMP	98%	80%	99.9%
Pyrometallurgical recycling	Recovery rate of chromium steel 18/8	92%	90%	99.9%
	Recovery rate of aluminium	95%	70%	99.9%
	Recovery rate of copper	98.7%/98.3%/97.78%	80%	99.9%
	Recovery rate of goethite	98.99%	60%	-
	Recovery rate of cobalt as $CoSO_4$	61.81%	60%	99.9%
	Recovery rate of nickel as $Ni(OH)_2$	95.71%	60%	99.9%

Table S20. Sensitivity analyses on recycling parameters of NMC622[31,81]

Recycling method	Parameter	Baseline	Low	High
Hydrometallurgical recycling	Recovery rate of chromium steel 18/8	92%	90%	99.9%
	Recovery rate of aluminium	95%	70%	99.9%
	Recovery rate of copper	98.7%/98.3%	80%	99.9%
	Recovery rate of graphite	0%	-	76.9%
	Recovery rate of NMC622	99.7%	60%	99.9%
	Recovery rate of NMP	98%	80%	99.9%
Direct cathode recycling	Recovery rate of chromium steel 18/8	92%	90%	99.9%
	Recovery rate of aluminium	95%	70%	99.9%
	Recovery rate of copper	98.7%/98.3%	80%	99.9%
	Recovery rate of graphite	0%	-	76.9%
	Recovery rate of NMC622	95%	60%	99.9%
	Recovery rate of $LiPF_6$	100%	70%	-
	Recovery rate of NMP	98%	80%	99.9%
Pyrometallurgical recycling	Recovery rate of chromium steel 18/8	92%	90%	99.9%
	Recovery rate of aluminium	95%	70%	99.9%
	Recovery rate of copper	98.7%/98.3%/97.78%	80%	99.9%
	Recovery rate of goethite	98.99%	60%	-
	Recovery rate of cobalt as $CoSO_4$	61.81%	60%	99.9%
	Recovery rate of nickel as $Ni(OH)_2$	95.71%	60%	99.9%

Table S21. Sensitivity analyses on recycling parameters of NCA[31,81]

Recycling method	Parameter	Baseline	Low	High
Hydrometallurgical recycling	Recovery rate of chromium steel 18/8	92%	90%	99.9%
	Recovery rate of aluminium	95%	70%	99.9%
	Recovery rate of copper	98.7%/98.3%	80%	99.9%
	Recovery rate of graphite	0%	-	76.9%
	Recovery rate of NCA	95.6%	60%	99.9%
	Recovery rate of NMP	98%	80%	99.9%
Direct cathode recycling	Recovery rate of chromium steel 18/8	92%	90%	99.9%
	Recovery rate of aluminium	95%	70%	99.9%
	Recovery rate of copper	98.7%/98.3%	80%	99.9%
	Recovery rate of graphite	0%	-	76.9%
	Recovery rate of NCA	95%	60%	99.9%
	Recovery rate of $LiPF_6$	100%	70%	-
	Recovery rate of NMP	98%	80%	99.9%
Pyrometallurgical recycling	Recovery rate of chromium steel 18/8	92%	90%	99.9%
	Recovery rate of aluminium	95%	70%	99.9%
	Recovery rate of copper	98.7%/98.3%/97.78%	80%	99.9%
	Recovery rate of goethite	98.99%	60%	-
	Recovery rate of cobalt as $CoCl_2$	59.27%	-	99.9%
	Recovery rate of nickel as $Ni(OH)_2$	95.81%	60%	99.9%

Figure S26. Sensitivity analyses for hydrometallurgical recycling on recycling parameters. (a), (b), (c), (d) correspond to the carbon footprint of LFP, LMO+NMC532, NMC622, and NCA LIBs; (e), (f), (g), (h) correspond to CED of LFP, LMO+NMC532, NMC622, and NCA LIBs, respectively.

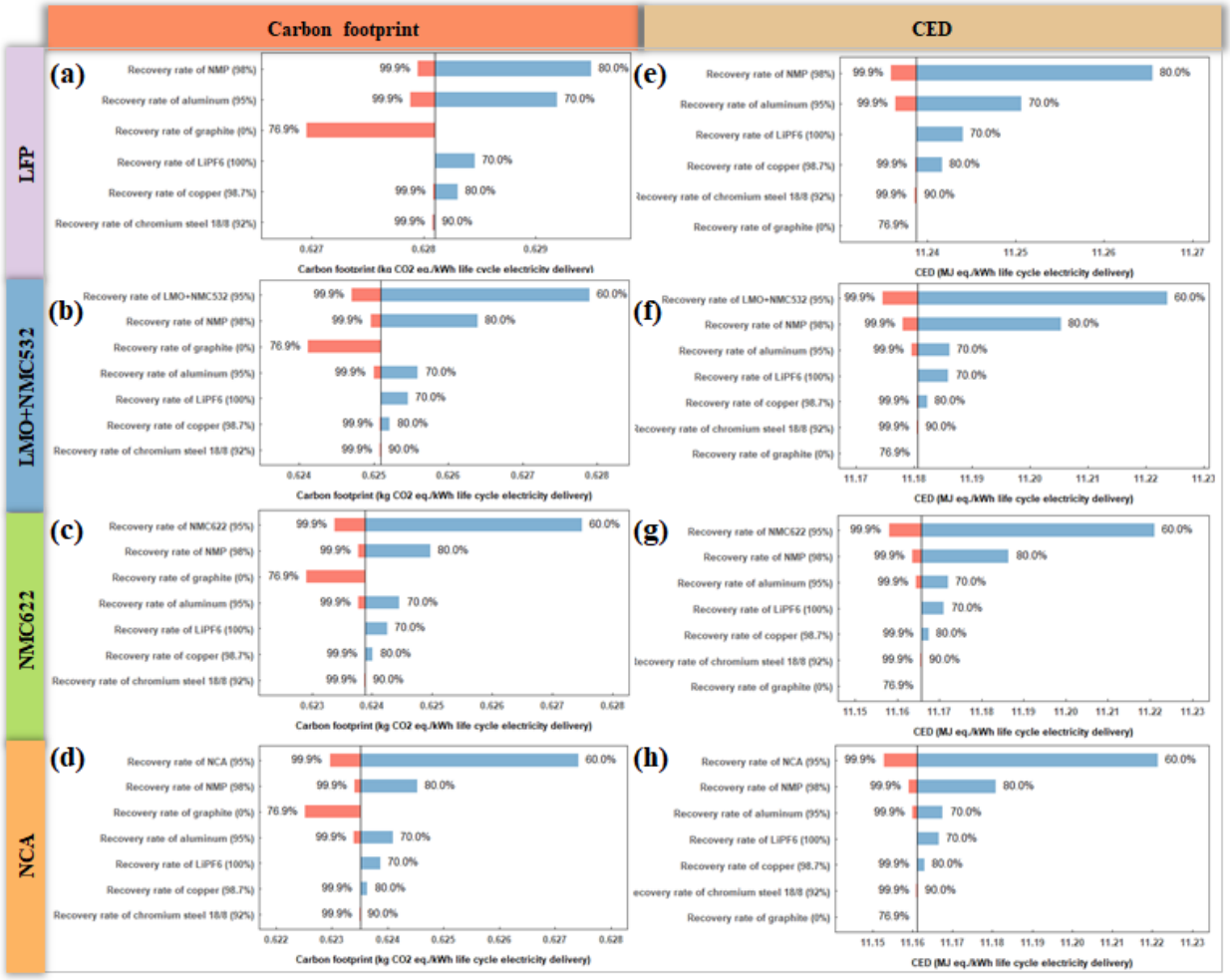

Figure S27. Sensitivity analyses for direct cathode recycling on recycling parameters. (a), (b), (c), (d) correspond to the carbon footprint of LFP, LMO+NMC532, NMC622, and NCA LIBs; (e), (f), (g), (h) correspond to CED of LFP, LMO+NMC532, NMC622, and NCA LIBs, respectively.

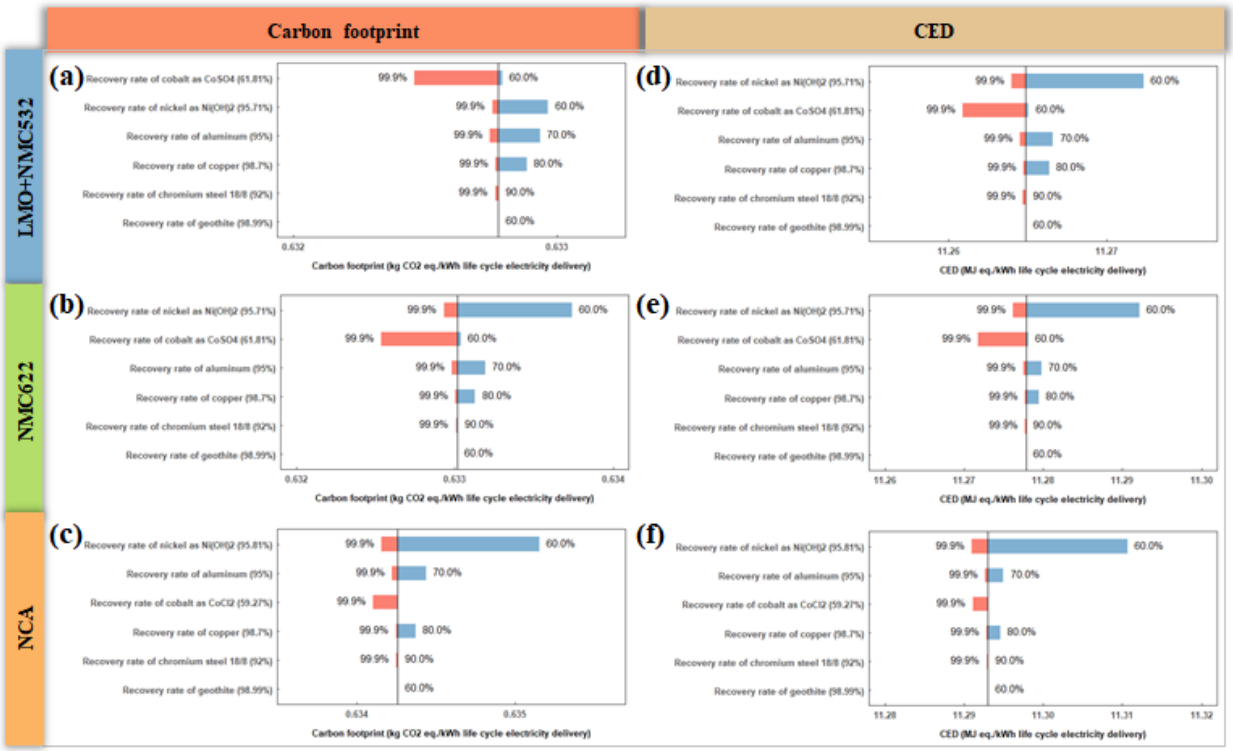

Figure S28. Sensitivity analyses for pyrometallurgical recycling on recycling parameters. (a), (b), (c) correspond to the carbon footprint of LMO+NMC532, NMC622, and NCA LIBs; (d), (e), (f) correspond to CED of LMO+NMC532, NMC622, and NCA LIBs, respectively.

S7. Economic parameters and breakdowns of life cycle costs

The economic parameters of the LIB production, repurpose and recycling are estimated from the EverBatt model as listed in Table S22.[52] Adjustments are made according to the optimized process flows of recycling technologies and the assumptions of LIB compositions in this study. The economic parameters of the use phase are obtained from NYSERDA.[91] The breakdowns of life cycle costs are presented in Table S23-Table S25 and the economic performance of reused automotive LIBs is discussed in the manuscript.

Table S22. Unit cost of materials used in LIB's life cycle[51,52,92]

Material	Unit cost	Plus cost
Aluminium cooling plate ($/kg)	4.00	0.10 ($/cell)
Aluminium current collector ($/m^2)	0.30	
Ammonia ($/kg)	0.46	
Battery jacket ($/kg)	7.00	
BMS ($/kg)	150.06	
Carbon black ($/kg)	6.60	
Cell container ($/kg)	3.00	0.20 ($/cell)
Citric acid ($/kg)	0.69	
Coke ($/kg)	0.09	
Coolant ($/gal)	4.74	
Copper current collector ($/m^2)	1.20	
Electricity (residential, average, New York State, 2020)	0.19	
Electrolyte ($/L)	15.00	
Glucose ($/kg)	0.50	
Graphite ($/kg)	12.50	
Hydrochloric acid ($/kg)	0.15	
Hydrogen peroxide ($/kg)	0.74	
Iron	0.27	
LFP ($/kg)	14.00	
Limestone	0.13	
Lithium carbonate	7.90	
Lithium hydroxide	12.18	
LMO+NMC532 ($/kg)	15.00	
Manganese oxide	2.16	
Module casing ($/kg)	3.00	1.00 ($/module)
Module compression plates and steel straps ($/kg)	2.00	
Module interconnects ($/kg)	5.00	1.00 ($/interconnect)
Module terminal ($/kg)	5.00	0.75 ($/module)
NCA ($/kg)	21.50	
Nitrogen ($/kg)	0.28	
NMC333 ($/kg)	21.00	
NMC532 ($/kg)	20.00	
NMC622 ($/kg)	20.60	
NMC811 ($/kg)	22.00	
Negative terminal assembly ($/kg)	6.00	0.25 ($/cell)
NMP ($/kg)	3.10	
Oxygen ($/kg)	0.20	
Phosphoric acid ($/kg)	0.06	
Positive terminal assembly ($/kg)	4.00	0.25 ($/cell)
PVDF ($/kg)	9.50	
Sand ($/kg)	0.06	
Separator ($/m^2)	1.10	

Slag ($/kg)	0.02
Soda ash ($/kg)	0.15
Sodium chlorate ($/kg)	0.40
Sodium hydroxide ($/kg)	0.40
Sulfuric acid ($/kg)	0.06

Table S23. Breakdowns of production cost for LIBs

Breakdown of production cost	LFP	LMO+NMC532	NMC333	NMC532	NMC622	NMC811	NCA
Material cost ($/EV pack)	5658.91	4771.59	5363.19	5102.60	4927.94	4809.01	4868.63
Direct labour cost ($/EV pack)	449.77	415.98	420.08	416.78	418.09	416.99	417.82
Capital equipment cost ($/EV pack)	884.61	830.63	833.19	827.03	824.68	841.61	822.00
Building cost ($/EV pack)	108.39	99.32	100.25	99.37	99.58	99.55	99.44
BMS and disconnect cost ($/EV pack)	540.25	540.25	540.25	540.25	540.25	540.25	540.25
Total ($/EV pack)	7641.93	6657.76	7256.95	6986.02	6810.54	6707.41	6748.14

Table S24. Breakdowns of life cycle cost for LIBs with second life

Breakdown of life cycle cost ($/kWh life cycle electricity delivery)		LFP	LMO+ NMC532	NMC333	NMC532	NMC622	NMC811	NCA
Production		5.50E-02	4.79E-02	5.22E-02	5.02E-02	4.90E-02	4.82E-02	4.85E-02
EV use		1.30E-02	1.30E-02	1.30E-02	1.30E-02	1.30E-02	1.30E-02	1.30E-02
Repurpose		1.34E-02	1.10E-02	1.12E-02	1.09E-02	1.08E-02	1.05E-02	1.06E-02
ESS use		4.65E-02	4.65E-02	4.65E-02	4.65E-02	4.65E-02	4.65E-02	4.65E-02
Recycling	Hydrometallurgical recycling	1.03E-02	1.18E-02	1.11E-02	1.09E-02	1.02E-02	1.12E-02	9.48E-03
	Direct cathode recycling	1.53E-02	1.03E-02	1.00E-02	9.84E-03	9.45E-03	1.07E-02	9.23E-03
	Pyrometallurgical recycling		6.48E-03	6.59E-03	6.52E-03	6.40E-03	6.30E-03	6.34E-03
Total	Hydrometallurgical recycling w/ second life	1.38E-01	1.30E-01	1.34E-01	1.31E-01	1.30E-01	1.29E-01	1.28E-01
	Direct cathode recycling w/ second life	1.43E-01	1.29E-01	1.33E-01	1.30E-01	1.29E-01	1.29E-01	1.28E-01
	Pyrometallurgical recycling w/ second life	-	1.25E-01	1.29E-01	1.27E-01	1.26E-01	1.25E-01	1.25E-01

Table S25. Breakdowns of life cycle cost for LIBs without second life

Breakdown of life cycle cost ($/kWh life cycle electricity delivery)		LFP	LMO+ NMC532	NMC333	NMC532	NMC622	NMC811	NCA
Production		2.50E-01	2.18E-01	2.38E-01	2.29E-01	2.23E-01	2.20E-01	2.21E-01
EV use		5.90E-02	5.90E-02	5.90E-02	5.90E-02	5.90E-02	5.90E-02	5.90E-02
Recycling	Hydrometallurgical recycling	4.70E-02	5.38E-02	5.04E-02	4.94E-02	4.66E-02	5.09E-02	4.31E-02
	Direct cathode recycling	6.98E-02	4.58E-02	4.46E-02	4.39E-02	4.22E-02	4.81E-02	4.13E-02
	Pyrometallurgical recycling	-	1.22E-02	1.27E-02	1.24E-02	1.18E-02	1.14E-02	1.16E-02
Total	Hydrometallurgical recycling w/o second life	3.56E-01	3.31E-01	3.47E-01	3.37E-01	3.29E-01	3.29E-01	3.23E-01
	Direct cathode recycling w/o second life	3.79E-01	3.23E-01	3.41E-01	3.32E-01	3.24E-01	3.27E-01	3.21E-01
	Pyrometallurgical recycling w/o second life	-	3.06E-01	3.27E-01	3.17E-01	3.11E-01	3.07E-01	3.09E-01

S8. Additional information and data

Figure S29 shows the electricity generation by energy sources in the Texas State used in this study.[93] The energy generated from renewable energy sources is responsible for under 30% of the total power generation. Natural gas, as the major source that accounts for 50% of electricity generation, contributes to 44% of the carbon footprint, 41% of the CED, 57% of fossil depletion, 91% of ozone depletion, and 68% of terrestrial ecotoxicity; Coal, as a pollutant emitting energy source, accounts for 23.5% of the energy source of Texas power grid and dominates most of the impact categories. Nuclear power accounts for 9% of the Texas electricity generation and contributes to 96% of ionizing radiation; In addition, although wood fuels result in only 0.2% of electricity generation, it could explain 31% of the agricultural land occupation. Therefore, the environmental impacts for electricity consumption (especially the use phase) are largely determined by characteristics of the environmental profiles of these energy sources.

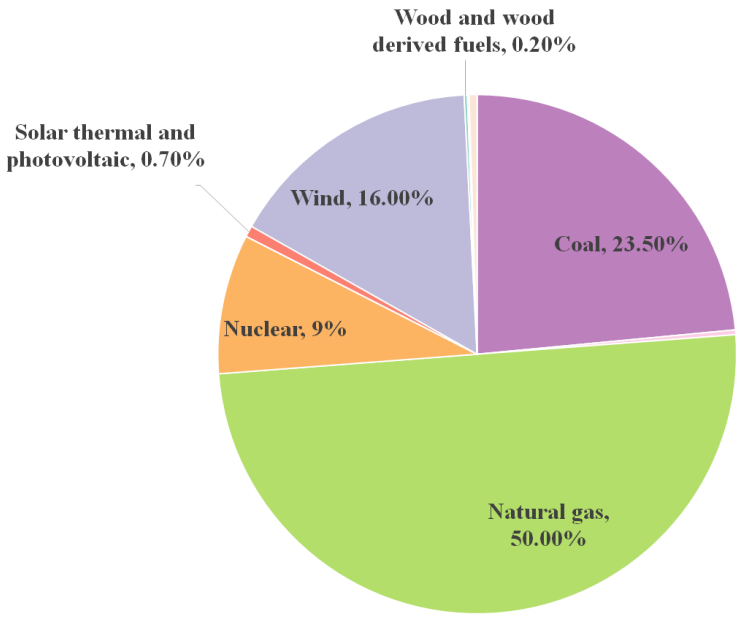

Figure S29. Electricity generation by energy sources in the Texas State in 2018

The electricity generation by energy source from 2020 to 2050 in the United State and China is presented on a percentage basis in Figure S30. This data is used to assess the impact of temporal and geographical variation in electricity generation to the environmental performance of reused automotive LIBs.

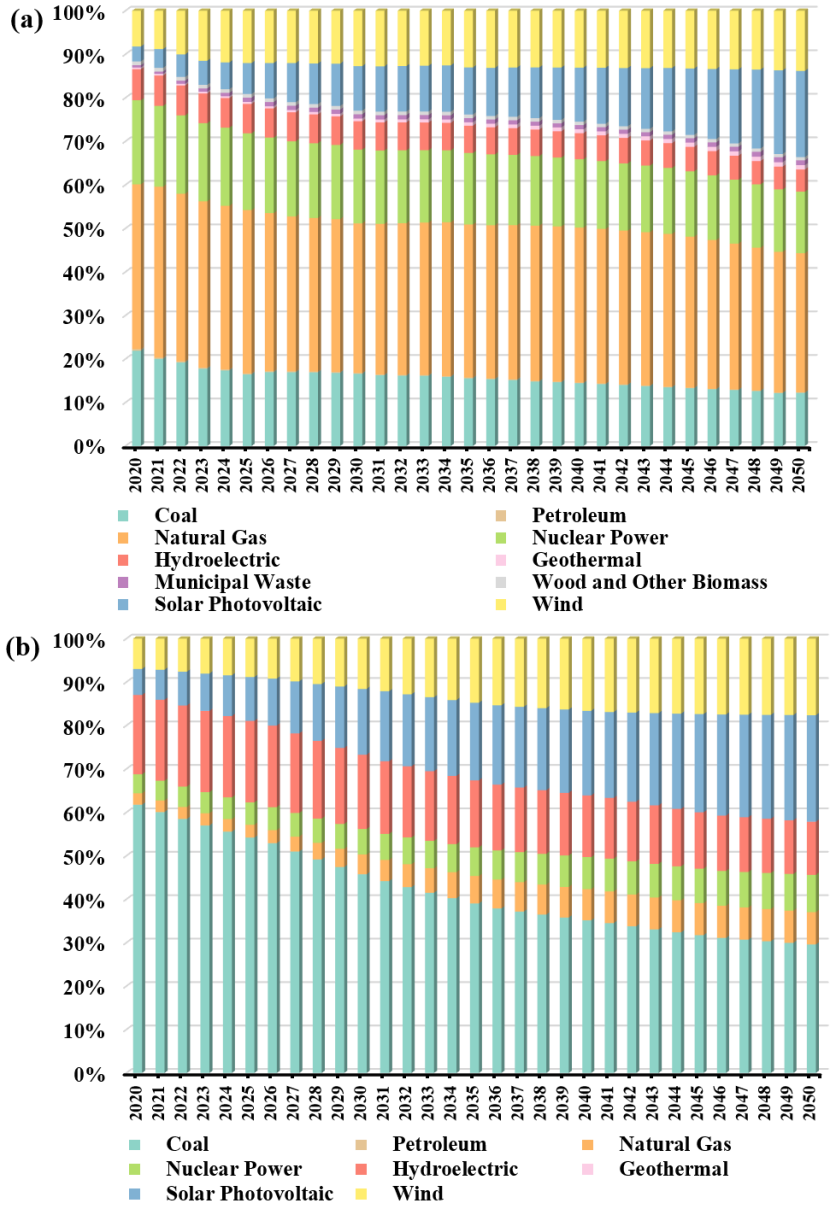

Figure S30. Electricity generation by energy sources in (a) United States[49] (b) China[50] from 2020 to 2050.

Table S26. Transportation of metal and chemicals on a ton basis[21,32]

Component	Water (km)	Rail (km)	Road (km)
$NiSO_4$	0	500	50
$CoSO_4$	0	1500	50
$MnSO_4$	0	1350	50
$Al_2(SO_4)_3$	0	600	50
Steel	8250	600	50
Iron	8250	600	50
Aluminium	0	700	50
Copper	0	650	50
Graphite	8250	600	50
PVDF	0	500	50
$LiPF_6$	0	500	50
EC	0	500	50
DMC	0	500	50
PP	0	500	50
PE	0	500	50
PET	0	500	50
NaOH	0	500	50
NH_3	0	500	50
ACN	0	500	50
PC	0	500	50
H_2O_2	0	500	50
Citric acid	0	500	50
H_2SO_4	0	500	50
HCl	0	500	50
H_3PO_4	0	500	50
$FeSO_4$	0	500	50
Na_2CO_3	0	500	50
$NaClO_3$	0	500	50
LI_2CO_3	0	500	50
LiOH	0	500	50
Mn_2O_3	0	0	500
Cathode active material	0	0	20
EOL LIBs (after EV use)	0	0	45
EOL LIBs (after stationary ESS use)	0	0	500

Table S27. Yield rates for battery materials and cells[51,94]

Component	Yield rate
Cathode materials	92.2%
Anode materials	92.2%
Aluminium current collector	90.2%
Copper current collector	90.2%
NMP recovery	98%
Separator	98%
Electrolyte	94%
Cells	95%